Appalachian State University
Boone, North Carolina

Southeastern Geology: Volume 41, No. 1
March 2002

Editor in Chief: S. Duncan Heron, Jr.

Abstract

Academic journal published quarterly by the Department of Geology, Duke University.

SOUTHEASTERN GEOLOGY

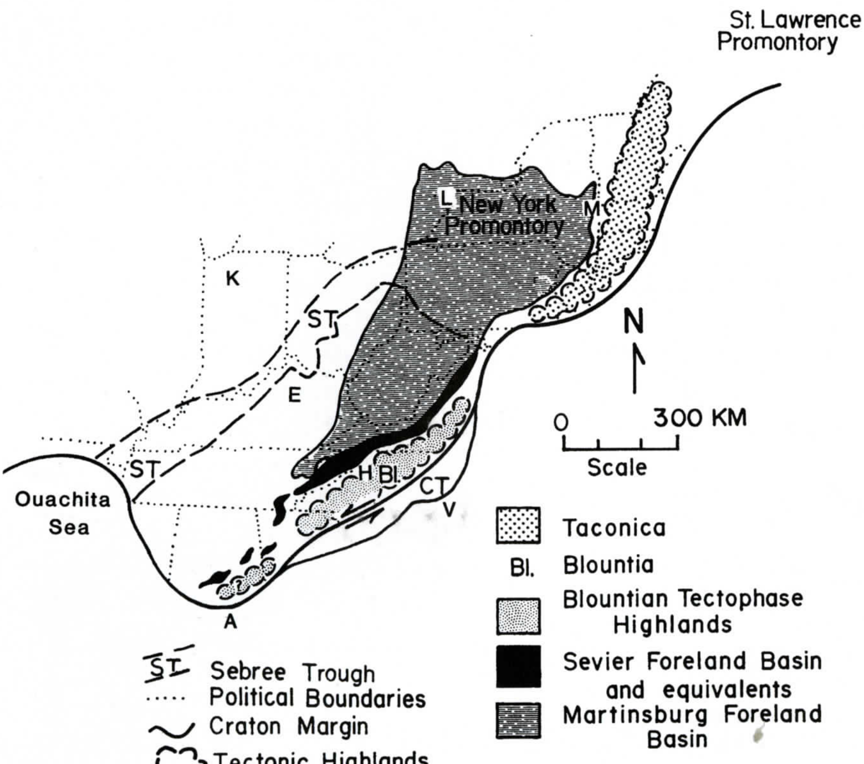

VOL. 41, NO. 1

MARCH 2002

SOUTHEASTERN GEOLOGY

Table of Contents

Volume 41, No. 1 March 2002

SOUTHEASTERN GEOLOGY

PUBLISHED

at

DUKE UNIVERSITY

Editor in Chief:

Duncan Heron

This journal publishes the results of original research on all phases of geology, geophysics, geochemistry and environmental geology as related to the Southeast. Send manuscripts to **DUNCAN HERON, DUKE UNIVERSITY, DIVISION OF EARTH & OCEAN SCIENCES, BOX 90233, DURHAM, NORTH CAROLINA 27708-0233**. Phone: 919-684-5321, Fax: 919-684-5833, Email: duncan.heron@duke.edu Please observe the following:

1) Type the manuscript with double space lines and submit in duplicate.
2) Cite references and prepare bibliographic lists in accordance with the method found within the pages of this journal.
3) Submit line drawings and complex tables reduced to final publication size (no bigger than 8 x 5 3/8 inches).
4) Make certain that all photographs are sharp, clear, and of good contrast.
5) Stratigraphic terminology should abide by the North American Stratigraphic Code (American Association Petroleum Geologists Bulletin, v. 67, p. 841-875).

Subscriptions to *Southeastern Geology* for volume 41 are: individuals - $22.00 (paid by personal check); corporations and libraries - $28.00; foreign $34. Inquires should be sent to: **SOUTHEASTERN GEOLOGY, DUKE UNIVERSITY, DIVISION OF EARTH & OCEAN SCIENCES, BOX 90233, DURHAM, NORTH CAROLINA 27708-0233**. Make checks payable to: *Southeastern Geology.*

Information about SOUTHEASTERN GEOLOGY is on the World Wide Web including a searchable author-title index 1958-2001 (Acrobat format). The URL for the Web site is:

http://www.southeasterngeology.org

SOUTHEASTERN GEOLOGY is a peer review journal.

ISSN 0038-3678

SOUTHEASTERN GEOLOGY
V. 41, No. 1, March 2002, p. 1-36

EVIDENCE AND IMPLICATIONS OF POSSIBLE FAR-FIELD RESPONSES TO TACONIAN OROGENY: MIDDLE-LATE ORDOVICIAN LEXINGTON PLATFORM AND SEBREE TROUGH, EAST-CENTRAL UNITED STATES

FRANK R. ETTENSOHN

Department of Geological Sciences, University of Kentucky, Lexington, KY 40506

JOHN C. HOHMAN

ExxonMobil Exploration Company, Houston, TX 77210

MARK A. KULP

Department of Geology & Geophysics, University of New Orleans, New Orleans, LA 70148

NICHOLAS RAST

Department of Geological Sciences, University of Kentucky, Lexington, KY 40506

ABSTRACT

Stratigraphic and structural differentiation of the shallow-water Blackriverian carbonate platform across east-central United States near the Blackriverian-Rocklandian (early Caradoc) transition coincides with inception of the Taconic tectophase of the Taconian Orogeny. Collapse of the Blackriverian carbonate platform and sequential development of the Galena Shelf, Lexington Platform, and Sebree Trough followed. The distribution of resulting facies parallels similarly trending basement structures with little or no surface expression, suggesting that facies changes reflect reactivation of basement structures at depth by far-field processes.

Bulge moveout at tectophase inception apparently reactivated old structures across the Black River Platform, leaving a series of structural lows and highs. The highs acted as foundations for extensive buildup of carbonates that would become the Galena Shelf and Lexington Platform. Intervening, linear low areas were sufficiently depressed to make contact with open seas to the south, which in the existing paleogeographic and paleoclimatic setting promoted quasi-estuarine circulation. This circulation funneled deep, cold, mineral-rich waters, inimical to carbonate deposition, from the southern margin of Laurentia into structural lows between the platforms, generating a Trenton surface of omission and corrosion there, expressed as a trough-like corridor of sediment starvation called the Sebree Trough. The resulting influx of cold water also changed broad sedimentary and faunal patterns during three million years of mid-Kirkfieldian to late Shermanian time.

More local responses across the Lexington Platform include development of a carbonate buildup, facies changes related to structural trends, and repeated horizons of widespread, seismically induced liquefaction. The diversity of responses across wide areas during narrow intervals of time, as well as coincidence and repetition of responses along basement structures, reflect the likely significance of far-field effects during craton-margin orogeny.

Literature review suggests that stratigraphic responses like those above are typical of orogenic complexes and probably reflect the distal transmission of stresses, focused on pre-existing zones of foreland, basement weakness. Hence, understanding basement structural framework and the paleogeographic and paleoclimatic settings in which it occurs, even in allegedly quiescent, distal, settings, can be critical in deciphering stratigraphic, sedimentary, and faunal relations of the foreland.

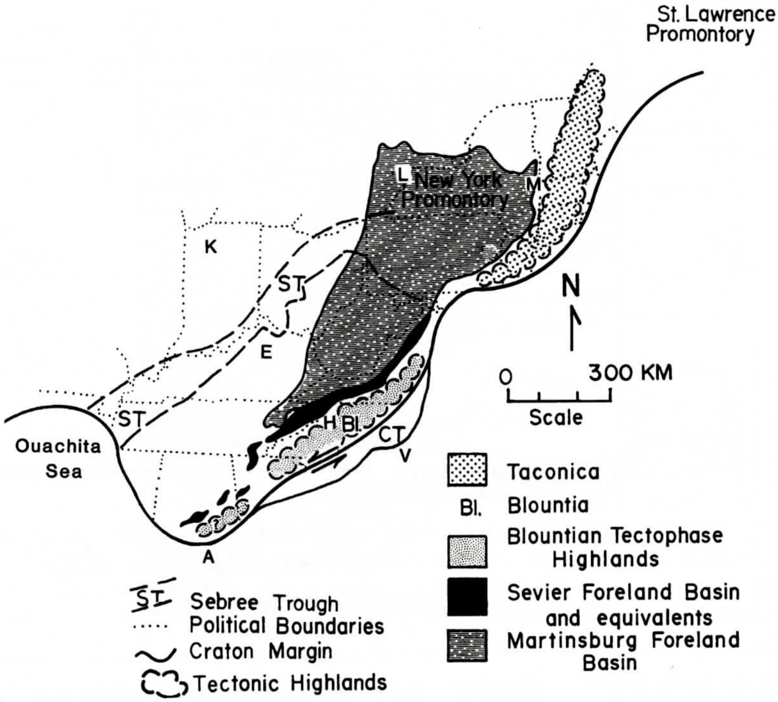

Figure 1. Generalized Middle-Late Ordovician paleogeographic framework on southeastern parts of Laurentia showing tectonic highlands and maximum extent of black-shale foreland basins relative to continental promontories. CT=Carolina Terrane; A=Alabama Promontory; V=Virginia Promontory (adapted from Ettensohn, 1991).

vergence (Kay and Colbert, 1965; Rodgers, 1970; Shanmugan and Lash, 1982; Bradley, 1989; Pollack, 1989, Ettensohn, 1991). Reflecting this shift is the fact that the earlier Blountian tectophase (late Whiterockian-early Rocklandian; Llanvirn-early Caradoc) was intense at the Virginia Promontory and perhaps at the Alabama Promontory, whereas the later Taconic tectophase (late Rocklandian-Gamachian; mid-Caradoc-Ashgill) was intense at the New York Promontory (Figure 1). The effects of each tectophase were nevertheless experienced to some extent along much of the orogen (Hiscott and others, 1986; Ettensohn, 1991). Promontories tended to localize deformation and were subject to greater compression and resulting strain (Dewey and Burke, 1974; Dewey and Kidd, 1974; Ettensohn, 1985, 1991). Hence, effects of lithospheric flexure related to unconformity formation, foreland-basin development, generation of associated stratigraphic sequences, and reactivation of basement structures, are commonly more pronounced behind promontories (Ettensohn, 1991, 1994). Moreover, each tectophase is characterized by an unconformity-bound stratigraphic sequence beginning with a transgressive unit of dark basinal shales, reflecting rapid subsidence due to deformational loading, followed by an overall regressive sequence of coarser clastic sediments indicating uplift and lithospheric relaxation (Figure 2). Although lithologies typical of foreland-basin sequences may not be present beyond the basin, the overall transgressive-regressive regime inherent in a foreland-basin sequence is commonly reflected in platform and ramp carbonates on adjacent parts of the foreland.

Two, and possibly three, flexural foreland-basin sequences, interpreted to represent Taconian tectophases, exist in the Appalachian Basin (Figure 2). Of these, the Middle to Late Ordovician Taconic tectophase, which generated the Martinsburg foreland basin (Figure 1), apparently had the most profound effects on the

INTRODUCTION

Major stratigraphic changes at the Early-Middle Ordovician transition on Laurentia mark the first major differentiation of sedimentary and tectonic regimes since Late Proterozoic formation of the craton. Many such changes across proximal parts of the Laurentian foreland reflect initiation of the Taconian Orogeny at the eastern craton margin, resulting in formation of the regional Knox unconformity and subsequent development of cratonic basins. The concurrent development of a facies mosaic across much of the foreland was also in part a response to far-field (distal), flexural deflections produced by vertical Taconian loading of the lithosphere (e.g., Jacobi, 1981; Quinlan and Beaumont, 1984; Ettensohn, 1991, 1994). However, horizontal compressive forces transmitted far into the foreland may also have controlled some facies distribution through synsedimentary reactivation of old structures (e.g., Lowell, 1995).

The influence of flexural processes, by which orogenies at the craton margin can affect the formation and reactivation of cratonic basins (e.g., Beaumont, 1981; Quinlan and Beaumont, 1984), is now broadly accepted, as is the idea that resulting basins exhibit distinctive sedimentary sequences (Ettensohn, 1991, 1994; Goodman and Brett, 1994; Lehmann and others, 1994). Large areas of the supposedly "more stable," interbasinal foreland are expected to exhibit local effects, and depending on the structural fabric of the underlying basement, may display a sedimentary mosaic that is different from basin-related patterns. Such patterns of interbasinal deposition and sediment remobilization are especially apparent in the foreland of Kentucky and nearby areas in upper Middle and lower Upper Ordovician strata deposited at the acme of the Taconian Orogeny (Ettensohn and Kulp, 1995; Ettensohn and others, 1996, 1998; Pope and others, 1997; Rast and others, 1999). Because many regional and local patterns tend to coincide with geophysically indicated basement structures, we will examine the nature, distribution and timing of the more salient, distal, foreland sedimentary patterns in and around Kentucky in order to discern possible Taconian far-field responses on interbasinal parts of the foreland.

TECTONIC AND STRUCTURAL FRAMEWORK

Large-scale, low-amplitude motions affecting the cratonic foreland, which can be linked through timing, stratigraphy or structural style to a coeval, craton-margin orogeny via supracrustal or subcrustal loading, have been called far-field tectonic responses (Klein, 1994; Coakley and Gurnis, 1995). With growing knowledge of crust-mantle relationships during convergence and the development of predictive models (Quinlan, 1987; Mitrovica and others, 1989; Coakley and Gurnis, 1995), the proposed correlation between distal deformations and coeval orogenies is becoming an increasingly acceptable model. Although the extent of far-field displacement overlaps the range of lithospheric flexure involved in forming foreland basins and their yoking with intracratonic basins, far-field effects have been reported more than 1300 km from the originating orogen (Karner and Watts, 1983; Ziegler, 1987; Mitrovica and others, 1989; Coakley and Gurnis, 1995). Aside from general cratonic tilting, some of the most apparent effects are commonly coincident with preexisting basement structural trends along which part of the displacement occurred (Ziegler, 1987).

For rocks considered in this study, the driving force for proposed far-field responses was the Taconian Orogeny, which marked closure of the Iapetus Ocean. The term "Taconian" is used in the sense of Kay (1969) to include all Ordovician and possibly Early Silurian deformation along the southeastern margin of Laurentia. The terms "Blountian" and "Taconic" are used in the sense of Kay and Colbert (1965) for phases of the Taconian Orogeny, more or less restricted to different times and places along that margin. Although the collision zone was heterogeneous in kinematic style and timing (Rodgers, 1971; Hiscott, 1984; Drake and others, 1989; Bock and others, 1996; Mac Niocaill and others, 1997), along U.S. parts of the zone there was a time-transgressive northeastward shift of con-

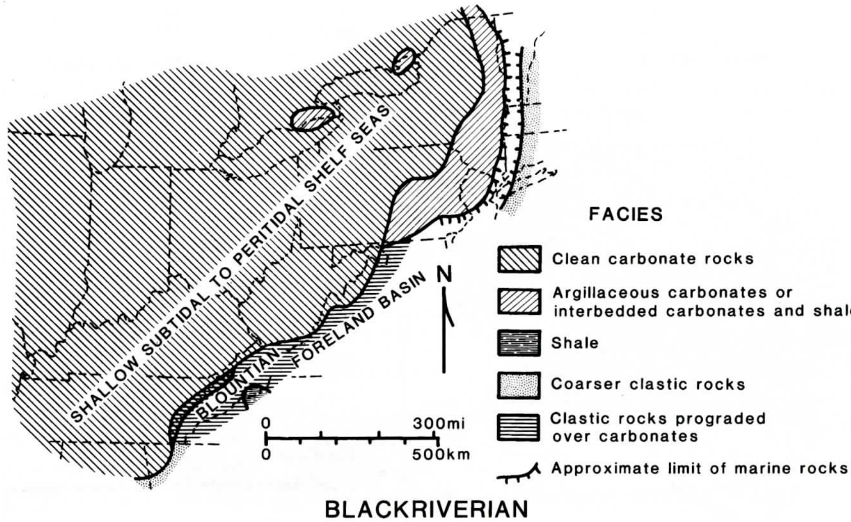

Figure 3. Schematic map view showing sedimentary and tectonic differentiation at the southeastern margin of Laurentia during the Blountian tectophase in Blackriverian time. Northwest of the foreland basin, facies were remarkably uniform consisting of shallow-subtidal to peritidal carbonates developed across the Blackriverian carbonate platform (adapted from Keith, 1989b).

1984), brittle deformation along basement zones of weakness may enhance the progress of flexure and far-field effects in the shallow crust. All of the above reflect responses to the transmission of vertical supra- or subcrustal forces, but the transmission of horizontal forces may also reactivate or invert old basement structures (Sibson, 1995; Lowell, 1995).

The upper lithosphere in Kentucky and adjacent states is diverse in composition and has many zones of structural weakness (Denison and others, 1984; Black, 1986; Shumaker, 1986; Drahovzal and others, 1992; Furer, 1996; Root, 1996; Shumaker and Wilson, 1996; Stark, 1997a). Most of the basement structures are related to Keweenawan extension (~1.1 Ga), Grenville compression (1.0 Ga), or Iapetan rifting (0.74 Ga), and the prevalence of southwest-northeast-trending basement dislocations largely reflects the orientations of Keweenawan and Iapetan rifts (Drahovzal and others, 1992; Shumaker and Wilson, 1996; Tullo and Aleinikoff, 1996; Stark, 1997a). In short, the basement throughout the study area is broken into many small blocks (Shumaker and Wilson, 1996; Stark, 1997a) capable of moving when subjected to stress.

The Taconic tectophase probably reflects the inception of a major episode of subduction and obduction at and near the New York Promontory, accompanied by volcanism, thrusting and formation of the tectonic upland, Taconica (Figure 1). To the south, however, oblique convergence of the Carolina Terrane with Laurentia also gave rise to coeval orogeny (Hibbard, 2000). Because the nature, apparent intensity, and positions of collision along the eastern margin of Laurentia make it likely that horizontal forces were also transmitted cratonward and that discernible far-field responses on and near the Lexington Platform were likely, we will examine rocks deposited during the most active, late Middle to early Late Ordovician (late Rocklandian-early Edenian; mid-Caradoc) period of the tectophase. These early parts of the tectophase, moreover, correspond to times of most active convergence and deformation; subsequent parts were largely relaxational and involved widespread inundation of the foreland basin and adjacent craton with clastic sediments (Figure 2) (Ettensohn, 1991, 1994). The sediments deposited on the craton during the early parts of the tectophase mainly comprise the Trenton Group and its equivalents. Widespread exposure of these rocks and their accessibility in the subsurface because of economic potential

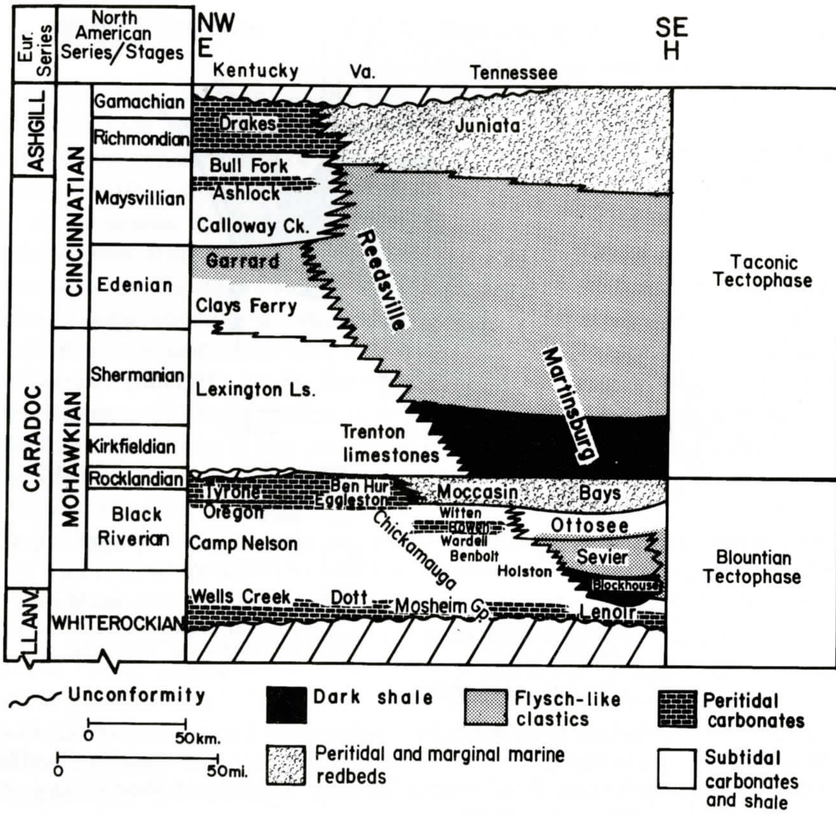

Figure 2. Schematic northwest-southeast section (E-H, located on Figure 1) perpendicular to the strike of the foreland basin showing two unconformity-bound stratigraphic sequences. Lenoir-Bays sequence represents sedimentation in the Sevier (Blountian) foreland basin; Martinsburg-Juniata and Lexington-Drakes sequences represent foreland-basin and foreland sedimentation during Taconic tectophase. The facies boundary between Lexington/Trenton limestones and Martinsburg Shale marks the boundary between Lexington Platform and foreland basin. The Lexington/Trenton limestones and Clays Ferry equivalents are the main units involved in formation of the Lexington Platform and Sebree Trough. Rocklandian, Kirkfieldian, Shermanian and early Edenian stages are largely equivalent to old concepts of a "Trenton Stage" (adapted from Ettensohn, 1991).

foreland, volcanicity, and differentiation along basement structural trends. This tectophase may reflect a major change in kinematic style from Blountian collision (e.g., Vick and others, 1987) to Taconic subduction. Although the polarity of subduction has been a subject of much debate, a west-dipping subduction zone (McKerrow and others, 1991) is consistent with some far-field effects (Coakley and Gurnis, 1995).

In addition to regional tilting (Quinlan and Beaumont, 1984; Q lan, 1987; Mitrovica and others, 1989; Coak y and Gurnis, 1995), flexural and far-field movements are interpreted to have reactivated foreland, basement structures or caused surface faulting (Bradley and Kusky, 1986; Knight and others, 1991; Ziegler, 1987; Coakley and Gurnis, 1995; Leighton, 1996), generating episodes of uplift or subsidence and concomitant unconformities and facies changes on local to regional scales. In fact, Coakley and Gurnis (1995) suggested the necessity of an inhomogeneous lithosphere for the full development of far-field effects, and in view of the fact that upper parts of the lithosphere are extremely viscous and experience stress relaxation over 10- to 200-Ma periods (Quinlan and Beaumont,

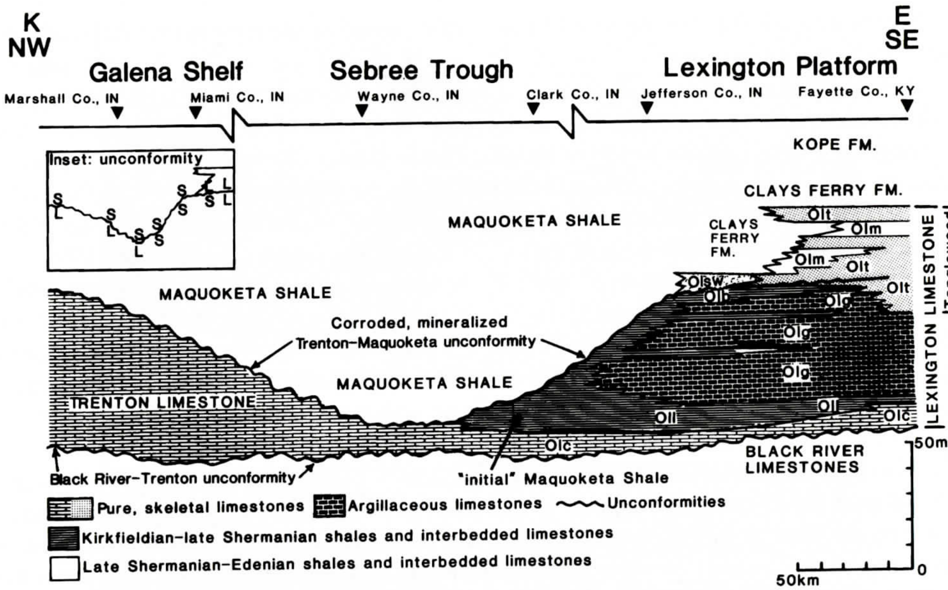

Figure 5. Schematic NW-SE cross section (K-E, located on Figure 1) from the Lexington Platform to the Galena Shelf, showing inferred stratigraphic relationships between Maquoketa Shale and its equivalents (central white area) in the Sebree Trough and limestones of the Galena Shelf and Lexington Platform based on five cores and exposures in Fayette County, Kentucky. Pronounced beveling of Trenton on Trenton-Maquoketa unconformity is misleading, and thinned Trenton section is largely due to lapping out of strata along the underlying Black River-Trenton unconformity. See Figure 15 for time-stratigraphic relationships. Members of Lexington Limestone: Olc=Curdsville Mbr., Oll=Logana Mbr., Olg=Grier Mbr., Olb=Brannon Mbr., Olt=Tanglewood Mbr., Olm=Millersburg Mbr. and Olsw=Sulphur Well Mbr. Shale tongues into Grier Mbr. represent the Macedonia and Cane Run beds in ascending order. Inset is a reduced view of the section showing lithology (L=limestone, S=shale) on either side of the corroded, mineralized, Trenton-Maquoketa (sub-Sulphur Well) unconformity (adapted from Keith and Wickstrom, 1993).

the northwest margin of the corridor where corrosion and nondeposition were greatest, and rises southeastwardly onto the Tanglewood buildup of the Lexington Platform (Figure 5) to become the sub-Sulfur Well unconformity noted by Cressman (1973) and Ettensohn and others (1986) (Keith and Wickstrom, 1993; Hohman, 1998). By Edenian time, the thicker accumulation of deeper water dark shales or interbedded fine-grained, argillaceous carbonates and shales on the most corroded part of the unconformity appeared to form a "trough," separating the shallow-water Galena carbonate shelf to the northwest from the shallow-water Lexington carbonate platform to the southeast (Figures 4 and 5) (Droste and Shaver, 1983; Keith, 1985, 1989b; Keith and Wickstrom, 1993). Although the Edenian reconstruction in Figure 4 suggests that shales infilling the trough were coeval with limestones comprising the Galena Shelf and Lexington Platform, stratigraphic relationships observed in cores and geophysical logs, as well as biostratigraphy, indicate that the shale infilling is largely younger than and unconformably overlies limestones on the adjacent shelves and platforms (Figure 5) (Keith and Wickstrom, 1993; Hohman and Keith, 1997b; Hohman, 1998).

This trough-like belt or corridor of deeper water sediments was probably the most prominent Ordovician bathymetric feature on east-central parts of cratonic Laurentia, extending southwestward from the Taconic (Martinsburg) foreland basin to the Illinois Basin area and most likely to the Ouachita embayment on the southern margin of Laurentia (Figure 1). In fact, the predominance of dark shales along the belt and the scarcity of benthic fauna in them (Gut-

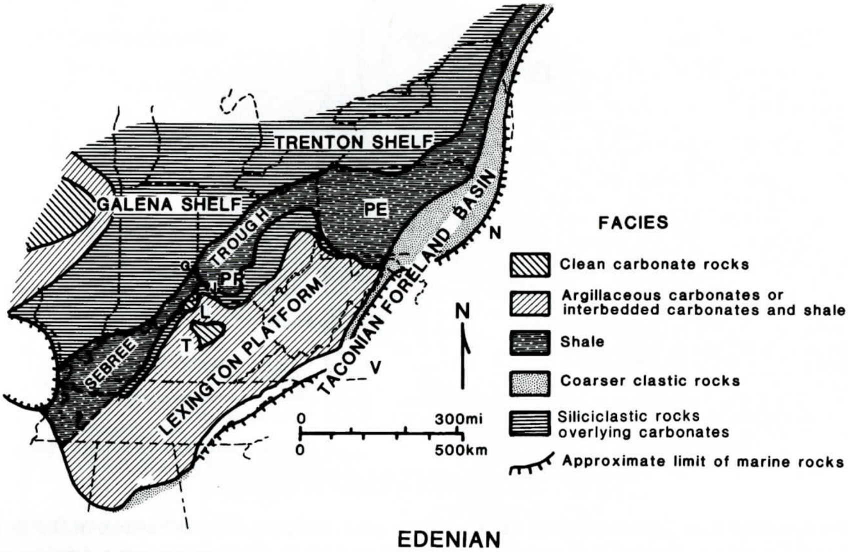

Figure 4. Schematic map view showing sedimentary and tectonic differentiation by early Edenian time of the Blackriverian carbonate platform into Galena and Trenton shelves, Sebree Trough, and Lexington Platform. The Tanglewood buildup (T) and Louisville High (L) were areas of likely local uplift. Along southern margins of the trough, shales have prograded out onto underlying platform carbonates. Note that Lexington Platform forms a barrier between eastern clastic sources and the Sebree Trough. PP=Point Pleasant basin; PE=Pennsylvania embayment; V=Virginia Promontory; N=New York Promontory (adapted from Keith, 1989b).

(Keith, 1989a; Roen and Walker, 1996) contribute to recognition of changing facies patterns.

STRATO-TECTONIC FRAMEWORK

Patterns of stratigraphic differentiation, or "division" of the extensive, shallow-water, Blackriverian carbonate platform (Figure 3) into a deep- to shallow-water facies mosaic of carbonates and siliciclastic sediments, was already apparent in late Whiterockian to Blackriverian time (Llanvirn-early Caradoc) on eastern parts of Laurentia, largely in the form of a foreland-basin complex developed on the subsiding continent margin (Figure 3). The greatest basin subsidence and development of diverse facies occurred in the Sevier foreland basin (Shanmugam, 1977; Shanmugam and Walker, 1980, 1983), just cratonward of the Virginia Promontory, the locus of Blountian tectonism (Figures 2 and 3). Much of the craton was part of an extensive carbonate platform (Figure 3) with restricted, peritidal to shallow-subtidal sedimentation represented by units like the Black River Group, High Bridge Group, Platteville Group, Plattin Limestone, and Stones River Group (Cressman and Noger, 1976; Cameron and Mangion, 1977; Droste and Shaver, 1983; Keith, 1989b; Bergström and Mitchell, 1994).

By Rocklandian time (mid-Caradoc), uniform patterns of deposition were abruptly disrupted, as parts of the platform experienced uplift and tilting along the margins of a nearly 1000-km-long "corridor," extending southwest to northeast from western Tennessee to central Pennsylvania (Figure 4). The corridor reflects development of two largely independent carbonate sequences on either side of an intervening area of nondeposition that is recognized by a pronounced thinning of Trenton limestones along a regional unconformity (Keith and Wickstrom, 1993; Hohman, 1998) (Figure 5). The unconformity is a pyritized and phosphatized corrosion surface or submarine hardground (Willman and Kolata, 1978; Delgado, 1983; Keith, 1985; Fara and Keith, 1989; Keith and Wickstrom, 1993) that is extensive across the Galena Shelf, appears to fall in section along

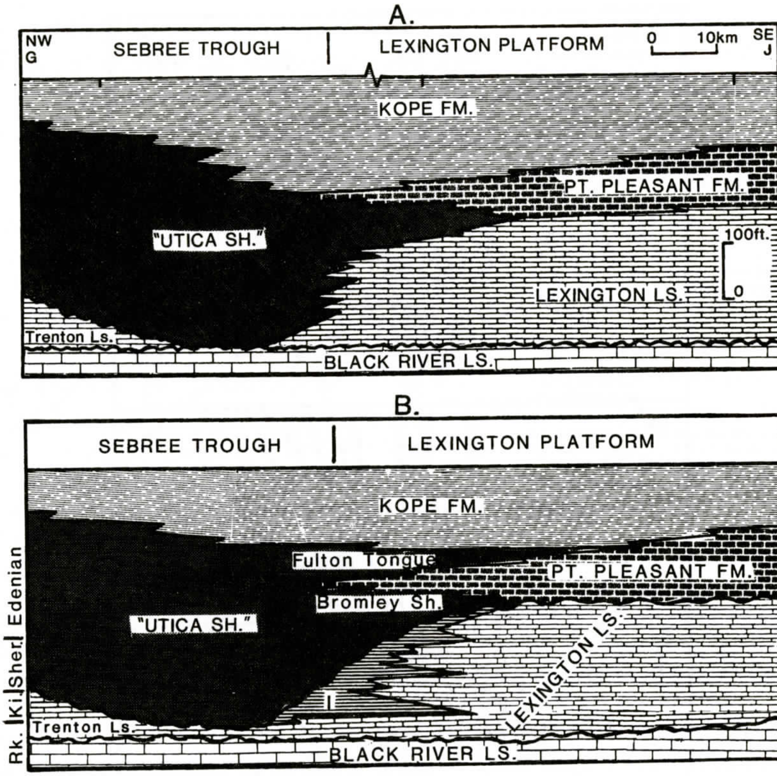

Figure 6. Schematic northwest-southeast cross-section across most of Sebree Trough in southeastern Indiana, southwestern Ohio, and northernmost Kentucky, showing A.) stratigraphic relationships between units in the trough and those on the Lexington Platform interpreted by Mitchell and Bergström (1991), B.) reinterpretation of stratigraphic relationships and ages based on more recent biostratigraphy and data from Hohman (1998) and Brett and Algeo (1999). Note that in B, ages differ from one side of the diagram to the other due to the Trenton-Maquoketa (sub-Sulphur Well) unconformity. See Figure 4 for location of the section G-J; I="initial Maquoketa" of Hohman (1998). Undulating line below Utica and Pt. Pleasant is the Trenton-Maquoketa (sub-Sulphur Well) unconformity. Rk.=Rocklandian; Ki.=Kirkfieldian; Sher.=Shermanian (adapted from Mitchell and Bergström, 1991).

which are latest Shermanian to early Edenian in age (Sweet and Bergström, 1971; Sweet, 1979). Hence, lower and middle parts of the Lexington Limestone cannot interfinger with most of the shales in the Sebree Trough as shown in Figure 6A. In contrast, on the Galena Shelf in Indiana, outcrop and subsurface data, augmented by limited biostratigraphy, indicate that deeper water Maquoketa shales are separated from underlying Trenton carbonates by an unconformity (Rooney, 1966; Schwalb, 1980; Fara and Keith, 1989; Mitchell and Bergström, 1991; Bergström and Mitchell, 1992; Wickstrom and Gray, 1989; Wickstrom and others, 1992; Kolata and others, 1998b) (Figure 5), with a hiatus represented by a mineralized hardground that at least locally is of late Shermanian to early Edenian age (Bergström and Mitchell, 1992). On the other side of the trough in Illinois, Galena Shelf carbonates (Galena Group) may be as young as late Edenian or early Maysvillian in age with a succeeding hiatus that may record Edenian-through-early Richmondian time (Shaver, 1985; Shaver and others, 1986; Norby, 1990; Hohman, 1998).

Keith and Wickstrom (1993), Hohman and Keith (1997b) and Hohman (1998) have traced this disconformity even farther into the trough using cores and geophysical logs and into outcrops on the Lexington Platform, showing that stadt, 1958b; Gray, 1972; Mitchell and Bergström, 1991; Wickstrom and others, 1992) indicate deposition in waters deep enough to have developed dysaerobic or anaerobic conditions, suggesting depths of 50- to 150-m based on modern dark-shale analogues (Rhoads and Morse, 1971; Byers, 1977). Minimum depths of 60-70 m, suggested by the difference in unconformity elevation between the "trough" and the Tanglewood buildup (see Cressman, 1973; Keith and Wickstrom, 1993; Hohman, 1998), also fall within this range. In contrast, depths on the Lexington Platform, based on modern analogues to the proximal tempestites (Aigner, 1985) which predominate there, must have largely fallen in the 15- to 20-m range.

Based on the geometry of thickened Cincinnatian shales unconformably overlying thinned Trenton carbonates in what appeared to be a valley along the corridor, Schwalb (1980) named this linear feature the "Sebree Valley" after the town of Sebree in Webster County, Kentucky, which is situated on the northwestern margin of the "valley." It has also been called the "Kope Trough" (Keith, 1985), but is now consistently designated the Sebree Trough (Bergström and Mitchell, 1987). Although the extent of this feature was not appreciated until the work of Rooney (1966), Gray (1972), Schwalb (1980), Droste and Shaver (1983), and Keith (1985, 1989b), observations on unit thinning and facies changes along the corridor had been made as early as the 1950's and 1960's in Ohio, Kentucky, and Indiana (Freeman, 1953; Gutstadt, 1958a,b; Calvert, 1962; Templeton and Willman, 1963). Rooney (1966) and Schwalb (1980) interpreted this trend of thinning and facies changes as either a structural hinge or a hinge line associated with "valley" erosion running from western Tennessee to north-central Ohio. However, not until the work of Cressman (1973) was it suggested to be a deeper, open-marine channel or trough that probably connected an oceanic domain at the southern margin of Laurentia with shallow platform areas as far north as central Ohio. Most subsequent workers adopted this interpretation (Keith, 1985; Bergström and Mitchell, 1989, 1990; Mitchell and Bergström, 1991), but in 1989, based on the presence of shales of similar age in central and western Pennsylvania (e.g., Patchen and others, 1985a), Keith suggested that in northeastern Ohio and northwestern Pennsylvania the trough, before joining the Taconic foreland basin (Figure 4), changed orientation to an easterly or southeasterly direction, and subsequent data (Ryder, 1991, 1992; Ryder and others, 1992) have supported this orientation. Somewhat similar interpretations (Wickstrom and others, 1992; Wickstrom, 1996) also concluded that the trough opened up into embayment-like basins in Ohio and Pennsylvania (Figure 4).

The fact that this trough-like feature is known almost wholly from the subsurface has made its origin difficult to interpret. However, the dark shales or argillaceous carbonates in the trough are included in parts of the Martinsburg Formation, Point Pleasant Formation, Utica Shale, or Maquoketa Group and contrast with shallow-water carbonates on either side (Figures 4, 5 and 6). In fact, a latest Shermanian to early Edenian tongue of dark "Utica Shale" is present in the Sebree Trough as far south as southeastern Indiana, where it joins dark shales of the Maquoketa Group that infill southwestern parts of the trough (Freeman, 1953; Mitchell and Bergström, 1991; Bergström and Mitchell, 1992) (Figure 6). Studies by Freeman (1953), Gutstadt (1958a), Rooney (1966), Gray (1972), Cressman (1973), Bergström and Mitchell (1989), and Mitchell and Bergström (1991) have suggested that these dark shales interfinger with carbonates on the northwestern margin of the Lexington Platform (Figure 6A). However, analysis of graptolite biostratigraphy from the trough (Mitchell and Bergström, 1991) indicates that the lowest graptolites in the trough filling lie near the *Corynoides americanus-Orthograptus reudemanni* zonal boundary, which based on newer work in the Mohawk Valley (Mitchell and others, 1994) occurs in the lowest Edenian Stage. This interpretation is also supported by conodont biostratigraphy from southeastern Indiana (Sweet, 1979, figure 3). This age means that the lowest shales analyzed in the Sebree Trough can only be equivalent to beds in the uppermost Lexington Limestone,

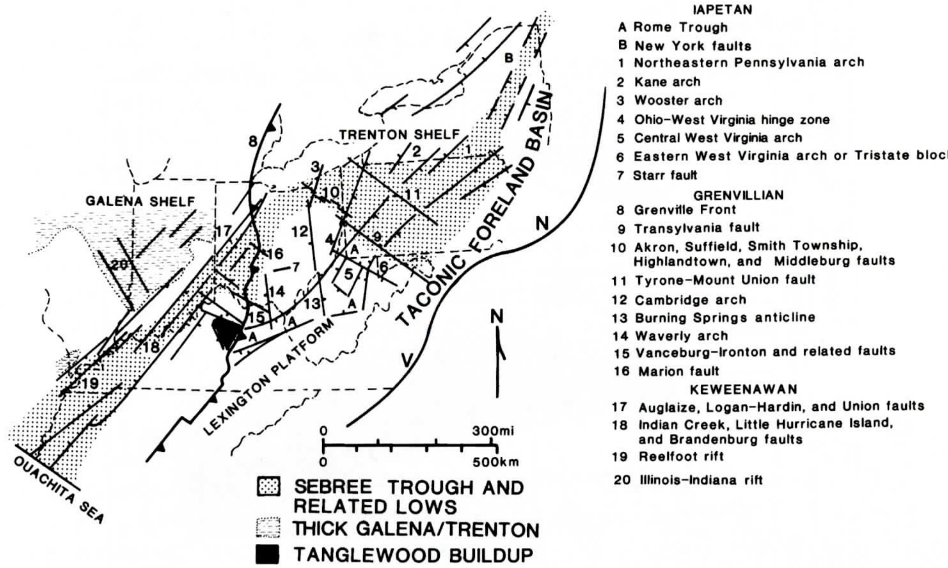

Figure 8. Map showing Edenian distribution (Keith, 1989b) of the Lexington Platform, Galena/Trenton shelf, Sebree Trough and Tanglewood buildup relative to apparently involved basement structures. Tick marks on downthrown side where predominant sense of movement is known.

trated along the hinge line during a sea-level lowstand. Schwalb (1980) found no evidence of structural control and suggested submarine channel erosion, but offered no location for the channel. Wickstrom and others (1992) showed that in parts of Ohio, trough orientation coincided with basement structural trends and that the deepest water facies developed over a basement graben. Bergström and Mitchell (1994) related trough formation to development of the Lexington Platform as a peripheral bulge, implying differential movement between the flexurally uplifted platform and the adjacent trough. Finally, Ettensohn and others (1996), Mitchell and others (1997), Stark (1997b) and Ettensohn (1999) suggested that the trough separated the Galena Shelf and Lexington Platform along northeasterly trending basement structures reactivated by Taconic orogeny.

STRATIGRAPHIC AND STRUCTURAL EVIDENCE

Galena-Trenton Shelf

The Galena-Trenton Shelf was a broad area of Middle-Late Ordovician (Rocklandian-early Edenian), shallow-water, generally coarse-grained carbonates with an open-marine fauna (e.g., Fisher, 1977; Hohman, 1998), which extended from central Illinois northeastwardly to central New York (Figure 4). Cross sections and isopach maps of the Galena Group and Trenton Limestone, which comprise the shelf in Illinois and Indiana (Kolata and Noger, 1990; Kolata and Nelson, 1990; Hohman, 1998), indicate that Galena carbonates unconformably overlie rocks of the Decorah, Platteville, or Black River groups and are relatively uniform in thickness through most of the present-day Illinois basin, which was at the time a stable shelf area. However, recent work by Hohman (1998) showed that Galena shelf carbonates thin prominently along a northeast-southwest trend (Figure 7A) that coincides with similarly oriented Keweenawan basement faults, which include the Reelfoot rift (Figure 8, nos. 18 and 19). Hohman's work also showed that thickest parts of the Galena, carbonate-shelf sequence overlie a northwest-southeast-oriented, Keweenawan, basalt-filled rift in east-central Illinois and adjacent parts of Indiana (see Denison and others, 1985, figure 5; Drahovzal and others, 1992, figure 8) and the northwestern margin of the Reel-

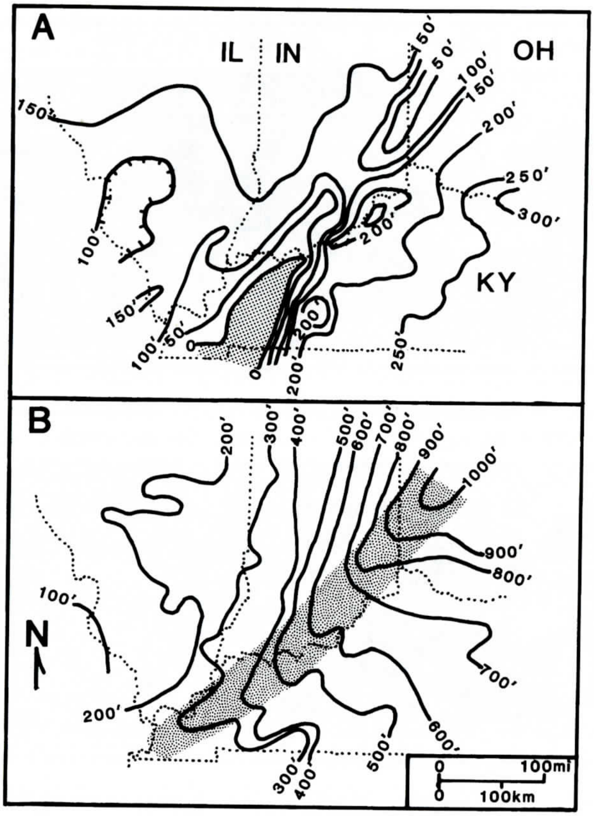

Figure 7. Isopach maps for the Trenton/Lexington and Maquoketa depositional sequences based on maps by Hohman (1998), which used data from 571 wells and outcrop sections. A.) Isopach map of the Trenton/Lexington deposition sequence (Galena, Trenton and lower Lexington formations). Note thick accumulations on the Galena Shelf (Galena/Trenton fms.) and on the Lexington Platform (lower Lexington Lms.) separated by a narrow, NE-SW-trending corridor of thin to absent deposits. Curdsville island stippled. B.) Isopach map of the Maquoketa depositional sequence (Maquoketa, Kope, Clays Ferry, "Utica," Point Pleasant and upper Lexington formations). The section thins to the northwest, but there is also a NE-SW thickening trend (stippled) that corresponds to the corridor noted in 7A above (adapted from Hohman, 1998).

the disconformity in the trough rises onto the Lexington Platform (Figures 5 and 6B) below the Sulphur Well and equivalent members of the Lexington Limestone (Cressman, 1973; Ettensohn and others, 1986) and is lost in adjacent, coarse Tanglewood limestones. Hence, tracking the unconformity from the trough onto the Lexington Platform also supports the biostratigraphy in indicating that most shales infilling the trough are no older than late Shermanian (Figure 6B). However, on the western and northwestern margin of the Lexington Platform, Keith and Wickstrom (1993) and Hohman (1998) have noted remnants of older, initial-stage, Maquoketa shales and their equivalents below the unconformity (Figures 5 and 6B).

The changes in lithofacies across the trough have been noted by many, but explanations have been few. Although structural influence has been a part of some interpretations, the evidence does not support structural subsidence characteristic of graben formation, as there is no evidence for associated faults or downdropped Trenton carbonates. Rooney (1966), however, suggested that the northwestern margin of the trough coincided with a structural hinge line that flexed down to the southeast due to epeirogenic upwarping and that wave erosion concenform largely coincides with these basement structures, points to their reactivation as a likely cause for its differentiation near the Blackriverian-Rocklandian transition.

Significant, but more localized, uplifts on the platform in the area of the Jessamine and Nashville domes in central Kentucky and central Tennessee, respectively, were apparently responsible for maintaining parts of the Lexington Platform until late Edenian or Maysvillian time (Wilson, 1962; Borella and Osborne, 1978; Keith, 1989b; Ryder, 1991, 1992; Ryder and others, 1992)). In particular, the origin of the Tanglewood buildup on the Jessamine Dome (Figure 10) will be discussed in the following section.

The first carbonates on the platform after Blackriverian-Rocklandian uplift were high-energy skeletal calcarenites associated with the uplift and included in the Curdsville Member and its equivalents. After subsequent flooding of the platform, up to 75 m of generally shallowing-upward, Kirkfieldian and early Shermanian carbonates were deposited across the platform (Figures 5 and 7A).

During Kirkfieldian time, deposition of the argillaceous carbonates that characterize much of the Lexington, or "Trenton," limestone became widespread across the Lexington Platform (Keith, 1989b) and continued until late Shermanian time. On the Jessamine Dome area of central Kentucky, Kirkfieldian to late Shermanian deposition is represented largely by the Curdsville, Logana, and Grier members of the Lexington Limestone (Figure 11), and beyond the Lexington area, rocks of this age represent the entirety of Lexington or Trenton limestones, attaining 60 m or less of thickness (Figure 11). In central Ohio and southeastern Indiana, however, the Trenton Limestone is no more than 20-m thick and is equivalent largely to the Curdsville Member of central Kentucky; overlying Lexington equivalents are interbedded shales and argillaceous limestones that would be included as parts of the Point Pleasant, Kope or Maquoketa formations respectively (Figure 5) (Brown and Lineback, 1966;Shaver, 1985; Wickstrom and others, 1992; "initial Maquoketa" of Hohman, 1998). In fact, subsurface mapping by Keith (1989b), Keith and Wickstrom (1993), and Hohman (1998) shows that by mid-Kirkfieldian time, deeper water shale and limestones were accumulating in the trough area in southeastern Indiana, north-central Kentucky, and southwestern Ohio. These deeper water,

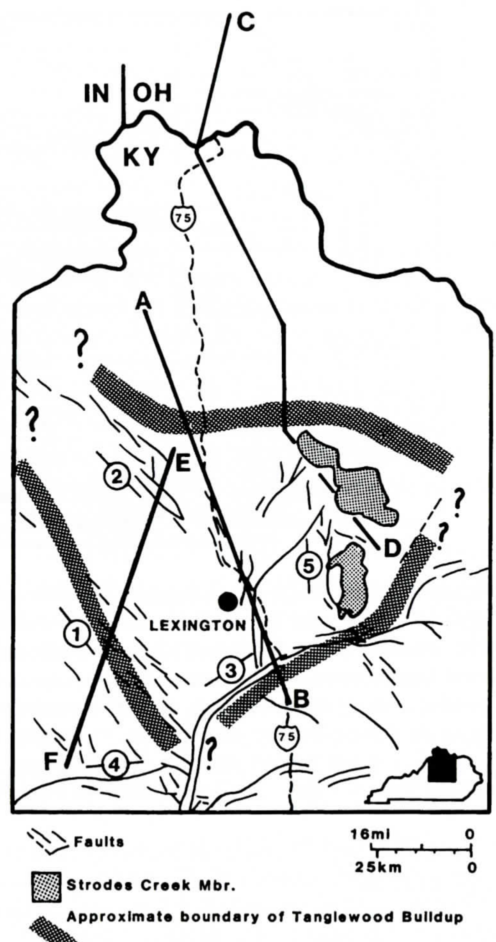

Figure 10. Location map showing the Jessamine Dome, position of the Tanglewood buildup, the distribution of related structures, and location of cross sections from Figures 11, 12 and 14. Outline of buildup is based on distribution of the Tanglewood Member from geologic quadrangle maps. Fault zones 1 and 2 are implicated in various facies changes (Figure 14) and in distribution of Brannon seismites (Figure 16). The Strodes Creek Member is a very local member confined to two small basins controlled by fault zone 5 (adapted from Ettensohn, 1992).

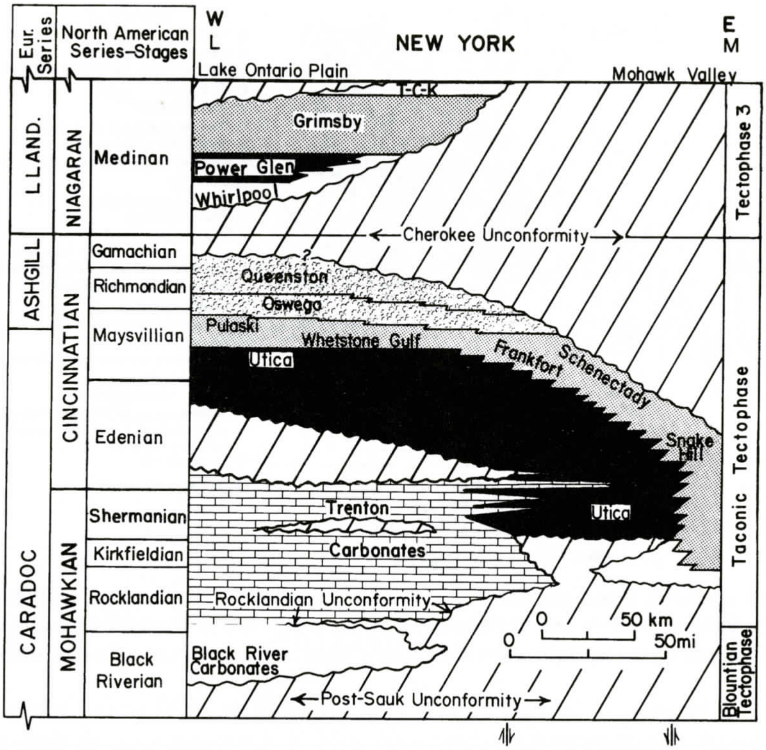

Figure 9. Schematic west-east section in New York nearly perpendicular to the strike of the Appalachian Basin (line L-M in Figure 1), showing the nature and disposition of three probable Taconian flexural sequences in the northern Appalachian Basin. Of special interest is the Trenton carbonate shelf (brick pattern) and its relationship to the Utica Basin (black shales) along basement faults (see Figure 8,B) shown by vertical lines below the section. Symbols: Black = dark shales; light stipple = flysch-like clastics; coarse stipple = peritidal and marginal-marine clastics; brick or no pattern = shallow-marine carbonates or clastics; wavy line = unconformity; diagonal lines = missing section. No vertical scale intended (adapted from Ettensohn, 1991, 1994).

foot rift (Figure 8). Inasmuch as shallow-water, carbonate sedimentation is generally enhanced on topographic highs (e.g., Wilson, 1975), the definition of the Galena shelf and the thickened carbonates along its margin (Figure 7A) may reflect reactivation or inversion of underlying structures.

The Galena shelf continues northeastward where it merges with the Trenton shelf of western and central New York. Here again, the eastern boundary of the carbonate shelf with the Utica basin is defined by a series of basement faults (Figures 8 and 9), suggesting that fault reactivation was influential in shelf development (Fisher, 1977).

Lexington Platform

Just as the Galena-Trenton shelf apparently reflects preferential carbonate buildup on reactivated Keweenawan structures, the Lexington platform to the south appears to represent a similar development. The northwestern and northeastern margins of the platform appear to coincide with a series of Keweenawan and Iapetan structures that were uplifted (Figures 7A and 8). Most notably, uplift on Iapetan faults controlled the Central West Virginia and East West Virginia arches, while uplift on the Grenvillian faults controlled the Vanceburg-Ironton, Waverly Arch and Cambridge-Burning Springs lineaments in southern and eastern Ohio (Figure 8). The fact that the northern margin of the plat-

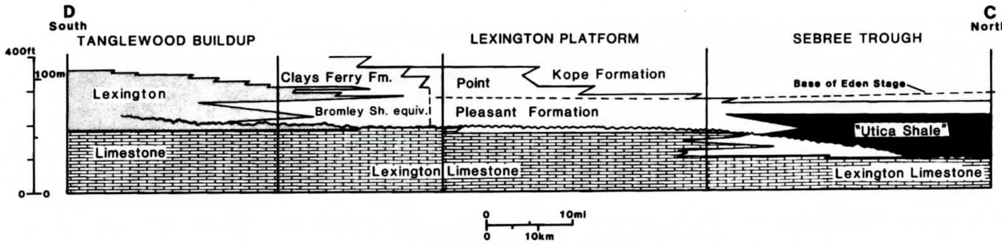

Figure 12. Schematic north-south cross section along line B-C in Figure 10, showing regional aspects of the relationship between the Tanglewood buildup and Sebree Trough. Note typical 50- to 60-m thicknesses of the Lexington Limestone that characterize parts of the Lexington Platform between the Tanglewood buildup and the Sebree Trough. Undulating line=sub-Sulphur Well unconformity (adapted from Cressman, 1973).

1994). This especially abrupt phase of deepening on the Lexington Platform and Trenton Shelf (Lehmann and others, 1994) was concurrent with Shermanian-Edenian expansion of the Sebree Trough (Mitchell and others, 1997), suggesting that the events may have been accompanied by a major episode of far-field tilting and subsidence.

Tanglewood Buildup

At the same time, however, but in contrast to the abrupt deepening that occurred nearly everywhere else on the platform, at the Jessamine Dome area of central Kentucky, a pronounced episode of regressive shoaling began in late Shermanian and continued into early Edenian time, resulting in an accumulation of Lexington Limestone in excess of 100 m (Figures 11 and 12). The effects of this shoaling also extended northward beyond the Jessamine Dome area to the margin of the Sebree Trough as a tongue of coarser grained limestones and interbedded shales equivalent to the upper Lexington Limestone, but called the Point Pleasant Formation (Cressman, 1973; Cuffy, 1998) (Figures 6B and 12). In central Kentucky, this shoaling produced a thicker (Cressman, 1973) and overall younger (Sweet and Bergström, 1971) Lexington Limestone as a carbonate buildup with an area of approximately 5500 km^2 grading laterally into deeper water facies in all directions (Figures 11 and 12). The anomalous thickness of Lexington Limestone on the Jessamine Dome was first recognized by Cressman (1973) and subsequently called the Tanglewood buildup by Ettensohn (1992), because it mainly consists of shoaling-upward calcarenites and calcirudites of the Tanglewood Member.

The Jessamine Dome, like the Nashville Dome to the south, is a culmination on the Cincinnati Arch, although the arch as a whole was not formed and did not become active until latest Ordovician time when regional lithofacies acquired trends parallel to its axis (Gutstadt, 1958b; Borella and Osborne, 1978; Weir and others, 1984). The dome area, however, is underlain by a series of Grenvillian and Iapetan faults with surface expression in extant fault zones (Black, 1986; Drahovzal and others, 1992; Rast and Goodmann, 1994), and abrupt changes in lithofacies along some of these faults have been interpreted to reflect Middle and Late Ordovician fault reactivation (Borella and Osborne, 1978; Ettensohn et al., 1986; Kulp, 1995; Kasl, 2001). The most important such change on the Jessamine Dome area is the change from mid-ramp, argillaceous carbonates of the Grier Member to very shallow, shoal-related, upper-ramp calcarenites and calcirudites of the Tanglewood Member that mark initiation of the Tanglewood buildup (Figures 11 and 12). Mapping the distribution of the member shows a roughly triangular body bound on two of the three sides by extant fault zones (Figure 10) (Ettensohn, 1992; Ettensohn and Kulp, 1995, 1997), suggesting that in the midst of regional subsidence and deepening, uplift on these fault zones helped to maintain a regressive buildup where Lexington carbonate deposition persisted

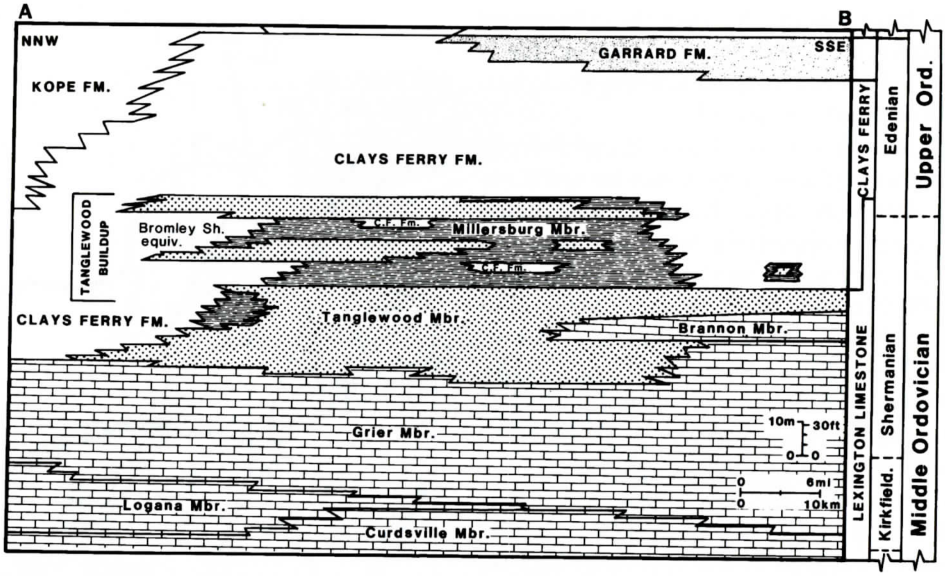

Figure 11. Schematic cross section along line A-B in Figure 10 showing the Lexington Limestone facies mosaic, the Tanglewood buildup and its relationship to deeper water units (Millersburg Mbr. and the Clays Ferry and Kope formations) that surround it, based on 11 measured sections from Cressman (1973). Coarse stipple represents calcarenites and calcirudites of Tanglewood buildup. Away from buildup, coeval deepening represented by the change from shallow-water Grier and Tanglewood carbonates to deeper water shales and argillaceous carbonates in the Clays Ferry Formation reflects a widespread, late Shermanian-early Edenian deepening event across the Lexington Platform (adapted from Ettensohn, 1992).

Kirkfieldian and Shermanian rocks occur in facies relationship with shallow-water limestones of the Lexington Platform (Figures 5 and 6B) and show that the trough-platform system was already well-developed by that time. Moreover, these "initial Maquoketa" shales are almost certainly equivalent to thinner tongues of deeper water shales and shaly carbonates in the Logana, Grier (Macedonian and Cane Run beds) and Brannon members of the Lexington Limestone in central Kentucky, as these tongues are coeval in age with initial Maquoketa shales and thicken to the north or northwest (Cressman, 1973; Grossnickle, 1985; Kulp, 1995) toward the trough where initial Maquoketa shales are best developed (Figures 5 and 6B). These shaly tongues probably reflect times of deeper water incursion onto the platform due to eustatic fluctuation and/or local structural downwarping. In the trough, only remnants of these rocks are left below the late Shermanian, Trenton-Maquoketa or sub-Sulfur Well unconformity (Figures 5 and 6B), as most deposition on and around the platform abruptly ended with a period of late Shermanian corrosion and nondeposition that is reflected in the sub-Sulphur unconformity. Off-platform in the Sebree Trough, this unconformity merges with a surface of nondeposition and corrosion (Hohman, 1998) (Figures 5 and 6B).

By late Shermanian time, widespread, regional deepening allowed deeper water, interbedded shales and argillaceous limestones, now included in the Clays Ferry, Point Pleasant, or Kope formations, to inundate most of the Lexington platform (Cressman, 1973) (Figures 11-14). Off-platform in the Sebree Trough, these units are largely equivalent to main parts of the Utica, Maquoketa, Scales, Bromley Shale, Point Pleasant and Kope formations (Shaver, 1985; Brett and Algeo, 1999) (Figure 6B). The deepening and associated influx of Point Pleasant, Clays Ferry and Kope siliciclastics may reflect foreland-basin subsidence accompanying initial Taconic relaxation (Ettensohn, 1991, uplifted areas that would define the Galena-Trenton shelf and the Lexington Platform. Although we cannot preclude the possibility of some erosion by bottom currents, examination of the unconformity in cores and exposures (Keith and Wickstrom, 1993; Hohman, 1998) indicates that the absence of Kirkfieldian and Shermanian carbonates in the corridor is related largely to nondeposition and corrosion. Moreover, as we will discuss further in a later section, the fact that limestones on both platforms are phosphorite-rich suggests that the trough corridor made contact with open sea to the south (Figures 1 and 4) and funneled deep, nutrient-rich waters onto the platforms, thereby accelerating carbonate production. Not only did increased carbonate production enhance trough-platform differences, but as the Lexington Platform accreted upward, it also formed a barrier to isolate the trough from eastern clastic influx, at least until late Shermanian time. So once the trough and platforms were initiated, they appear to have had continuous synergetic effects on the development of each other.

Throughout much of the trough, Kirkfieldian-through-middle Shermanian time is represented by a series of corroded, merged omission surfaces that form a Trenton-Maquoketa unconformity that merges upsection on the Lexington Platform with the sub-Sulphur Well unconformity (Keith and Wickstrom, 1993; Hohman, 1998). Based on the previously described late Shermanian age for the oldest, major trough filling, sediment starvation continued until late Shermanian time, when clastic influx from the east moved into the trough. By mapping the distribution of sediment types that began filling the trough at that time, Keith (1989b) noted that dark Utica shales from the foreland basin to the east had joined dark Maquoketa shales from the west at the Indiana-Kentucky-Ohio Tristate area (Figures 7 and 15), implying a genetic relationship between trough sedimentation and the Taconic foreland basin. In fact, this infilling may be related to the concurrent tilting of northwestern and central parts of the old Blackriverian carbonate platform noted by Droste and Shaver (1983, cf. figures 20 and 22), Wickstrom and others (1992, cf. figures 8 and 10), and Hohman (1998), which was part of an overall southeastward tilt of the Laurentian craton toward the subduction zone (Mitrovica and others, 1989; Coakley and Gurnis, 1995) and a reactivation of basement structures (Leighton, 1996) accompanying the Taconic tectophase.

The trend of the trough infill mapped by Keith (1989b) is clearly aligned with preexisting basement structures (Ettensohn and others, 1996) (Figure 8). This does not necessarily mean that growth faulting along these structures initiated trough development, although this possibility cannot be ruled out everywhere. More likely, however, is the possibility already mentioned that accelerated carbonate buildup on structurally high areas receiving high nutrient input continued to amplify the effects of Blackriverian-Rocklandian structural discontinuities now manifest as trough-platform boundaries. In north-central Ohio, the trend of the trough is directionally related to the Grenville front and associated structures (Figure 8). West of the front boundary, the northeast-southwest orientation of the trough probably reflects influence of the of the Keweenawan Illinois-Indiana and Midcontinental rift system, called the East Continent Rift Complex (e.g., Denison et al., 1984; Stark, 1997a), whereas east of the point of trough inflection in north-central Ohio, the main northwest-southeast and subsidiary northeast-southwest trough orientations seem to reflect influence of Grenvillian and Iapetan trends respectively (Figure 8). In extreme western Kentucky and adjacent parts of Tennessee, the boundaries of the trough coincide with the extent of the Reelfoot Rift and related faults (Figure 8, no. 19) (Stearns and Reesman, 1986; Drahovzal and others, 1992; Kolata and Nelson, 1997). One of these Reelfoot faults continues northeastward as the Indian Creek Fault into southeastern Indiana, and along with the Brandenberg Fault, seems to have controlled trough margins in the Tristate region. Furer (1996) has documented Middle Ordovician movement along these faults (Figure 8, no. 18) attesting to their activity at the time. In Indiana, the northwestern trough boundary similarly coincides with the Little Hurricane Island Fault (Furer, 1996), a basement fault that continues into east-

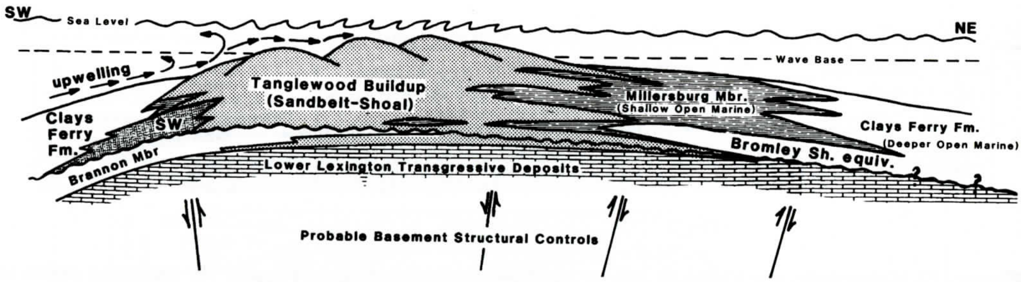

Figure 13. A highly schematic, environmental reconstruction across an approximately 70-km expanse of the Tanglewood buildup for upper regressive parts of the Lexington Limestone (Tanglewood-Millersburg-Clays Ferry continuum) showing probable structural control on buildup development and presence of upwelling from the Sebree Trough. SW=Sulphur Well Mbr.; undulating line=sub-Sulphur Well unconformity (adapted from Ettensohn, 1992).

(Figures 11-13). Although the northern boundary of the buildup does not coincide with an extant fault zone, in the subsurface a Grenvillian fault zone is present (Figure 8). In Figure 13, a schematic environmental reconstruction suggests how reactivation of basement faults may have contributed to the buildup; originally related to Precambrian and Cambrian rifting, Ordovician movement on some of these faults appears to reflect inversion of the original displacement (e.g., Ziegler, 1987; Sibson, 1995; Lowell, 1995).

Keith (1989b) noted another likely buildup of skeletal sands in the Louisville area (Figure 4). Although known only from the subsurface, it also coincides with a basement structural high, the Louisville High of Black (1986). The high is interpreted to be a horst-like block in the Keweenawan fault zone (Drahovzal and others, 1992; Stark, 1997a,b) bounding the southern margin of the Sebree Trough (Figure 8) and probably reflects basement reactivation. These two late Shermanian-early Edenian buildups reflect final stages of the Lexington Platform. After early Edenian time, deeper water clastics of the Kope and Clays Ferry formations completely overspread the buildups.

Together with the surrounding shales into which it grades, the limestones of the Tanglewood buildup were included by Hohman (1998) in the Maquoketa depositional sequence, which is separate from underlying Lexington/Trenton limestones. These Tanglewood rocks overlie the sub-Sulphur Well unconformity and are continuous into Upper Ordovician rocks that are truncated by the Ordovician-Silurian unconformity (Figure 15). Not only did the clastics that predominate in this systems tract end major carbonate production across the Lexington Platform, but they form the principal filling of the Sebree Trough (Figure 6B).

Sebree Trough

Comparing isopach maps of thickness trends for the Trenton-Lexington depositional system of Hohman (1998) (Figure 7A) and the overlying Maquoketa depositional sequence (Figure 7B) shows clearly that the Sebree Trough began as a corridor of drastically reduced limestone thickness between the Galena-Trenton Shelf and the Lexington Platform, which was subsequently filled with Maquoketa deposits. What Trenton-Lexington carbonates that do floor this corridor are largely equivalent to the Curdsville and thin due to onlap and nondeposition on and around the Curdsville island or high (Hohman, 1998) (Figures 7A and 15). However, the event that formed the Curdsville island seems to have also reactivated basement structures across the old Blackriverian carbonate platform, and on those uplifted areas like the Curdsville island, production of shallow-water carbonates proliferated. In the intervening, deeper corridor, carbonate production was effectively arrested, generating an omission surface or unconformity. Hence, after Curdsville deposition, most carbonate deposition was restricted to structurally

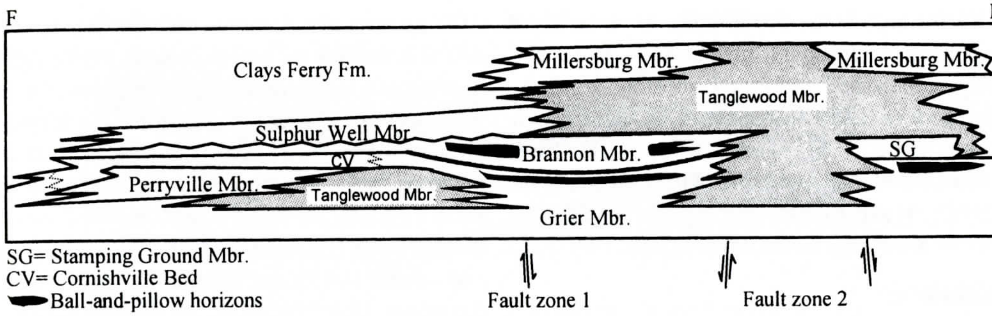

Figure 14. Schematic, southwest-northeast section (located on Figures 10 and 16) based on 18 measured sections from Kulp (1995) across an approximately 75-km expanse of the Tanglewood buildup and fault zones 1 and 2, showing coincidence of facies boundaries with fault zones. The dark, thickened lines represent horizons of soft-sediment deformation, or likely seismites, in the Grier and Brannon members (adapted from Ettensohn and Kulp, 1995).

vergence and deformation. Deformational loading and resulting flexural forces are expected to have been especially effective in reactivating zones of basement weakness just behind the promontory, and these zones may have transmitted far-field forces westward and northwestward into the foreland.

Local Patterns of Response

Locally, responses are reflected in facies changes and occurrences of "seismites" (Seilacher, 1984) that broadly coincide with extant fault zones. Smaller scale, local manifestations like the above are common throughout east-central United States, and although they are possibly related to far-field reactivation of basement structures, specifically demonstrating such relationships and relating them to particular events are difficult because many of structures were reactivated repeatedly. Nonetheless, as examples of types of changes to expect, we emphasize local facies changes and likely seismites (Rast and Ettensohn, 1995, 1999; Pope and others, 1997; Ettensohn and others, 1998; Rast and others, 1999) that were contemporaneous with the late Shermanian origin of the Tanglewood buildup.

Facies changes:

Facies changes involving peritidal to deeper open-marine environments abound in the Tanglewood buildup (Cressman, 1973; Ettensohn and others, 1986; Ettensohn, 1992; Kulp, 1995; Ettensohn and Kulp, 1995, 1997; Kasl, 2001; Jewell, 2001). The facts that so many of these changes are local and coincide with extant structural trends suggest the likelihood of structural influence, well-illustrated in the interval of the Grier-Tanglewood transition (Figures 11 and 14). Not only was this transition coeval with other mid- to late Shermanian regional changes, but the range of facies changes in it is the greatest in the Lexington Limestone.

Figure 14 is a schematic representation showing possible relationships between facies development at the transition and underlying fault zones. At the transition, the Grier Member grades vertically and laterally along two linear trends into coarse, crossbedded Tanglewood calcarenites and calcirudites. These trends apparently reflect linear shoals developed due to reactivation and uplift on fault zones 1 and 2 (Mackey, 1972; Kulp, 1995) (Figures 10 and 14). Other present facies, including peritidal (Perryville), shallow open-marine (Cornishville, Sulphur Well, Millersburg, Stamping Ground), and deeper open-marine (Brannon, Clays Ferry), have distributions that also indicate control by fault zones 1 and 2. Even the sub-Sulphur Well unconformity in this area (Figures 13 and 14) has been related to control by fault zone 1 (Ettensohn and others, 1986), and the fact that this facies control was coeval with late Shermanian structural activity and tilting across the Sebree Trough and Lexington central and northwestern Ohio as the Auglaize, Logan-Hardin, and Union fault zones (Figure 8, no. 17) (Wickstrom and Gray, 1989; Wickstrom and others, 1992; Wickstrom, 1996; Root, 1996). These fault zones parallel the northwestern margin of the trough and seem to have localized deeper water deposition of black, Utica shales (Wickstrom and others, 1992).

The southeastern trough margin in central Ohio is more irregular and seems to reflect control by a series of basement structures, including the Vanceburg-Ironton Fault, the Waverly Arch, the Marion Fault, the Starr Fault and the Cambridge Arch-Burning Springs Anticline (Figure 8) (see Root, 1996; Shumaker and Wilson, 1996). These structures are mostly oriented northwest or north-northwest and have been interpreted as Grenvillian in origin (Shumaker and Wilson, 1996); they outline a small embayment off the main trend of the trough in south-central Ohio that Wickstrom and others (1992) called the Pt. Pleasant Basin (Figures 4 and 8).

In northeastern Ohio and northwestern Pennsylvania, the trough opens into an embayment-like basin, the Pennsylvania Embayment, that joins the foreland basin in southeastern Pennsylvania (Figure 4). The widening of the trough begins at the Wooster Arch and Ohio-West Virginia hinge, northeasterly oriented Iapetan structures that are part of the widening of the Rome Trough in western and central Pennsylvania (Ryder, 1992; Ryder and others, 1992). Southern and northern trough boundaries in Pennsylvania and northeastern Ohio nearly coincide with the Transylvania Fault System of Pennsylvania and a series of smaller, related fault systems in Ohio (40th parallel lineament of Shumaker, 1986) and the Tyrone-Mt. Union Fault System to the north (Ryder, 1992; Ryder and others, 1992; Wickstrom, 1996), both of which Shumaker and Wilson (1996) indicated to be Grenvillian structures (Figure 8). Later, as flexurally controlled subsidence and/or eustatic sea-level rise continued, the extent of the Pennsylvania Embayment expanded southward as far as the Central West Virginia and Eastern West Virginia arches and northward as far as the Kane and Northeastern Pennsylvania arches (Figure 8), all of which reflect uplifted basement blocks associated with Iapetan development of the Rome Trough (Ryder, 1991, 1992). The further northeastward development of this embayment and its merger with the foreland basin in northeastern Pennsylvania and southeastern New York were probably related to subsidence along faults bounding the northern end of the Rome Trough where it extends into New York (Figure 8). Nearly parallel, northeast-southwest-trending, Iapetan faults in east-central New York (Fisher, 1977) apparently define the western margin of the foreland basin near its merger with the trough (Figures 8B and 9).

The corridor of sediment infill outlined by this Middle to Late Ordovician zone of reactivated basement structures stretching from western Kentucky and Tennessee to central Pennsylvania is considered herein to reflect the Sebree Trough (Figures 4 and 8). Thus interpreted, the trough attained its greatest extent (Keith, 1989b) and thickest fill of dark shales (Ryder and others, 1992) in the Pennsylvania Embayment (Figures 4 and 8). The embayment area is especially broad because it coincides with a northwest-southeast widening of the Rome Trough and is box-like in outline because the Rome Trough in this area is nearly at right angles to two Grenvillian structural lineaments (Transylvania and Tyrone-Mt. Union faults). Moreover, the involved structures have a predominant sense of movement that is down toward the interior of the embayment, which opens up southeastwardly into the foreland basin. That this segment of the Rome Trough experienced more subsidence than other parts of the trough is probably related to the fact that the trough in this area was bound by horst-like uplifts to the south (Central West Virginia and Eastern West Virginia arches) and north (Kane and Northeastern Pennsylvania arches) that were situated just cratonward of the locus of most intense Taconic convergence at the New York Promontory (Figures 4 and 8). The location of this area behind the promontory and the fact that the promontory was the source for much of the later Ordovician clastic wedge (Colton, 1970; Meckel, 1970) indicate that it must have been the focal point for Taconic con-

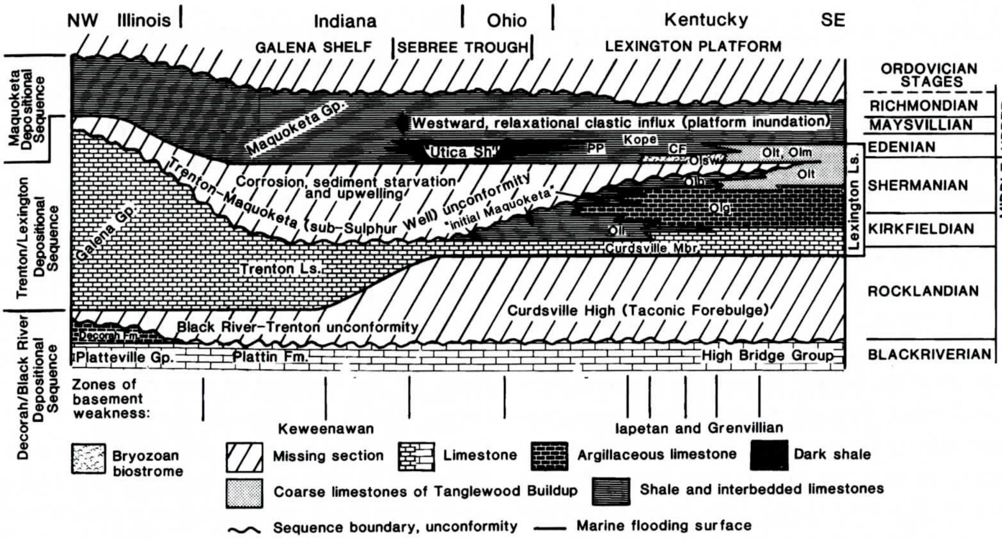

Figure 15. NW-SE chronostratigraphic section from the Lexington Platform in central Kentucky to the Galena Shelf in central Illinois, showing the overall diachroneity of the Galena Shelf, Lexington Platform and Sebree Trough. Vertical lines below the section are relative positions of basement fault zones that apparently influenced parts of the above stratigraphic configuration. Text in diagonally hatched gaps names unconformities and indicates likely cause of missing section. Lexington member abbreviations as in Figure 5; PP=Point Pleasant Fm.; CF=Clays Ferry Fm. (adapted from Hohman, 1998).

ure 4 is somewhat misleading in suggesting that carbonates of the Galena Shelf, siliciclastics of the Sebree Trough, and carbonates of the Lexington Platform are contemporaneous. In fact, this is generally not the case, as the Trenton-Maquoketa unconformity separates carbonates of the Galena Shelf and most carbonates on the Lexington Platform from the largely siliciclastic fill of the Sebree Trough (Keith and Wickstrom, 1993; Hohman, 1998) (Figures 5, 6B and 15). This unconformity has been widely recognized on the Galena Shelf because of contrasting lithologies at the Galena-Maquoketa boundary, but on and near the Lexington Platform the unconformity has been largely missed because of the shale-on-shale and carbonate-on-carbonate nature of the contact (Figure 5, inset). The tracing of this unconformity from the Galena Shelf through the Sebree Trough and onto the Lexington Platform by Keith and Wickstrom (1993) and Hohman (1998) is an extremely important finding, and as they have suggested, can only mean that the most of the trough infilling is largely post-Galena and post-Lexington in age, a fact now supported by reinterpretation of available biostratigraphic data. Hohman (1998) has furthermore pointed out that the Galena Shelf, Sebree Trough, and Lexington Platform are largely of different ages and reflect shifting loci and types of deposition, apparently controlled in large part by the tectonic and structural framework (Figure 15). During Rocklandian and early Kirkfieldian time, carbonate deposition was initially focused on the Galena Shelf, but by mid-Kirkfieldian through late Shermanian time the focus of deposition had shifted to the Lexington Platform. By latest Shermanian and earliest Edenian time, however, carbonate deposition became even more narrowly focused on distant parts of the Galena Shelf and on the Tanglewood buildup of the Lexington Platform as siliciclastic sediments inundated the area, initially via the Sebree Trough. Despite the fact that most of the trough was infilled after late Shermanian time, it is important to note that the physical trough had an earlier origin. This is indicated by remnants of Middle Ordovician Maquoketa Shale in facies

Platform argues for the likelihood of far-field responses. Additional information on facies development in the Lexington Limestone and Tanglewood buildup is reported by Black and others (1965), Mackey (1972), Cressman (1973), Ettensohn and others (1986), Ettensohn (1992), Kulp (1995) Ettensohn and Kulp (1995), Kasl (2001) and Jewell (2001).

Seismites:

Seismites, or probable, post-depositional, seismogenically deformed sediments (Seilacher, 1969, 1984), are commonly associated with ancient and recent faults (Sims, 1973; Anand and Jain, 1987; Guiraud and Plaziat, 1993; Obermeier, 1996), and similar structures have been interpreted from the Lexington Limestone (Rast and Ettensohn, 1995; Pope and others, 1997; Rast and others, 1999). Pope and others (1997) have extensively documented seismites in the central Kentucky area, as well as in nearby parts of Ohio and Virginia. Differentiating structures of seismic origin from similar structures of other origins is disputed, but Obermeier (1996) has suggested that widespread development of features and their repetition in the stratigraphic record around a core area, as well as morphologies consistent with sudden liquefaction accompanying seismic shaking, are critical criteria.

Horizons of formerly liquefied sediment are found throughout the Lexington Limestone, but are especially common and well-developed near the Grier-Tanglewood transition (Figure 14) that represents changeover from widespread, transgressive Lexington deposition to localized regression on the Tanglewood buildup (Figures 11-14). Because soft-sediment deformation of non-seismogenic origin may be confused with that of seismogenic origin, we have adopted several concurrent criteria as indicators of likely seismic origin (Obermeier, 1996). The most important of these include: presence of multiple deformed horizons bound above and below by undeformed strata in close stratigraphic proximity, evidence for strong upward-directed hydraulic force in the form of carbonate dikes, evidence of sediment liquefaction or fluidization, presence of structures consistent with historically documented, earthquake-induced deformation, and association with faults in presently or formerly seismically active regions. These characteristics have been documented from three, consecutive, deformed horizons in the Brannon Member, which occur across an area of nearly 1800 km^2 in central Kentucky (Ettensohn and others, 1998; Rast and others, 1999), and from a deformed bed in the upper Grier Member, so distinctive as to bear its own formal name, the Cane Run Bed (Black and others, 1965; Cressman, 1973; Jewell, 2001), which occurs across an area of nearly 700 km^2 (Figure 16). What is most telling about these deformed horizons is that their mapped distributions show clear proximity to extant fault zones (Figure 16) developed over known basement precursors. Likely seismites in the Brannon Member (Figure 16) are associated with a segment of the Kentucky River Fault System (with an Iapetan precursor) and with fault zones 1 and 2 (with Grenvillian precursors), for which there are also facies-related examples of synsedimentary structural control (Figures 10 and 14). The Cane Run Bed, on the other hand, is a deformed horizon along a segment of the Lexington Fault System (with a Grenvillian precursor) (Figure 16). Although it is difficult to relate any of the seismite horizons to specific far-field effects of Taconic subduction over 500 km to the east, the facts that mechanisms are in place to explain their occurrence and that they occur in abundance at a time and place in which likely regional effects have been demonstrated, suggest localized responses to far-field foreland stresses.

DISCUSSION

Regional Situation

There is clearly a pronounced stratigraphic differentiation between the time of the Blackriverian carbonate platform (Figure 3) and the deep- to shallow-water facies mosaic of carbonates and siliciclastics that comprise the Edenian Galena Shelf, Sebree Trough, and Lexington Platform (Figure 4). However, as already suggested, the Edenian facies mosaic shown in Fig-

Shallow-water carbonate deposition continued on the Galena Shelf and Lexington Platform into early Kirkfieldian time, but neither area had fully differentiated because carbonate deposition was continuous across them (Hohman, 1998) (Figure 15). By mid-Kirkfieldian time, however, differentiation had become very apparent. With regional flooding (Curdsville-Logana transition), carbonate deposition became restricted to the two platform/shelf areas, while the intervening area became a linear corridor of sediment starvation and omission, and it was this linear corridor that would become the Sebree Trough, largely through the absence of deposition. That this corridor was in fact a low, trough-like area with little carbonate deposition is indicated by the abrupt facies change along the northwest margin of the Lexington Platform, where shallow-water, platform carbonates pass into deeper water shales and fine-grained limestones of Hohman's initial Maquoketa (Figures 5, 6B and 15). In view of the regional flooding indicated by the initial Maquoketa and the transition from Curdsville to Logana lithologies, the persistence of shallow-water, carbonate deposition on the platform/shelf areas would have required that they were already uplifted or in the process of uplift. Although parts of the Lexington Platform around the Curdsville island had already experienced uplift, the coincidence of major facies changes in the lower Lexington Limestone with basement structures (e.g., Mackey, 1972; Grossnickle, 1985; Kulp, 1995; Ettensohn and Kulp, 1995; Jewell, 2001) suggests that uplift continued on the platform throughout Lexington time. The same kind of detailed facies work is not now available for most of the Galena-Trenton Shelf, but the fact that this shelf continued to be an area of shallow-water, carbonate deposition for the rest of Kirkfieldian, Shermanian and early Edenian time (Fisher, 1977; Shaver, 1985; Shaver et al., 1986; Norby, 1990) suggests that it also experienced relative uplift compared to the Sebree Trough. The absence of direct evidence for synsedimentary faulting along platform/shelf margins probably reflects gentle flexure in response to growth faulting at depth. Although initial uplift and structural reactivation in the platform area (Curdsville island) was probably related to bulge moveout, cratonward bulge moveout is an early aspect of tectophase flexure (Quinlan and Beaumont, 1984) and may not be adequate to explain continued uplift. However, far-field responses related to subduction (Coakley and Gurnis, 1995) or to transfer of external horizontal forces (Lowell, 1995) during transgressive accretion of the Carolina Terrane (Hibbard, 2000) could well explain continued uplift on reactivated structures.

The flooding associated with the initial Maquoketa and post-Curdsville Lexington may have also had tectonic causes, possibly reflecting cratonic subsidence and tilting related to the subsiding Taconic foreland basin, but other components like the Shermanian, mid-Lexington flooding events that resulted in the deeper water shales and fine-grained limestones of the Macedonia and Cane Run beds, as well as the Brannon Member of the Lexington Limestone, may partially represent eustatic events (e.g., Ross and Ross, 1992, 1995; Diecchio and Broderson, 1994). Hence, it is the mid-Kirkfieldian to late Shermanian facies changes at the northwestern margin of the Lexington Platform that first indicate inception of the Sebree Trough in the Tristate area (Figure 15). In contrast, closer to the Galena Shelf, it is the lack of deposition that defines much of the Sebree Trough until latest Shermanian time (Figure 15), a contrast in depositional regimes that is most easily explained via the interaction of paleogeographic, paleoclimatic and tectonic factors.

Based on interpolation from the time scales of Harland et al. (1989) and Webby (1995), the Sebree Trough was generated in about 3 million years during middle Kirkfieldian to late Shermanian time. Although depositional thinning of Trenton carbonates is present in parts of the trough, this thinning reflects earlier onlap and has little bearing on the sediment starvation and corrosion that are the real reasons for the trough. Once the Lexington Platform began development, it and the subsiding foreland basin to the east acted as barriers to westward transport of siliciclastic sediment from Taconic highlands (Figure 4), except during times of high sea level. In fact, extensive shaly intervals like the relationship with Lexington Platform carbonates, the initial phase of Hohman's (1998) Maquoketa Shale (Figures 5 and 6B) that occurs below the Trenton-Maquoketa unconformity (Keith and Wickstrom, 1993; Hohman, 1998) (Figure 15). Presence of these remnant sediments indicates that the trough had already begun to form along structural lines in the Tristate region in mid-Kirkfieldian to late Shermanian time (Figures 5 and 6B). So, although collapse of the Blackriverian carbonate platform and inception of the Sebree Trough are apparent from Rocklandian through much of late Shermanian time, why is there so little record of sedimentation in or near the trough until latest Shermanian or Edenian time? This is an important question, because it is the absence of sedimentation and unconformity development, more than structural reactivation, that defines the Sebree Trough.

Origins

The first changes on the Blackriverian carbonate platform coincided with inception of the Taconic tectophase in Rocklandian time. During this Blackriverian-Rocklandian transition, parts of the peritidal Blackriverian platform collapsed in southern Illinois, southwestern Indiana, and western Kentucky, and were succeeded locally by deeper water, fossiliferous shales and fine-grained carbonates (Decorah Gp.) (Hohman, 1998) and a widespread, regional erosional surface, the Blackriver-Trenton unconformity (Figure 15). At about the same time to the east, an area of major erosion and reduced deposition ensued along a northeast-southwest-trending high in west-central Tennessee, west-central and central Kentucky, south-central Indiana, and southwestern Ohio, called the Curdsville island or Curdsville high (Wilson, 1962; Hohman, 1998). The timing and location of the collapse and erosional trends, as well as the presence of local, low-angle stratal discordance on the unconformity (Kolata et al., 1998a; Hohman, 1998) strongly implicate bulge uplift and moveout, accompanied by reactivation of basement structures, during initiation of the Taconic tectophase (Figure 15). Although Wilson (1962) suggested the necessity of subaerial exposure for unconformity formation, absence of subaerial exposure features on the unconformity suggests that erosion was entirely subaqueous (Cressman, 1973; Kolata et al., 1998a), having been generated by bulge uplift into the surf zone.

The bulge, however, seems to have done more than just generate the Blackriver-Trenton unconformity; it also apparently reactivated many regional structures that served as foundations for the buildup of new carbonate platforms. Uplift on Keweenawan structures in Illinois, Indiana and Ohio and on Iapetan structures in New York formed the basis of the Galena-Trenton Shelf, while uplift on a combination of Keweenawan, Grenvillian, and Iapetan structures provided foundations for the Lexington Platform. When deposition resumed in mid- to late Rocklandian time, relatively thick (7-53 m), shallow-water carbonates (lower Galena Group) developed across the Galena Shelf in off-bulge areas to the northwest, while equivalent carbonates (Curdsville Mbr., Lexington Lms., and equivalents) were absent or thinner (0-8 m) at on-bulge areas that would become the Lexington Platform (Figure 15). Clearly, the thickness and duration of middle Rocklandian through early Kirkfieldian carbonates equivalent to the Curdsville indicate that the off-bulge Galena Shelf was the major focus of deposition at this time (Hohman, 1998) (Figure 15). The facts that the Curdsville and equivalent Trenton thin along an on-bulge trend that parallels northeast-southwest-trending Keweenawan structures (cf. Figure 8 and Hohman, 1998, figure 47), and that Curdsville deposition in the on-bulge, central Kentucky area was largely controlled by reactivated structures (Grossnickle, 1985), suggest that bulge moveout must have reactivated older basement structures that established later patterns of deposition in the area. In fact, regional correlations and cross sections (Hohman, 1998) indicate that the Curdsville and its equivalents are the only parts of the Trenton-Lexington sequence present throughout most of the area of the Sebree Trough in southern Indiana, western Kentucky and southwestern Ohio.

and the sediment starvation in the trough would have encouraged mineralization of the surface in the decreasing-pressure and increasing-temperature conditions encountered as Ouachita bottom waters moved higher onto the craton. In fact, the phosphorite-rich nature of the Lexington Limestone and equivalents on the Nashville Dome probably reflects upwelling of trough waters onto nearby parts of the Lexington Platform (Wilson, 1962; Cressman, 1973) (Figure 17).

Major sedimentation in the Sebree Trough did not begin until latest Shermanian or earliest Edenian time. Before this, the trough area had mainly experienced sediment starvation, possibly enhanced by an episode of late Shermanian sea-level drop (e.g., Diecchio and Broderson, 1994; Ross and Ross, 1995; Holland, 1993; Pope and Read, 1997a,b). By latest Shermanian time, however, the region apparently experienced abrupt deepening, tilting and local structural reactivation, and this, combined with a nearly filled foreland basin, allowed siliciclastic sediments to be shunted across the basin onto the Lexington Platform and into the Sebree Trough. On the platform, these siliciclastics inundated former shallow-water carbonate environments, and they are represented by fossiliferous, gray interbedded shales and fine-grained limestones of the Clays Ferry and Kope formations (Figures 11, 12 and 15), deposited in deeper, oxic conditions. In the Sebree Trough, siliciclastics are represented by the dark, poorly fossiliferous "Utica" and Maquoketa shales (Figures 6B, 7B, 12 and 15), basal parts of which must represent even deeper, oxygen-deficient, dysoxic to anoxic conditions. In the Tristate area, tongues of this dark shale lap onto the Lexington Platform as the Bromley Shale and Fulton Submember of the Kope Formation (Brett and Algeo, 1999) (Figure 6B). Inasmuch as apparently equivalent tongues of the Clays Ferry Formation lap onto the Tanglewood buildup to the south at about the same times (Figures 11 and 12) (Cressman, 1973; Ettensohn, 1992), respective tongues of shale probably reflect brief periods of rapid sea-level rise.

In the face of rising sea level and inundation by siliciclastic sediments from the east, shallow-water carbonate deposition on the Lexington Platform became centered on the Tanglewood buildup until mid-Edenian time (Figures 12 and 15). The fact that buildup margins coincide with structural lineaments (Figures 8, 10 and 14) suggests that uplift related to reactivation of structures was responsible for continuation of shallow-water carbonate deposition in this isolated area (Ettensohn, 1992; Ettensohn and Kulp, 1995). Moreover, this buildup apparently served as the source for the package of finer grained Point Pleasant carbonates transported north toward the trough (Figures 6B and 12) as distal tempestites by storm currents. Most of these distal carbonates were dumped in a structurally defined northwest-southeast-oriented low area on the margin of the trough called the Pt. Pleasant Basin by Wickstrom and others (1992) (Figure 4).

Implications

Much of what we have suggested for the origin of the Sebree Trough and Lexington Platform, as well as for other features on the platform, is related to the apparent reactivation of foreland basement structures during the Taconian Orogeny. Although the concept of far-field, foreland responses to carton-margin orogeny has only been recognized in the United States for the last 30 years, such responses have been widely recognized in Europe and Asia as an integral part of orogenic complexes since the pioneering work of Stille (1920) and subsequent modifications by Sengör (1984) based on work in the classic Alpine, Cimmeride, and Himalayan orogenic complexes. The reactivation of older basement structures, as is proposed here, is a common foreland response to craton-margin orogenies and is widely reported from other craton-orogen settings (Ziegler, 1978, 1987; Gordon and Hempton, 1986; Sanford, 1987; Zalán and others, 1991; Holbrook, 1993; Sengör, 1984; Leighton, 1996). Hence, on eastern parts of the Middle and Late Ordovician Laurentian craton where Keweenawan, Grenvillian, and Iapetan basement structures abound and where major phases of the Taconian Orogeny were ongoing, there is little reason to sus-

Logana and Brannon members in part probably reflect such high-stand periods, and the otherwise argillaceous nature of many Lexington platform carbonates indicates that the platform successfully intercepted the westward influx of siliciclastics. So not only were waters in the Sebree Trough too deep for carbonate sedimentation, but they were also largely bereft of siliciclastic influx because of intervening foreland-basin and platform sediment sinks.

The resulting sediment starvation and deepening waters easily explain the shut-down of sedimentation in the early Sebree Trough. This shut-down is represented by a pyritic/phosphoritic hardground or corrosion surface with several centimeters of relief or by lag deposits of phosphorite clasts on the Trenton-Maquoketa unconformity (Fara and Keith, 1989; Keith and Wickstrom, 1995; Kolata and others, 1998b) that apparently reflects most of mid-Kirkfieldian to late Shermanian time (Figure 15). Latest Shermanian to Edenian shales and fine-grained carbonates of the Maquoketa, "Utica," Kope, Bromley, and Pt. Pleasant formations may sharply overlie this surface in and near the trough (Figures 5, 6B and 15). The same pyritic and phosphoritic surface rises onto the Tanglewood buildup below the Sulphur Well and equivalent members in the Lexington Limestone (Hohman, 1998) and disappears in a conformable succession of the coarse-grained Tanglewood limestones (Figures 5 and 15). Several other mineralized, hardgrounds occur below the Sulphur Well surface, and they may merge northwestwardly with the main surface in the trough.

Although the absence of Trenton section below the unconformity/corrosion surface has been ascribed to subaerial erosion (Rooney, 1966), the presence of marine trace-fossil bores on the surface, the absence of karstic or other subaerial features, and the presence of mineralized crusts typical of marine environments largely preclude this possibility (Fara and Keith, 1989; Keith and Wickstrom, 1993; Kolata and others, 1998b). However, an intricately scalloped surface with centimeters of relief (Keith and Wickstrom, 1993), bores and encrustations suggest the combined effects of bioerosion and submarine, chemical corrosion along this surface (Willman and Kolata, 1978; Keith and Wickstrom, 1993; Kolata and others, 1998b).

To understand how corrosion and encrustation might have happened, it is necessary to examine the Middle Ordovician paleogeography and paleoclimate of Laurentia. At this time, the study area was located south of the paleoequator in the southern trade-wind belt (Scotese and Golonka, 1992) (Figure 17). Prevailing winds and storms would have come from the southeast and approached the Sebree Trough at high angles, but because of Coriolis deflection to the left in the southern hemisphere, the dominant surface currents would have carried shallow foreland waters southwestwardly off the craton into the Ouachita Sea (Figure 17). Eventually, this surface-water movement seems to have generated quasi-estuarine circulation in the study area, drawing cold, mineral-rich, oxygen-poor waters at depth from the Ouachita Sea onto the Laurentian craton (cf. Cressman, 1973) via Reelfoot Rift parts of the Sebree Trough where it apparently met the Ouachita Sea (Figures 1, 8 and 17). Although the trough area probably did not initially have the geometry that we infer for Edenian time (Figure 4), continued upward growth of carbonate platform/shelf areas, abetted by nutrient influx from the trough and by structural reactivation, acted to funnel Ouachita waters at depth between the growing Lexington Platform and Galena Shelf. Carbonate dissolution by the cold bottom waters must have caused much of the corrosion observed on the unconformity, and the periodic input of sands transported from the Lexington Platform by storms may have provided materials for mechanical bottom scour. Hence, the resulting "channel" or "trough" was largely produced during approximately three million years of mid-Kirkfieldian to late Shermanian sediment starvation and corrosion. As the trough became better developed and more canalized by growing platform margins, incoming, northeastwardly directed bottom current velocities would have increased. The combination of high velocity and oxygen-poor waters may explain the near absence of fossil life along this surface,

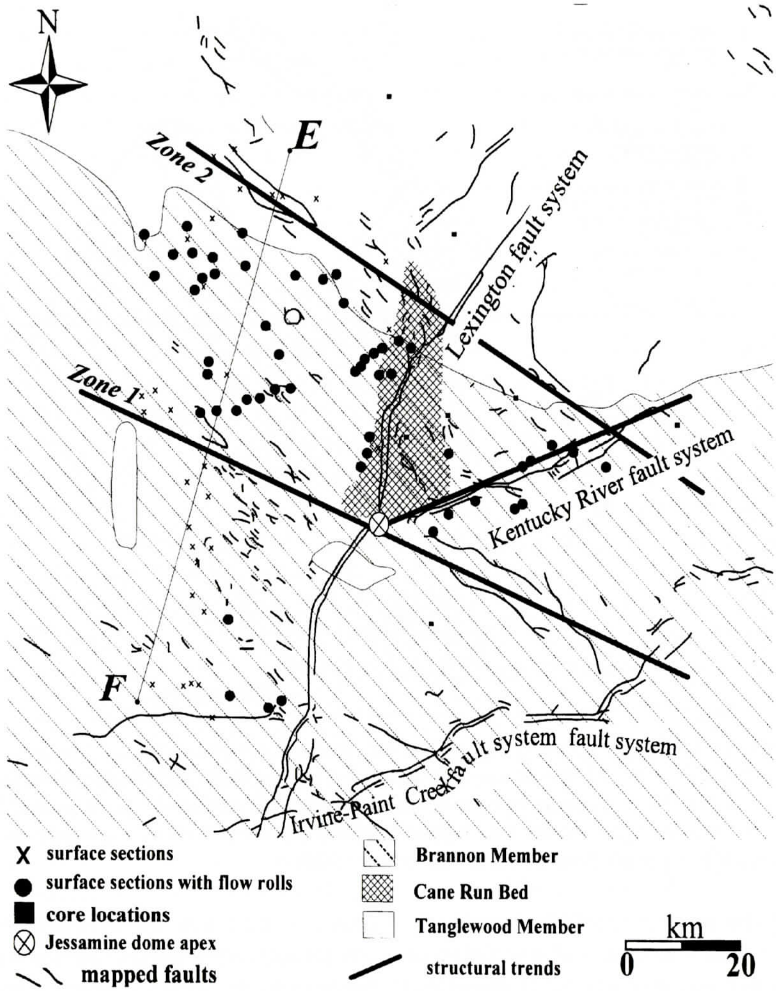

Figure 16. Map of the Jessamine Dome area in central Kentucky, showing the association of Brannon seismites (blackened circles) with fault zones 1 and 2 from Figure 10 and with the Kentucky River Fault Zone. Note that distribution of the Cane Run Bed, a seismically deformed interval in the Lexington Limestone (upper Grier Mbr.), coincides with a segment of the Lexington Fault Zone. Note also that northern limit of Brannon distribution approximately coincides with the northernmost structural trend, fault zone 2 on Figure 10. The northern limit of Brannon distribution reflects the northeasterly pinchout of the member into the Tanglewood seen on Figure 14. Structural trends are defined as lineations along which facies changes coincide with extant fault zones (adapted from Kulp, 1995).

the craton interior, cold water and chemical corrosion insured that no carbonate deposition would occur in the lows, but as these nutrient-rich waters upwelled onto shallower structural highs, they enhanced carbonate buildup along old structural lines and further canalized the trough, where most of this time is represented by a corroded, mineralized omission surface (Trenton-Maquoketa unconformity) (Kolata and others, 1998b). In contrast, trough waters that upwelled onto the Lexington Platform (Figure 17) generated many small, mineralized hardgrounds. However, because the platform was elevated into shallower, warmer waters, many of these minerals were immediately available as nutrients to organisms living there. This scenario not only explains the generally cold-water nature of the fauna (Patzkowsky and Holpect that similar responses were not present. In fact, the Rocklandian to Edenian (mid-late Caradoc) stratigraphic record shows major depositional changes on regional to local scales across the former Blackriverian carbonate platform (Keith, 1989b, figure 2; Ettensohn, 1992; Hohman, 1998) that parallel or coincide with basement structures, suggesting that the stratigraphic differentiation of the platform reflects a coeval structural differentiation (Figure 15). Although stratigraphic differentiation may also partly reflect major eustatic or tectono-eustatic changes at the time (Ross and Ross, 1992, 1995; Patzkowsky and Holland, 1993; Pope and Read, 1997 a, b), the timing, location, and progression of stratigraphic changes relative to foreland, basement structures and concurrent Taconic tectonism (Figures 4 and 8) suggest the likelihood of far-field responses.

Although structural and related facies changes should be expected in proximal parts of the foredeep or foreland basin (Bradley and Kidd, 1991), the most prominent regional changes reported here are in the somewhat distal foreland and involve a change in the tilt of the eastern Laurentian foreland toward the southeast (Droste and Shaver, 1983; Wickstrom and Gray, 1989; Wickstrom and others, 1992; Coakley and Gurnis, 1995) and developments leading to formation of the Sebree Trough in western Kentucky and Tennessee more than 500 km from the orogen. Such responses would have necessitated transmission of stresses across 500 km of the foreland in ways that both modelling and comparative examples suggest can only happen through flexural or far-field interactions between the foreland and an orogen (Karner and Watts, 1983; Gordon and Hempton, 1986; Quinlan, 1987; Ziegler, 1987; Mitrovica and others, 1989; Coakley and Gurnis, 1995; Lowell, 1995).

Ultimately, foreland differentiation brought on by craton-margin orogeny depends in large part on pre-existing intraplate discontinuities (Ziegler, 1987). "Horizontal" discontinuities resulting in thinned or thickened crust and in detachment or decoupling horizons can also control the occurrence and rate of differentiation, but in most cases are difficult to demonstrate. "Vertical" discontinuities, on the other hand, are reflected in better known patterns of basement structural weakness and commonly control surface patterns of far-field response, of which the trough-platform/shelf complex discussed herein is a probable example. The trough-platform complex stretches nearly 1000 km from the Illinois basin area to the Taconic foreland basin as a trend of thickened, deeper water sediment (Keith, 1989b) bound on either side by an older carbonate platform and shelf, largely coinciding with known basement structures (Figure 8). Where the trough is narrow as in southern Indiana (Figure 8), it coincides with narrow Keweenawan rifts, and where it broadens into embayment-like basins as in south-central Ohio (Pt. Pleasant Basin) and western Pennsylvania (Pennsylvanian Embayment) (Figure 4), the trough coincides with "structural embayments" defined by areas where the widened Rome Trough is crossed by Grenvillian structures at high angles (Figure 8). Even the change in trough orientation in northern Ohio (Keith, 1989b) seems related to a major structural discontinuity, the Grenville front, east of which the effect of Keweenawan structures is largely masked and the influence of Grenvillian and Iapetan structures begins. Although subsequent relative sea-level rises have blurred structural boundaries as deeper water sediments lapped out of trough onto adjacent platform margins (Keith, 1989b, figures 4-6), the basic structural outline of the trough-platform/shelf complex and the fact that it roughly parallels the Taconic orogen are still apparent.

However, it is how the trough-platform complex interacted with Laurentian paleogeography and paleoclimate at the time that underscores the importance of its orientation. While the elevated Lexington carbonate platform, along with regional deepening and cratonic tilting, advanced the isolation of the trough area behind it, the configuration of the trough-platform complex combined with Ordovician wind and circulation patterns to develop a quasi-estuarine circulation that funneled cold, mineral-rich, deep-sea waters from the Ouachita Sea into low areas between the two platform/shelf areas. As deep-sea waters followed structural lows into of Ordovician time, the continued high faunal diversity and abundance for which the Tristate area is so famous probably signals the persistence of a low trough area and a resulting quasi-estuarine system that pumped nutrient-rich waters into it.

CONCLUSIONS

The Lexington Platform and Sebree Trough reflect the structural and stratigraphic differentiation of the older, Blackriverian carbonate platform during Rocklandian-to-early Edenian (mid-Caradoc) parts of the Taconic tectophase of the Taconian Orogeny. The fact that many resulting facies changes coincide with basement structures that had little or no surface expression during Ordovician time suggests reactivation through growth faulting at depth. The large area over which these structures were reactivated, the different origins and orientations of basement structures involved, and the fact that trough evolution coincided with and paralleled Taconic, foreland-basin development strongly suggest that parts of trough and platform development must have been related to interaction between basement discontinuities and far-field forces generated by coeval Taconic subduction and transgression.

The interregional extent of the Lexington Platform and Sebree Trough make them some of the most prominent far-field responses to Taconic orogeny, but likely, less extensive, regional and local responses were also present. More restricted events, particularly from late Shermanian through early Edenian time, like tilting and deepening across the Lexington Platform and the concomitant reactivation of basement structures to form the Tanglewood buildup (Figures 5 and 10-12), seem to be characteristic, as on a local scale are facies variations (Figures 13 and 14) and seismites (Figure 16). Admittedly, the smaller and more localized the response, the more difficult it is to relate that response directly to far-field effects. Nonetheless, the diversity of responses (abrupt deepening, uplift along structures, subsidence along others, seismic liquefaction), the fact that various responses were contemporaneous across wide areas during specific intervals of time, as well as the coincidence and repetition of responses along basement structural trends, all provide important support for far-field tectonic effects.

Most responses were dependent on pre-existing zones of basement weakness, but their reactivation was just the initial step in collapse of the Blackriverian carbonate platform. The resulting development of the Galena Shelf, Lexington Platform, and Sebree Trough was sequential (Figure 15) and moderated by the way in which regional tectonic features interacted with the paleogeographic and paleoclimatic setting. Sediment starvation, quasi-estuarine circulation, carbonate corrosion, upwelling, and rapid aggradation of skeletal carbonates on structural highs were all formative processes related to the interaction between far-field tectonism, paleogeography and paleoclimate during Trenton time and are best understood in terms of the prominent Trenton-Maquoketa unconformity. Hence, not only did these interactions control "Trenton" stratigraphic differentiation of the old Blackriverian carbonate platform, but in the process they changed the warm-water, faunal and sedimentary realm of the area to a cold-water realm that endured for the rest of Ordovician time.

Far-field, foreland responses, like those described above, are characteristic of orogenic complexes. Called "Germanotype" deformation by Stille (1920) and compressional foreland deformation by Ziegler (1988), these syn-, late-, and post-orogenic, foreland responses reflect the distal transmission of compressional intraplate stresses across the foreland, commonly facilitated by preexisting zones of basement weakness. Although such responses should be expected in foreland areas, their diversity and abundance in the studied stratigraphic record at regional to local scales suggest the importance of understanding regional and local tectonic frameworks in interpreting stratigraphic sequences. Even locally, facies changes and seismic remobilization of sediments near reactivated structures like those associated with the Tanglewood buildup demonstrate the effects of rapid, short-term changes during syn-sedimentary faulting and the accompanying chang-

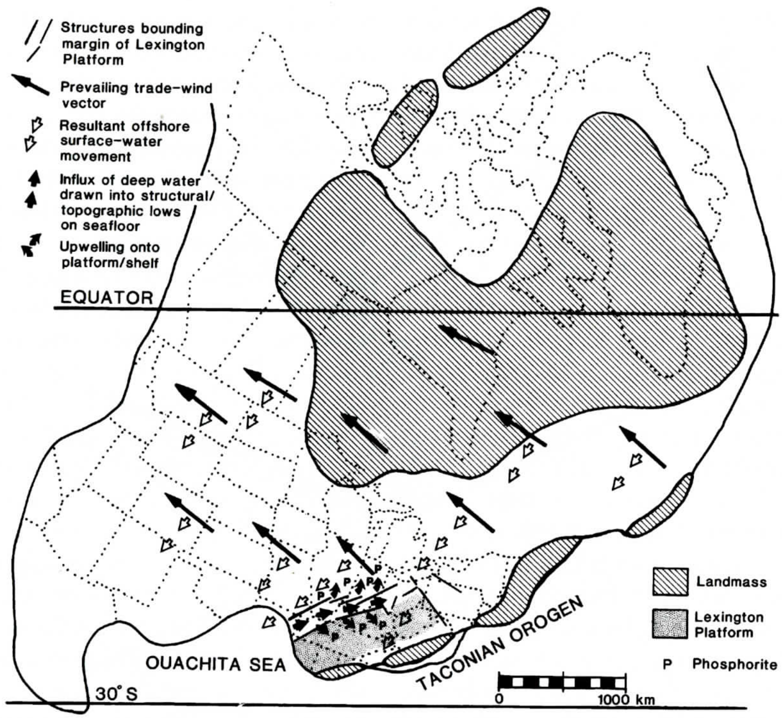

Figure 17. Middle Ordovician paleogeographic reconstruction of Laurentia, showing how resultant surface-water movement (interaction of trade-wind vector and Coriolis force) advanced quasi-estuarine circulation, forcing deep waters northeastward into structural lows (position of Sebree trough) on northern margins of the Lexington Platform to upwell onto the platform and Galena Shelf (paleogeography from Scotese and Golonka, 1992).

land, 1993; Pope and Read, 1997b), but also the high diversity and abundance of that fauna on the platform and the rapid accretion of skeletal sands comprising the platform and the Tanglewood buildup. Even the location of major bryozoan biostromes on the northwestern margin of the buildup (Sulphur Well Mbr., Lexington Lms.; Figures 13 and 14) was probably related to proximity of upwelling.

Major sediment accumulation in the trough, however, was not present until latest Shermanian and Edenian time. Although sub-unconformity facies changes on the northwestern side of the platform (initial Maquoketa; Figures 5, 6B and 15) indicate presence of a trough area during most of Kirkfieldian and Shermanian time, not until latest Shermanian time with the advent of major deepening, far-field tilting, and structural reactivation did siliciclastics begin flooding into the trough from the northeast. The first sediments to infill the trough were dark Maquoketa and Utica shales deposited in deeper, oxygen-deficient waters that initially occupied the trough. By Edenian time, the regressive, relaxational phase of the Taconic tectophase had begun and vast amounts of siliciclastic sediment inundated the foreland (Ettensohn, 1991), first filling the foreland basin and trough and then inundating the Lexington Platform and Galena Shelf (Keith 1989b; Hohman and Keith, 1997a) (Figure 15). As siliciclastics engulfed the platform, only on the Tanglewood buildup did major carbonate sedimentation continue, apparently reflecting continued uplift along reactivated faults (Ettensohn, 1992; Ettensohn and Kulp, 1995) and the rapid aggradation of skeletal carbonates thereon. By late Edenian time, all carbonate-platform sedimentation in the area had been snuffed out, as even the buildup was buried by siliciclastics of Clays Ferry and Kope formations (Figures 5, 11, 12, and 15). Despite ongoing clastic influx for the rest

Paper 768, 61 p.

Cressman, E.R., and Noger, M.C., 1976, Tidal-flat carbonate environments in the High Bridge Group (Middle Ordovician) of central Kentucky: Kentucky Geological Survey Report of Investigations 18, 15 p.

Cuffey, R.J., 1998, An introduction to the type Cincinnatian, *in* Davis, R.A., and Cuffey, R.J., eds., Sampling the layer cake that isn't: The stratigraphy and paleontology of the type Cincinnatian: Ohio Division of Geologic Survey, Guidebook No. 13. 194 p.

Delgado, D.J., 1983, Deposition and diagenesis of the Galena Group in the upper Mississippi Valley, *in* Delgado, D.J., ed., Ordovician Galena Group of the upper Mississippi Valley — deposition, diagenesis, and paleoecology: Guidebook for 13th Annual Field Conference, Great Lakes Section, SEPM, p. A1-A17.

Denison, R.E., Lidiak, E.G., Bickford, M.E., and Kisvarsanyi, E.V., 1984, Geology and geochronology of Precambrian rocks in the Central Interior Region of the United States: U.S. Geological Survey Professional Paper 1241-C, 20 p.

Dewey, J.F., and Burke, K.C.A., 1974, Hot spots and continental breakup: Implications for collisional orogeny: Geology, v. 2, p. 57-60.

Dewey, J.F., and Kidd, W.S.F., 1974, Continental collisions in the Appalachian-Caledonian belt: Variations related to complete and incomplete suturing: Geology, v. 2, p. 543-546.

Diecchio, R.J., and Brodersen, B.T., 1994, Recognition of regional (eustatic?) and local (tectonic?) relative sea-level events in outcrop and gamma-ray logs, Ordovician, West Virginia, *in* Dennison, J.M., and Ettensohn, F.R., eds., Tectonic and eustatic controls on sedimentary cycles: SEPM Concepts in Sedimentology and Paleontology, v. 4, p. 171-180.

Drahovzal, J.A., Harris, D.C., Wickstrom, L.H., Walker, D., Baranoski, M.T., Keith, B., and Furer, L.C., 1992, The East Continental Rift basin: A new discovery: Kentucky Geological Survey Special Publication 18, Series XI, 25 p.

Drake, A.A., Jr., Sinha, A.K., Laird, J., and Guy, R.E., 1989, The Taconic orogen, *in* Hatcher, R.D., Jr., Thomas, W.A., and Viele, G.W., eds., The Appalachian-Ouachita orogen in the United States: Boulder, Colorado, Geological Society of America, The Geology of North America, v. F-2, p. 101-177.

Droste, J.B., and Shaver, R.H., 1983, Atlas of early and middle Paleozoic paleogeography of the southern Great Lakes area: Indiana Geological Survey Special Report 32, 32 p.

Ettensohn, F.R., 1985, The Catskill Delta complex and the Acadian orogeny, *in* Woodrow, D.W., and Sevon, W.D., eds., The Catskill Delta: Geological Society of America Special Paper 201, p. 39-49.

Ettensohn, F.R., 1991, Flexural interpretation of relationships between Ordovician tectonism and stratigraphic sequences, central and southern Appalachians, U.S.A., *in* Barnes, C.R., and Williams, S.H., eds., Advances in Ordovician geology: Geological Survey of Canada Paper 90-9, p. 213-224.

Ettensohn, F.R., 1992, Regressive facies in the upper Lexington Limestone: Tanglewood-Millersburg relationships, *in* Ettensohn, F.R., ed., Changing interpretations in Kentucky geology — layer-cake, facies, flexure, and eustasy: Ohio Division of Geologic Survey Miscellaneous Report No. 5, p. 62-66.

Ettensohn, F.R., 1994, Tectonic control on the formation and cyclicity of major Appalachian unconformities and associated stratigraphic sequences, *in* Dennison, J.M., and Ettensohn, F.R., eds., Tectonic and eustatic controls on sedimentary cycles: SEPM Concepts in Sedimentology and Paleontology, v. 4, p. 217-242.

Ettensohn, F.R., 1999, Taconian far-field effects and the origin of the Middle-Late Ordovician Lexington Platform and the Sebree Trough, east-central United States: Geological Society of America Abstracts with Programs, v. 31, p. A-15.

Ettensohn, F.R., Amig, B.C., Pashin, J.C., Greb, S.F., Harris, M.Q., Black, J C., Cantrell, D.J., Smith, C.A., McMahan, T.M., Axon, A.G., and McHargue, C.J., 1986, Paleoecology and paleoenvironments of the bryozoan-rich Sulphur Well Member, Lexington Limestone (Middle Ordovician), central Kentucky: Southeastern Geology, v. 26, p. 199-219.

Ettensohn, F.R., and Kulp, M.A., 1995, Structural-tectonic control on Middle-Late Ordovician deposition of the Lexington Limestone, central Kentucky, *in* Cooper, J.D., Droser, M.L., and Finney, S.C., eds., Ordovician odyssey: Short papers for the Seventh International Symposium on the Ordovician System: Pacific Section, Society for Sedimentary Geology (SEPM), Book 77, p. 261-264.

Ettensohn, F.R., and Kulp, M.A., 1997, Stratigraphic and structural framework of Granville-like lithologies in the Tanglewood Member, Middle and Upper Ordovician Lexington Limestone, central Kentucky: American Association of Petroleum Geologists Bulletin, v. 81. p. 1549-1550.

Ettensohn, F.R., Kulp, M.A., and Rast, N., 1996, Far-field, foreland responses to Taconian orogeny: Evidence from the Jessamine dome region and the Lexington Limestone, central Kentucky: Geological Society of America Abstracts with Programs, v. 28, p. 52.

Ettensohn, F.R., Rast, N., and Kulp, M.A., 1998, Paleoseismites in the Ordovician Lexington Limestone, central Kentucky: Evidence and implications for marine epicontinental sedimentation: Geological Society of America Abstracts with Programs, v. 30, p. A-399.

Fara, D.R., and Keith, B.D., 1989, Depositional facies and diagenetic history of the Trenton Limestone in northern Indiana, *in* Keith, B.D., ed., The Trenton Group (Upper Ordovician Series) of eastern North America, deposition, diagenesis, and petroleum: American Association of Petroleum Geologists Studies in Geology #29, p. 277-298.

Fisher, D.W., 1977, Correlation of the Hadrynian, Cam-

es in relative sea level. At other scales, however, the interplay between these effects and the ambient paleogeography and paleoclimate may generate impacts far more widespread and intense than the initial reactivation of structures.

ACKNOWLEDGEMENTS

We wish to thank C.E. Brett and K. DeJong for their very helpful comments toward improvement of the manuscript.

REFERENCES CITED

Aigner, T., 1985, Storm depositional systems: Lecture Notes in Earth Sciences, v. 3, Berlin, Springer-Verlag, 174 p.

Anand, A., and Jain, A.K., 1987, Earthquakes and deformation structures (seismites) in Holocene sediments from the Himalayan-Andaman Arc, India: Tectonophysics, v. 133, p. 105-120.

Beaumont, C., 1981, Foreland basins: Geophysical Journal of the Royal Astronomical Society, v. 65, p. 291-329.

Bergström, S.M., and Mitchell, C.E., 1987, Geology of Middle to Upper Ordovician Sebree trough northwest of Cincinnati arch, Ohio, Indiana, and Kentucky [abs.]: American Association of Petroleum Geologists Bulletin, v. 71, p. 1101.

Bergström, S.M., and Mitchell, C.E., 1989, Relations between the Ordovician Trenton Group and associated strata in the northern Appalachian foreland basin - shelf region and their lateral equivalents in the eastern midcontinent, *in* Shumaker, R.C., ed., Spring Program, April, 1989, Appalachian Basin Industrial Associates: Morgantown, West Virginia University, v. 15, p. 7-41.

Bergström, S.M., and Mitchell, C.E., 1990, Trans-Pacific graptolite faunal relations: The biostratigraphic position of the base of the Cincinnatian Series (Upper Ordovician) in the standard Australian graptolite zone succession: Journal of Paleontology, v. 64, p. 992-997.

Bergström, S.M., and Mitchell, C.E., 1992, The Ordovician Utica Shale in the eastern midcontinental region: Age lithofacies, and regional relationships, *in* Chaplin, J.R., and Barrick, J.E., eds., Special papers in paleontology: A special tribute to Thomas W. Amsden: Oklahoma Geological Survey Bulletin 145, p. 67-89.

Bergström, S.M., and Mitchell, C.E., 1994, Regional relationships between late Middle and early Late Ordovician standard successions in New York and Quebec and the Cincinnati region in Ohio, Indiana, and Kentucky, *in* Landing, E., ed., Studies in stratigraphy and paleontology in honor of Donald W. Fisher: New York State Museum Bulletin No. 481, p. 5-20.

Black, D.F.B., 1986, Basement faulting in Kentucky: Proceedings of the Sixth International Conference on Basement Tectonics, p. 125-139.

Black, D.F.B., Cressman, E.R., and MacQuown, W.C., Jr., 1965, The Lexington Limestone (Middle Ordovician) of central Kentucky: U.S. Geological Survey Bulletin 1224-C, 29 p.

Bock, B., McLennan, S.M., and Hanson, G.N., 1996, The Taconian orogeny in southern New England: Nd-isotope evidence against addition of juvenile components: Canadian Journal of Earth Sciences, v. 33, p. 1612-1627.

Borella, P.E., and Osborne, R.H., 1978, Late Middle and early Late Ordovician history of the Cincinnati arch Province, central Kentucky to central Tennessee: Geological Society of America Bulletin, v. 89, p. 1559-1573.

Bradley, D.C., 1989, Taconic plate kinematics as revealed by foredeep stratigraphy, Appalachian orogen: Tectonics, v. 8, p. 1037-1049.

Bradley, D.C., and Kidd, W.S.F., 1991, Flexural extension of the upper continental crust in collisional foredeeps: Geological Society of America Bulletin, v. 103, p. 1416-1438.

Bradley, D.C., and Kusky, T.M., 1986, Geologic evidence for rate of plate convergence during the Taconic arc-continent collision: Journal of Geology, v. 94, p. 667-681.

Brett, C.E., and Algeo, T.J., 1999, Stratigraphy of the Upper Ordovician Kope Formation in its type area (northern Kentucky) including a revised nomenclature, *in* Algeo, T.J., and Brett, C.E., eds., Sequence, cycle & event stratigraphy of Upper Ordovician & Silurian strata of the Cincinnati Arch region: Field Trip Guidebook, 1999 SEPM-GLS/KSPG Field Conference, Cincinnati, University of Cincinnati, p. 47-64.

Brown, G.D., Jr., and Lineback, J.A., 1966, Lithostratigraphy of the Cincinnatian Series (Upper Ordovician) in southeastern Indiana: American Association of Petroleum Geologists Bulletin, v. 50, p. 1018-1023.

Byers, C.W., 1977, Biofacies patterns in euxinic basins: A general model: Society of Economic Paleontologists and Mineralogists Special Paper No. 25, p. 5-17.

Calvert, W.L., 1962, Sub-Trenton rocks from Lee County, Virginia, to Fayette County, Ohio: Ohio Division of Geological Survey Report of Investigations 45, 57 p.

Cameron, B., and Mangion, S., 1977, Depositional environments and revised stratigraphy along the Black River-Trenton boundary in New York and Ontario: American Journal of Science, v. 277, p. 486-502.

Coakley, B., and Gurnis, M., 1995, Far-field tilting of Laurentia during the Ordovician and constraints on the evolution of a slab under an ancient continent: Journal of Geophysical Research, v. 100, p. 6313-6327.

Colton, G.W., 1970, The Appalachian basin — its depositional sequences and their geologic relationships, *in* Fisher, G.W., Pettijohn, F.J., Reed, J.C., and Weaver, K.N., eds., Studies of Appalachian geology: New York, Interscience Publishers, p. 5-47.

Cressman, E.R., 1973, Lithostratigraphy and depositional environments of the Lexington Limestone (Ordovician) of central Ohio: U.S. Geological Survey Professional

Wilson, J.L., and Yurewicz, D.A., eds., Paleokarst related hydrocarbon reservoirs: SEPM Core Workshop No. 18, p. 167-179.

Klein, G.D., 1994, Depth determination and quantitative distinction of the influence of tectonic subsidence and climate on changing sea level during deposition of Mid-continent Pennsylvanian cyclothems, *in* Dennison, J.M., and Ettensohn, F.R., eds., Tectonic and eustatic controls on sedimentary cycles: SEPM Concepts in Sedimentology and Paleontology, v. 4, p. 35-50.

Knight, I., James, N.P., and Lane, T.E., 1991, The Ordovician St. George unconformity, northern Appalachians: The relationship of plate convergence at the St. Lawrence Promontory to the Sauk/Tippecanoe sequence boundary: Geological Society of America Bulletin, v. 103, p. 1200-1225.

Kolata, D.R., Huff, W.D., and Bergström, S.M., 1998a, Nature and regional significance of unconformities associated with the Middle ordovician Hagan K-bentonite complex: Geological Society of America Bulletin, v. 110, p. 723-739.

Kolata, D.R., Huff, W.D., and Bergström, S.M., 1998b, Carbonate starvation events in the Illinois Basin during the Middle Ordovician: Geological Society of America Abstracts with Programs, v. 30, p. A-316.

Kolata, D.R., and Nelson, W.J., 1990, Tectonic history of the Illinois Basin, *in* Leighton, M.W., Kolata, D.R., Oltz, D.F., and Eidel, J.J., eds.,Interior cratonic basins: American Association of Petroleum Geologists Memoir 51, p. 263-285.

Kolata, D.R., and Nelson, W.J., 1997, Role of the Reelfoot Rift/Rough Creek Graben in the evolution of the Illinois Basin, *in* Ojakangas, R.W., Cickas, A.B., and Green, J.C., eds., Middle Proterozoic to Cambrian rifting, central North America, Geological Society of America Special Paper 312, p. 287-298.

Kolata, D.R., and Noger, M.C., 1990, Tippecanoe I Subsequence, Middle and Upper Ordovician series, *in* Leighton, M.W., Kolata, D.R., Oltz, D.F., and Eidel, J.J., eds.,Interior cratonic basins: American Association of Petroleum Geologists Memoir 51, p. 89-99.

Kulp, M. A., 1995, Paleoenvironmental interpretation of the Brannon Member of Middle-Upper Ordovician Lexington Limestone, central Bluegrass region of Kentucky [M.S. thesis]: Lexington, University of Kentucky, 222 p.

Lehmann, D., Brett, C.E., and Cole, R., 1994, Tectonic and eustatic influences upon the sedimentary environments of the Upper Ordovician strata of New York and Ontario, *in* Dennison, J.M., and Ettensohn, F.R., eds., Tectonic and eustatic controls on sedimentary cycles: SEPM Concepts in Sedimentology and Paleontology, v. 4, p. 181-201.

Leighton, M.W., 1996, Interior cratonic basins: A record of regional tectonic influence, *in* van der Pluijm, B.A., and Catacosinos, P.A., eds., Basement and basin of eastern North America: Geological Society of America Special Paper 308, p. 77-93.

Lowell, J.D., 1995. Mechanics of basin inversion from worldwide examples, *in* Buchanan, J.G., and Buchanan, P.G., eds., Basin inversion: Geological Society Special Publication No. 88, p. 39-57.

Mackey, R.T., 1972, Lithostratigraphy and depositional environments of the Perryville Limestone and related members of the lower Lexington Limestone [M.S. thesis]: Lexington, University of Kentucky, 94 p.

Mac Niocaill, C., van der Pluijm, B.A., and Van der Voo, R., 1997, Ordovician paleogeography and the evolution of the Iapetus ocean: Geology, v. 25, p. 159-162.

McKerrow, W.S., Dewey, J.F., and Scotese, C.R., 1991, The Ordovician and Silurian development of the Iapetus Ocean, *in* Basset, M.G., Lane, P.D., and Edwards, D., eds., The Murchison Symposium: Proceedings of an international conference on the Silurian System: Special Papers in Paleontology, v, 44, p. 165-178.

Meckel, L.D., 1970, Paleozoic alluvial deposition in the central Appalachians: A summary, *in* Fisher, G.W., Pettijohn, F.J., Reed, J.C., and Weaver, K.N., eds., Studies of Appalachian geology: New York, Interscience Publishers, p. 49-67.

Mitchell, C.E., and Bergström, S.M., 1991, New graptolite and lithostratigraphic evidence from the Cincinnati region, U.S.A., for the definition and correlation of the base of the Cincinnatian Series (Upper Ordovician), *in* Barnes, C.R., and Williams, S.H., eds., Advances in Ordovician geology: Geological Survey of Canada Paper 90-9, p. 59-77.

Mitchell, C.E., Bergström, S.M., and Schumacher, G.A., 1997, Stratigraphic sequences of the Sebree Trough and Jessamine Dome as an expression of basement reactivation during the Taconic Orogeny: Geological Society of America Abstracts with Programs, v. 29, p. 61.

Mitchell, C.E., Goldman, D., Delano, J.W., Samson, S.D., and Bergström, S.M., 1994, Temporal and spatial distribution of biozones and facies relative to geochemically correlated K-bentonites in the Middle Ordovician Taconic foredeep: Geology, v. 22, p. 715-718.

Mitrovica, J.X., Beaumont, C., and Jarvis, G.T., 1989, Tilting of continental interiors by the dynamical effects of subduction: Tectonics, v. 8, p. 1079-1094.

Norby, R.D., 1990, Biostratigraphic zones in the Illinois Basin, *in* Leighton, M.W., Kolata, D.R., Oltz, D.F., and Eidel, J.J., eds.,Interior cratonic basins: American Association of Petroleum Geologists Memoir 51, p. 179-194.

Obermeier, S.F., 1996, Use of liquefaction-induced features for paleoseismic analysis — An overview of how seismic liquefaction features can be distinguished from other features and how their regional distribution and properties of source sediment can be used to infer the location and strength of Holocene paleo-earthquakes: Engineering Geology, v. 44, p. 1-76.

Patchen, D.G., Avary, K.L., and Erwin, R.B., 1985a, Northern Appalachian region: American Association of Petroleum Geologists COSUNA Chart NAP.

Patchen, D.G., Avary, K.L., and Erwin, R.B., 1985b, South-brian, and Ordovician rocks in New York State: New York State Museum Map and Chart Series No. 25.

Freeman, L.B., 1953, Regional subsurface stratigraphy of the Cambrian and Ordovician in Kentucky and vicinity: Kentucky Geological Survey, Series IX, Bulletin No. 12, 352 p.

Furer, L.C., 1996, Basement tectonics in the southeastern part of the Illinois basin and its effect on Paleozoic sedimentation, *in* van der Pluijm, B.A., and Catacosinos, P.A., eds., Basement and basins of eastern North America: Geological Society of America Special Paper 308, p. 109-126.

Goodman, W.M., and Brett, C.E., 1994, Roles of eustasy and tectonics in development of Silurian stratigraphic architecture of the Appalachian foreland basin, *in* Dennison, J.M., and Ettensohn, F.R., eds., Tectonic and eustatic controls on sedimentary cycles: SEPM Concepts in Sedimentology and Paleontology, v. 4, p. 147-169.

Gordon, M.B., and Hempton, M.R., 1986, Collision-induced rifting: The Grenville orogeny and the Keweenawan rift of North America: Tectonophysics, v. 127, p. 1-25.

Gray, H.H., 1972, Lithostratigraphy of the Maquoketa Group (Ordovician) in Indiana: Indiana Geological Survey Special Report 7, 31 p.

Grossnickle, E.A., 1985, Tempestites and depositional interpretations of the Middle Ordovician Curdsville Limestone of central Kentucky [M.S. thesis]: Lexington, University of Kentucky, 107 p.

Guiraud, M., and Plaziat, J.-C., 1993, Seismites in the fluviatile Bima sandstones: Identification of paleoseisms and discussion of their magnitudes in a Cretaceous synsedimentary strike-slip basin (Upper Benue, Nigeria): Tectonophysics, v. 225, p. 493-522.

Gutstadt, A.M, 1958a, Cambrian and Ordovician stratigraphy and oil and gas possibilities in Indiana: Indiana Geological Survey Bulletin 14, 103 p.

Gutstadt, A.M., 1958b, Upper Ordovician stratigraphy in eastern interior region: American Association of Petroleum Geologists Bulletin, v. 42, p. 513-547.

Harland, W.B., Armstrong, R.L., Cox, A.V., Craig, L.E., Smith, A,G., and Smith, D.G., 1989, A geologic time scale: Cambridge, Cambridge University Press, 263 p.

Hibbard, J., 2000, Docking Carolina: Mid-Paleozoic accretion in the southern Appalachians: Geology, v. 28, p. 127-130.

Hiscott, R.N., 1984, Ophiolitic source rocks for Taconic-age flysch: Trace-element evidence: Geological Society of America Bulletin, v. 95, v. 1261-1267.

Hiscott, R.N., Pickering, K.T., and Beeden, D.R., 1986, Progressive filling of a confined Middle Ordovician foreland basin associated with the Taconic orogeny, Quebec, Canada: Special Publications of the International Association of Sedimentologists, v. 8, p. 309-325.

Hohman, J.C., 1998, Depositional history of the Upper Ordovician Trenton Limestone, Lexington Limestone, Maquoketa Shale and equivalent lithologic units in the Illinois Basin: An application of carbonate and mixed carbonate - siliciclastic sequence stratigraphy [Ph.D. dissertation]: Bloomington, Indiana University, 186 p.

Hohman, J.C., and Keith, B.D., 1997a, Buried Alive! The demise of the Upper Ordovician carbonate platform in the Illinois Basin and Cincinnati Arch areas: American Association of Petroleum Geologists Bulletin, v. 81, p. 1554.

Hohman, J.C., and Keith, B.D., 1997b, The Sebree Trough - did it really exist? Upper Ordovician sequence stratigraphy provides an answer: American Association of Petroleum Geologists Bulletin, v. 81, p. 1554.

Holbrook, J.M., 1993, Evidence for and potential tectonic origin of regional intraplate deformation throughout the Early Cretaceous United States western interior: Geological Society of America Abstracts with Programs, v. 25, p. A-70.

Holland, S.M., 1993, Sequence stratigraphy of a carbonate-clastic ramp: The Cincinnatian Series (Upper Ordovician) in its type area: Geological Society of America Bulletin, v. 105, p. 306-322.

Jacobi, R.D., 1981, Peripheral bulge — a causal mechanism for the Lower/Middle Ordovician disconformity along the western margin of the northern Appalachians: Earth and Planetary Science Letters, v. 56, p. 245-251.

Jewell, H.E., 2001, The origin of the Cane Run Bed, Lexington Limestone, central Kentucky [M.S. thesis]: Lexington, University of Kentucky, 170 p.

Karner, G.D., and Watts, A.B., 1983, Gravity anomalies and flexure of the lithosphere at mountain ranges: Journal of Geophysical Research, v. 88 (B12), p. 10449-10477.

Kasl, J.M., 2001, The nature and origin of the Devils Hollow Member, Lexington Limestone, central Kentucky [M.S. thesis]: Lexington, University of Kentucky, 209 p.

Kay, M., 1937, Stratigraphy of the Trenton Group: Geological Society of America Bulletin, v. 48, p. 233-302.

Kay, M., 1969, Introduction, *in* Kay, M., ed., North Atlantic geology and continental drift, a symposium: American Association of Petroleum Geologists Memoir 12, p. 3-4.

Kay, M., and Colbert, E.H., 1965, Stratigraphy and life History: New York, John Wiley & Sons, Inc., 736 p.

Keith, B.D., 1985, Facies, diagenesis, and the upper contact of the Trenton Limestone of northern Michigan: Michigan Basin Geological Society Special Paper No. 4, p. 15-32.

Keith, B.D., ed., 1989a, The Trenton Group (Upper Ordovician Series) of eastern North America, deposition, diagenesis, and petroleum: American Association of Petroleum Geologists Studies in Geology #29, 317 p.

Keith, B.D., 1989b, Regional facies of the Upper Ordovician Series of eastern North America, *in* Keith, B.D., ed., The Trenton Group (Upper Ordovician Series) of eastern North America, deposition, diagenesis, and petroleum: American Association of Petroleum Geologists Studies in Geology #29, p. 1-16.

Keith, B.D., and Wickstrom, L.H., 1993, Trenton Limestone — the karst that wasn't there, or was it?, *in* Fritz, R.D., graphic atlas: Paleomap Progress Report #20, Arlington, University of Texas at Arlington.

Seilacher, A., 1969, Fault-graded beds interpreted as seismites: Sedimentology, v. 13, p.155-159.

Seilacher, A., 1984, Sedimentary structures tentatively attributed to seismic events: Marine Geology, v. 55, p. 1-12.

Sengör, A.M.C., 1984, The Cimmeride orogenic system and the tectonics of Eurasia: Geological Society of America Special Paper 195, 82 p.

Shanmugam, G., 1977, Shelf to basinal sequences at Boyds Creek, *in* Ruppel, S.C., and Walker, K.R., eds., The ecostratigraphy of the Middle Ordovician of the southern Appalachians (Kentucky, Tennessee, and Virginia), U.S.A.: A field excursion: University of Tennessee Department of Geological Sciences Studies in Geology No. 77-1, p. 106-117.

Shanmugam, G., and Lash, G.G., 1982, Analogous tectonic evolution of the Ordovician foredeeps, southern and central Appalachians; Geology, v. 10, p. 562-566.

Shanmugam, G., and Walker, K.R., 1980, Sedimentation, subsidence, and evolution of a foredeep basin in the Middle Ordovician, southern Appalachians: American Journal of Science, v. 280, p. 479-496.

Shanmugam, G., and Walker, K.R., 1983, Anatomy of the Middle Ordovician Sevier Shale basin, eastern Tennessee: Sedimentology, v. 34, p. 315-337.

Shaver, R.H., 1985, Midwestern basin and arches region: American Association of Petroleum Geologists COSUNA Chart MBA.

Shaver, R.H., and 16 others, 1986, Compendium of Paleozoic rock-unit stratigraphy in Indiana — a revision: Indiana geological Survey Bulletin 59, 203 p.

Shumaker, R.C., 1986, Structural development of Paleozoic continental basins of eastern North America: Proceedings of the Sixth International Conference on Basement Tectonics, p. 82-95.

Shumaker, R.C., and Wilson, T.H., 1996, Basement structure of the Appalachian foreland in West Virginia: Its style and effect on sedimentation, *in* van der Pluijm, B. A., and Catacosinos, P. A., eds., Basement and basin of eastern North America: Geological Society of America Special Paper 308, p. 139-155.

Sibson, R.H., 1995, Selective fault reactivation during basin inversion: Potential for fluid redistribution through fault-valve action, *in* Buchanan, J.G., and Buchanan, P.G., eds., Basin inversion: Geological Society Special Publication No. 88, p. 3-19.

Sims, J.D., 1973, Earthquake-induced sedimentary structures in Van Norman Lake, San Fernando, California: Geological Society of America Abstracts with Programs, v. 5, p. 107-108.

Stark, T.J., 1997a, The East Continental Rift Complex: evidence and conclusions, *in* Ojakangas, R.W., Cickas, A.B., and Green, J.C., eds., Middle Proterozoic to Cambrian rifting, central North America, Geological Society of America Special Paper 312, p. 253-266.

Stark, T.J., 1997b, The English graben: A possible Precambrian rift segment of the eastern Midcontinent, *in* Ojakangas, R.W., Cickas, A.B., and Green, J.C., eds., Middle Proterozoic to Cambrian rifting, central North America, Geological Society of America Special Paper 312, p. 267-285.

Stearns, R.G., and Reesman, A.L., 1986, Cambrian to Holocene structural and burial history of the Nashville dome: American Association of Petroleum Geologists Bulletin, v. 70, p. 143-154.

Stille, H., 1920, Über Alter und Art der Phasen varischer Gebirgsbildung: Nachrichten der königlichen Gesellschaft der Wissenschaften zu Göttingen, mathematische-physikalische Klasse, 1920, p. 218-224.

Sweet, W.C., 1979, Conodonts and conodont biostratigraphy of post-Tyrone Ordovician rocks of the Cincinnati region: U.S. Geological Survey Professional Paper 1066-G, 26 p.

Sweet, W.C., and Bergström, S.M., 1971, The American Upper Ordovician standard: XIII A revised time-stratigraphic classification of North American upper Middle and Upper Ordovician rocks: Geological Society of America Bulletin, v. 82, p. 613-628.

Templeton, J.S., and Willman, H.B., 1963, Champlainian Series (Middle Ordovician) in Illinois: Illinois State Geological Survey Bulletin 89, 260 p.

Tullo, R.P., and Aleinikoff, J.N., 1996, Petrology and U-Pb geochronology of the Robertson River Igneous Suite, Blue Ridge province, Virginia — evidence for multistage magmatism associated with an early stage of Laurentian rifting: American Journal of Science, v. 296, p. 1045-1090.

Vick, H.K., Channell, J.E.T., and Opdyke, N.D., 1987, Ordovician docking of the Carolina Slate Belt: Paleomagnetic data: Tectonics, v. 6, p. 573-583.

Webby, B.D., 1995, Towards an Ordovician time scale, *in* Cooper, J.D., Droser, M.L., and Finney, S.C., eds., Ordovician odyssey: Short papers for the Seventh International Symposium on the Ordovician System: Pacific Section, Society for Sedimentary Geology (SEPM), Book 77, p. 5-9.

Weir, G.W., Peterson, W.L., and Swadley, W.C., 1984, Lithostratigraphy of Upper Ordovician strata exposed in Kentucky. Geological Survey Professional Paper, 1151-E, 121 p.

Wickstrom, H.H., 1996, Play MOf: Middle Ordovician fractured carbonates, *in* Roen, J.B., and Walker, B.J., eds., The atlas of major Appalachian gas plays: West Virginia Geological and Economic Survey Publication V-25, p. 172-176.

Wickstrom, L.H., and Gray, J.D., 1989, Geology of the Trenton Limestone in northwestern Ohio, *in* Keith, B.D., ed., The Trenton Group (Upper Ordovician Series) of eastern North America, deposition, diagenesis, and petroleum: American Association of Petroleum Geologists Studies in Geology #29, p. 159-172.

Wickstrom, L.H., Gray, J.D., and Stieglitz, R.D., 1992, Stratigraphy, structure, and production history of the Trenton Limestone (Ordovician) and adjacent strata in ern Appalachian region: American Association of Petroleum Geologists COSUNA Chart SAP.

Patzkowsky, M.E., and Holland, S.M., 1993, Biotic response to a Middle Ordovician paleoceanographic event in eastern North America: Geology, v. 21, p. 619-622.

Pollock, S.J., 1989, Mélanges and olistostromes associated with ophiolitic metabasalts and their significance in Cambro-Ordovician forearc accretion in the northern Appalachians, *in* Horton, J.W., Jr., and Rast, N., eds., Mélanges and olistostromes of the U.S. Appalachians: Geological Society of America Special Paper 228, p. 43-64.

Pope, M.C., and Read, J.F., 1997a, High-resolution surface and subsurface sequence stratigraphy of late Middle to Late Ordovician (Late Mohawkian-Cincinnatian) foreland basin rocks, Kentucky and Virginia: American Association of Petroleum Geologists Bulletin, v. 81, p. 1866-1893.

Pope, M.C., and Read, J.F., 1997b, High-resolution stratigraphy of the Lexington Limestone (Late Middle Ordovician), Kentucky, U.S.A.: A cool-water carbonate-clastic ramp in a tectonically active foreland basin, *in* James, N.P., and Clarke, J.A.D., eds., Cool-water carbonates: SEPM Special Publication No. 56, p. 411-429.

Pope, M.C., Read, J.F., Bambach, R., and Hofmann, H.J., 1997, Late Middle to Late Ordovician seismites of Kentucky, southwest Ohio and Virginia: Sedimentary recorders of earthquakes in the Appalachian basin: Geological Society of America Bulletin, v. 109, p. 489-503.

Quinlan, G.M., 1987, Models of subsidence mechanisms in intracratonic basins and their applicability to North American examples, *in* Beaumont, C., and Tankard, A. J., eds., Sedimentary basins and basin-forming mechanisms: Canadian Society of Petroleum Geologists Memoir 12, p. 483-505.

Quinlan, G.M., and Beaumont, C., 1984, Appalachian thrusting, lithospheric flexure, and the Paleozoic stratigraphy of the eastern interior of North America: Canadian Journal of Earth Science, v. 21, p. 973-996.

Rast, N., and Ettensohn, F.R., 1995, Effects of seismic disturbance on epicontinental depositional systems in the Ordovician and Devonian rocks of central Kentucky: Geological Society of America Abstracts with Programs, v. 27, p. A-381.

Rast, N., and Ettensohn, F.R., 1999, Far-field orogenic effects at convergent boundaries of cratons — Laurentian-Iapetus border during Taconian orogeny: Geological Society of America Abstracts with Programs, v. 331, p. A-475.

Rast, N., Ettensohn, F.R., and Rast, D.E., 1999, Taconian seismogenic deformation in the Appalachian Orogen and the North American craton, *in* Mac Niocaill, C., and Ryan, P.D., eds., Continental tectonics: London, Geological Society Special Publication 164, p. 127-137.

Rast, N., and Goodmann, P.T., 1994, Tectonic and sedimentary consequences of Late Proterozoic and early and mid-Paleozoic overthrusting in Kentucky and adjacent states: Northeastern Geology, v. 17, p. 2-9.

Rhoads, D.C., and Morse, J.W., 1971, Evolutionary and ecologic significance of oxygen-deficient basins: Lethaia, v. 4, p. 413-438.

Rodgers, J., 1970, The tectonics of the Appalachians: New York, Wiley-Interscience, 271 p.

Rodgers, J., 1971, The Taconic Orogeny: Geological Society of America Bulletin, v. 82, p. 1141-1178.

Roen, J.B., and Walker, B.J., eds., 1996, The atlas of major Appalachian gas plays: West Virginia Geological and Economic Survey Publication V-25, 201 p.

Rooney, L.F., 1966, Evidence of unconformity at the top of Trenton Limestone in Indiana and adjacent states: American Association of Petroleum Geologists Bulletin, v. 50, p. 533-546.

Root, S., 1996, Recurrent basement faulting and basin evolution, West Virginia and Ohio: The Burning Springs-Cambridge fault zone, *in* van der Pluijm, B.A., and Catacosinos, P.A., eds., Basement and basin of eastern North America: Geological Society of America Special Paper 308, p. 127-137.

Ross, C.A., and Ross, J.R.P., 1995, North American Ordovician depositional sequences and correlations, *in* Cooper, J.D., Droser, M.L., and Finney, S.C., eds., Ordovician odyssey: Short papers for the Seventh International Symposium on the Ordovician System: Pacific Section, Society for Sedimentary Geology (SEPM), Book 77, p. 309-313.

Ross, J.R.P., and Ross, C.A., 1992, Ordovician sea-level fluctuations, *in* Webby, B.D., and Laurie, J.R., eds., Global perspectives on Ordovician geology: Rotterdam, A. A. Balkema, p. 327-335.

Ryder, R.T., 1991, Stratigraphic framework of Cambrian and Ordovician rocks in the central Appalachian basin from Richland County, Ohio, to Rockingham County, Virginia: U.S. Geological Survey Miscellaneous Investigation Series Map I-2264.

Ryder, R.T., 1992, Stratigraphic framework of Cambrian and Ordovician rocks in the central Appalachian basin from Lake County, Ohio, to Juniata County, Pennsylvania: U.S. Geological Survey Miscellaneous Investigation Series Map I-2200.

Ryder, R.T., Harris, A.G., and Repetski, J.E., 1992, Stratigraphic framework of Cambrian and Ordovician rocks in the central Appalachian basin from Medina County, Ohio, through southwestern and south-central Pennsylvania to Hampshire County, West Virginia: U.S. Geological Survey Bulletin 1839-K, 32 p.

Sanford, B.V., 1987, Paleozoic geology of the Hudson platform, *in* Beaumont, C., and Tankard, A.J., eds., Sedimentary basins and basin-forming mechanisms: Canadian Society of Petroleum Geologists Memoir 12, p. 483-505.

Schwalb, H., 1980, Hydrocarbon entrapment along a Middle Ordovician disconformity: Kentucky Geological Survey, Series XI, Special Publication 2, p. 35-41.

Scotese, C.R., and Golonka, J., 1992, Paleomap paleogeo-

SOUTHEASTERN GEOLOGY
V. 41, No. 1, March 2002, p. 37-62

GEOCHEMISTRY AND PETROLOGY OF CRYSTALLINE BASEMENT BENEATH COASTAL PLAIN SEDIMENTS AT THE SAVANNAH RIVER SITE, SOUTH CAROLINA, U.S.A.

MICHAEL RODEN

(mroden@gly.uga.edu)
Department of Geology,
University of Georgia,
Athens, GA 30602

TIMOTHY E. LA TOUR

(geotel@panther.gsu.edu)
Department of Geology
Georgia State University
Atlanta, GA 30303

JAMES WHITNEY

V. MICHELLE ANDERSON

RICHARD C. CAPPS

Department of Geology,
University of Georgia,
Athens, GA 30602

ABSTRACT

Drill core samples of crystalline rocks which occur beneath Coastal Plain sediments at the Savannah River Site (SRS) consist primarily of greenschist to amphibolite grade schists of variable bulk composition (43-86 wt.% SiO_2, 0.24-13 wt.% MgO). These rocks are samples of the Appalachian orogen to the east of surface exposures of orogenic rocks. Evaluation of rock geochemistry suggests that they are mainly igneous (or immature sediments derived from igneous sources) in origin and probably constitute a series of fundamentally calc-alkaline volcanic, volcaniclastic, and hypabyssal plutonic rocks. Hence, these rocks are similar in origin to other Paleozoic or Late Proterozoic rocks of the Carolina (Avalon) terrane of the southern Appalachians. Relict igneous mineralogy, including calcic plagioclase (to An_{56}) cores, oscillatory zoning in plagioclase, and magnesiohornblende cores rimmed by metamorphic pargasitic amphibole, attest to the survival of some primary features of the rocks. Amphibole textures indicate multiple metamorphic events which probably occurred in distinct tectonic environments. Relict igneous amphiboles were variably replaced or overgrown by actinolite, probably during seafloor metamorphism after formation of the igneous suite. Subsequent regional metamorphism produced an overprint of amphibolite grade metamorphism as indicated by overgrowths on or complete replacement of magnesiohornblende and/or actinolite by edenitic/pargasitic blue-green hornblende in association with relatively calcic plagioclase.

INTRODUCTION

The southern Appalachians consist of a series of northeast trending "belts" or terranes that are defined on the basis of their bulk compositions, metamorphic grade, geochronology and inferred geologic history (e.g., Hatcher and others, 1989). Proceeding from northwest to south-

northwestern Ohio: Ohio Division of Geological Survey Report of Investigations No. 143, 77 p.

Willman, H.B., and Kolata, D.R., 1978, The Platteville and Galena groups in northern Illinois: Illinois State Geological Survey Circular 502, 75 p.

Wilson, C.W., Jr., 1962, Stratigraphy and geologic history of Middle Ordovician rocks of central Tennessee: Geological Society of America Bulletin, v. 73, p. 481-504.

Wilson, J.L., 1975, Carbonate facies in geologic history: New York, Springer-Verlag, 471 p.

Zalán, P.V., and eight others, 1991, The Paraná basin, Brazil, *in* Leighton, M.W., Kolata, D.R., Oltz, D.F., and Eidel, J.J., eds., Interior cratonic basins: American Association of Petroleum Geologists Memoir 51, p. 681-708.

Ziegler, P.A., 1978, Northeastern Europe: Tectonics and basin development: Geologie en Mijnbouw, v. 57, p. 589-626.

Ziegler, P.A., 1987, Late Cretaceous and Cenozoic intraplate compressional deformations in the Alpine foreland — a geodynamic model: Tectonophysics, v. 137, p. 389-420.

Ziegler, P.A., 1988, Evolution of the Arctic—North Atlantic and the western Tethys: American Association of Petroleum Geologists Memoir 43, 198 p.

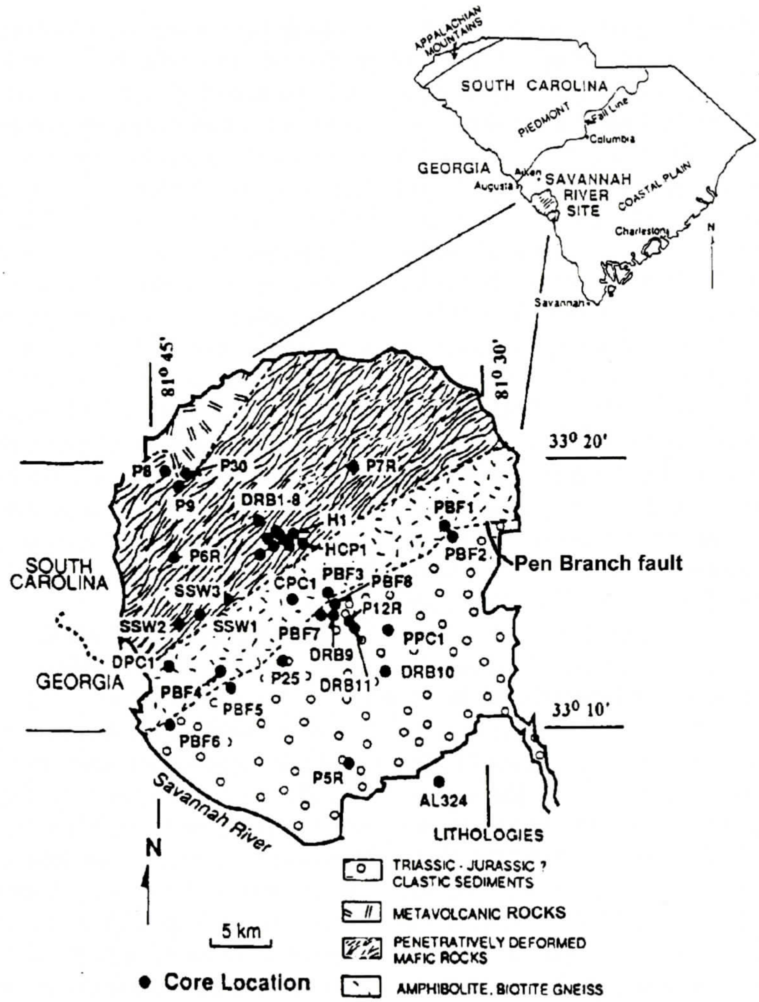

Figure 1. Map of Savannah River Site, with locations of core drill holes (modified from Snipes et al., 1993).

one, Anderson (1997) studied the metamorphic assemblages in 8 samples from throughout the site. An important conclusion in her study is that the assemblages include retrograde minerals, predominantly chlorite but including some biotite and epidote. Utilizing mineral equilibria, she estimated peak metamorphic conditions consistent with amphibolite facies metamorphism (540- 700°C and P = 5.5-6.5 kbars) for the rocks of the penetratively deformed terrane of Snipes and others (1993) and upper greenschist to epidote amphibolite facies (400-530°C and P = 7-10 Kb) for the metavolcanic rocks in the northwestern corner of the SRS.

SAMPLING AND ANALYTICAL TECHNIQUES

Locations of the drill holes at the SRS are shown in Figure 1. Drill cores were logged (Capps and others, 1995; LaTour and others, 1996) and then sampled to obtain representative specimens for petrographic and mineralogic characterization and for the analysis of bulk rock compositions by X-ray fluorescence spectrometry (XRF). Approximately 20 cores were logged and typical samples were selected for petrographic study. Most sample cores are concentrated in the two northwestern terranes (Fig-east, these terranes include the Valley and Ridge, the Blue Ridge, the Inner Piedmont, and the Carolina terrane and represent lithotectonic packages assembled by plate tectonic processes during the Paleozoic. The southeastern margin of the Appalachian orogen is an unconformity coincident with the Fall Line and defined by Coastal Plain sediments in contact with the crystalline rocks of the Appalachians. Metamorphic rocks of the Appalachian orogen extend beneath the Coastal Plain sediments as inferred from drill core samples, aeromagnetic surveys and seismic profiles (Thomas and others, 1989a). The Savannah River Site (SRS, Figure 1) is located 25 km southeast of the unconformity and the crystalline basement here is likely part of the Avalonian Carolina terrane (Rankin and others, 1989; Thomas and others, 1989b). Here, 200-400 meters of Coastal Plain sediments overlie Paleozoic or older greenschist to amphibolite grade metavolcanic rocks, schists, and gneisses in the northwestern half of the site and terrigenous sediments of the Triassic Dunbarton basin in the southeastern half (Marine and Siple, 1974; Snipes and others, 1993). The boundary between these two pre-Cretaceous terranes is a northeast striking, southeast dipping fault, the Pen Branch fault (Snipes and others, 1993; Stieve and Stevenson, 1995).

The closest exposed crystalline rocks to the SRS are greenschist facies metavolcanics and metasediments of the Belair belt or Augusta terrane and amphibolite facies schists and gneisses of the Kiokee belt or Savannah River terrane (Thomas and others, 1989b; Maher and others, 1994). These two terranes are juxtaposed along the northeast-striking Augusta fault zone near Augusta, GA, and Thomas and others (1989b) inferred that the two terranes interfinger in the subsurface of the SRS based on a synthesis of well data, surface mapping and geophysical data. Both terranes are part of the complex assemblage of accreted rocks that make up the Appalachian orogen southeast of the Inner Piedmont.

Starting in the late 1950s the Department of Defense oversaw deep drilling of the crystalline basement beneath the SRS with the aim of understanding the basement geology of the site as well as exploring the possibility of using the basement as a repository for nuclear waste. The crystalline cores have been preserved and due to the close spacing of the drill holes (Figure 1), and extensive amount of crystalline basement sampled (commonly several hundred meters, LaTour and others, 1996), the cores provide a unique opportunity to examine the petrology, geochemistry, and structure of the crystalline rocks of the Appalachian orogen to the east of surface exposures of crystalline rock. In this paper we report results of a petrologic and geochemical investigation of these crystalline drill cores. Our aim was to provide a general geologic characterization of the crystalline basement at the SRS and to interpret the geology in the context of the tectonics of the southern Appalachians.

Snipes and others. (1993) summarized previous work on the SRS crystalline basement and examined the crystalline rock samples retrieved during the drilling program. An important result of their work was a geologic map of the basement (Figure 1) which we used to guide our sampling program. They recognized three metamorphic terranes in the basement: a small metavolcanic terrane which occupies the northwestern corner of the site, a terrane composed of penetratively deformed mafic to ultramafic rocks which underlies most of the northwestern 1/3 of the SRS, and a northeast trending band of amphibolite and biotite gneiss adjacent to the mafic rocks (Figure 1). Mauldin and others (1997) and La Tour and others (1997) reported preliminary results showing that the bulk compositions of the basement rocks were consistent with a dominantly meta-igneous source.

In a companion study to this paper, Capps and others (1995) logged the drill core which allowed us to choose representative samples for study. In another companion study, Vanko and Capps (1995) documented the occurrence of two types of veining in the core: an early, high temperature veining event probably related to peak metamorphism, and a second, much later and lower temperature event which produced crosscutting calcite- and zeolite-dominated veins. In a third companion study to the present

Table 1. Whole-rock chemical compositions of crystalline cores, Savannah River Site

Core	DRB-1	DRB-1	DRB-1	DRB-1	DRB-1	DRB-1	DRB-1	DRB-1	DRB-1	DRB-1	DRB-1	DRB-1	DRB-2	DRB-2	DRB-2	DRB-2	DRB-2	DRB-2	DRB-2	DRB-3
Sample	DRB1-01	DRB1-02	DRB1-03	DRB1-04	DRB1-05	DRB1-06	DRB1-07	DRB1-08	DRB1-09	DRB1-10	DRB1-11	DRB1-12	DRB2-05	DRB2-11	DRB2-14	DRB2-16	DRB2-19	DRB2-20	DRB2-21	DRB3-03
Depth (ft)	903.0	1011.5	1011.5	1117.0	1153.0	1572.0	1234.0	1234.0	1729.0	1879.0	1885.0	1885.0	1153.0	1448.0	1632.0	1730.0	1805.0	1866.0	1945.0	1074.0
Depth (m)	273.6	306.5	306.5	338.5	349.4	476.4	373.9	373.9	523.9	569.4	571.2	571.2	349.4	438.8	494.5	524.2	547.0	565.5	589.4	325.5
Rock Type	1	3	1	2	3	1	3	3	1	3	3	3	3	1*	1*	1	1	1	1	1
SiO_2	61.74	58.86	50.91	49.15	54.09	80.35	57.49	58.00	47.20	48.77	59.90	56.73	48.95	58.02	57.51	60.51	53.80	54.97	48.60	51.06
TiO_2	0.78	0.70	0.71	0.99	1.07	0.28	0.94	0.67	1.32	0.89	0.75	0.73	0.85	1.10	1.18	0.77	0.87	0.91	1.05	1.03
Al_2O_3	13.76	17.29	15.37	16.84	15.45	6.68	17.47	16.61	14.43	19.60	17.68	17.33	17.94	16.61	17.40	16.88	20.82	17.92	17.61	19.48
$Fe_2O_3{}^a$	8.93	6.58	10.90	10.71	11.31	3.30	8.48	8.36	13.10	9.59	6.60	8.26	10.64	9.59	9.76	7.25	8.51	8.78	11.14	9.72
MnO	0.19	0.10	0.20	0.17	0.14	0.05	0.17	0.18	0.20	0.15	0.10	0.13	0.18	0.20	0.17	0.14	0.12	0.15	0.23	0.18
MgO	2.78	2.27	8.84	7.73	4.33	0.67	3.11	4.01	5.14	5.21	2.51	4.05	6.02	2.90	3.06	3.10	2.70	4.13	5.73	3.63
CaO	6.63	9.57	8.36	10.21	7.83	5.63	6.66	6.63	9.67	11.26	6.31	7.08	11.00	6.38	4.93	6.24	7.97	6.22	10.20	7.82
Na_2O	2.08	3.11	2.85	1.65	2.95	0.15	4.32	3.99	2.97	2.57	4.59	4.48	2.77	3.08	3.72	3.96	4.23	2.66	2.53	4.61
K_2O	0.50	0.53	0.39	0.43	0.94	0.04	0.48	0.42	0.21	0.25	0.07	0.67	0.84	1.23	1.74	0.78	0.47	2.76	1.16	1.56
P_2O_5	0.14	0.18	0.10	0.12	0.16	0.07	0.22	0.13	0.17	0.15	0.21	0.14	0.30	0.48	0.21	0.17	0.17	0.31	0.35	0.31
LOI^c	1.74	0.67	2.53	2.62	0.80	1.19	1.21	0.48	0.49	1.66	0.74	0.59	0.95	0.55	0.83	0.70	1.35	1.23	1.28	1.37
Total	99.27	99.86	101.16	100.62	99.07	98.41	100.55	99.48	94.90	100.10	99.46	100.19	100.44	100.14	100.51	100.50	101.01	100.04	99.88	100.77
FeO^b	8.04	5.92	9.81	9.64	10.18	2.97	7.63	7.52	11.79	8.63	5.94	7.43	9.57	8.63	8.78	6.52	7.66	7.90	10.02	8.75
trace elements (ppm)																				
Ba	119	170	46	98	349	<10	243	186	24	54	313	243	219	588	846	328	148	812	256	590
Cr	18	37	511	288	32	9	24	14	65	140	14	27	91	16	33	21	24	72	41	33
Nb	<3	<3	<3	<3	<3	<3	<3	<3	<3	<3	<3	<3	<3	<3	<3	<3	<3	<3	<3	<3
Ni	61	54	148	109	52	76	40	41	52	47	44	53	43	38	40	37	41	37	46	42
Rb	10	12	6	11	18	3	11	9	<3	6	18	15	17	28	37	17	11	61	22	27
Sr	275	413	141	227	242	307	342	294	256	315	370	295	493	542	354	429	617	426	501	553
V	187	150	252	267	340	81	182	173	363	245	125	191	232	152	180	144	142	202	299	275
Y	21	22	10	14	21	6	19	18	14	11	16	21	15	31	27	20	18	28	19	21
Zr	82	120	30	46	76	59	74	51	54	49	148	67	64	144	103	151	109	118	79	90

(a) Total iron given as Fe_2O_3.
(b) Total iron as FeO. Not included in totals.
(c) LOI not corrected for weight gain during oxidation of Fe and others. Complete oxidation cannot be assumed

Rock Types:
1. Mafic schist (Figure 2A)
1* Garnet-bearing mafic schist
2. Blastoporphyritic mafic schist (Figure 2B)
3. Meta-quartz diorite (Figure 2C)
4. Muscovite schist
5. Metagranitoid
6. Biotite gneiss
7. Sediment from above basement
8. Metabase
9. Metavolcanic with well-preserved textures

ure 1) recognized by Snipes and others (1993). Samples with the prefix "P9R", "P11R" or "P30" are from within or near the "metavolcanic" terrane which underlies the northwest corner of the SRS (Snipes and others, 1993). Samples with the prefix "DRB" (excluding DRB-9), "SSW" or "P6R" are from the "penetratively deformed mafic to ultramafic" terrane which underlies most of the northern half of the SRS (Snipes and others, 1993). The DRB 1 through 8 holes are all closely spaced and from the central portion of the SRS near the Pen Branch fault (Figure 1). Holes P6R, SSW-1, SSW-2 and SSW-3 are more widely spaced and located southwest of the DRB cluster. We also examined a few samples from core that penetrated the "amphibolite-biotite gneiss" terrane just to the northwest of the Pen Branch fault - these samples have the prefix "PBF" and "CPC", and one sample from core DRB-9 which penetrated a metagranitoid beneath the Triassic sediments of the Dunbarton basin.

Eighty-seven polished thin sections were examined to characterize mineral assemblages and rock textures. Eighty two of these samples were analyzed for major and trace element abundances by XRF at Georgia State University following Norrish and Hutton (1969) and LaTour (1989) (Table 1). Samples for major elements were a mix of rock powder and lithium tetraborate in a ratio of 1:9. Trace elements were analyzed on pressed pellets of rock powder mixed with crystalline cellulose. The X-ray spectrometer is a Rigaku 3070 wavelength dispersive spectrometer and analyses were carried out at 50 kV accelerating voltage and 50 Ma X-ray tube current. Natural rock standards were used for calibration curves and analyses were corrected for mass absorption and overlap effects. Analytical reproducibilities are generally lower than 1 relative percent except for MnO (2.6%) and P_2O_5 (3%). Loss on ignition measurements were carried out following heating of rock powders for 2 hours at 950-1000^oC.

Based on petrographic analysis, samples with typical metamorphic assemblages, or unusual examples of mineral zoning or those with what appeared to be preserved igneous zoning were studied with a JEOL 833 electron microprobe at the University of Georgia. Analytical techniques followed those outlined in Roden and Shimizu (1993). Typical operating conditions were 15 kV accelerating voltage and electron beam currents ranging from 5 to 15 nA. The beam was defocused to a 10 micron diameter area when analyzing feldspar and occasionally epidote and chlorite. X-ray intensities were converted to weight percent oxides using a Bence-Albee correction scheme and X-ray intensities for natural mineral standards. Major element oxides are reproducible to +/- 1.5 relative percent and minor elements to +/- 5 relative percent. Data abstracted from Anderson (1997) was gathered following similar analytical procedures. Mineral compositions are reported for plagioclase, biotite, chlorite, epidote, garnet, and amphibole in Tables 2 through 7.

MINERAL ASSEMBLAGES AND ROCK TEXTURES

The majority of the rocks we examined are from the "penetratively deformed mafic to ultramafic" terrane of Snipes and others (1993). Most of these rocks are green, schistose, and dominated by chlorite, amphibole (pargasitic), and epidote with varying amounts of biotite, plagioclase (oligoclase) and quartz. Oxides and sulphides are distributed throughout the core but were not examined in detail. The most common rock type is a mafic schist (Figure 2A) dominated by chlorite, biotite, or amphibole; quartz is ubiquitous, and plagioclase neoblasts and porphyroclasts (commonly replaced by mosaic intergrowths of epidote) are common. Some rocks have blastoporphyritic (i.e., meta-igneous) textures with relatively large plagioclase porphyroclasts (or mosaic pseudomorphs of epidote after plagioclase; interpreted as former igneous phenocrysts) in a fine-grained, dark green schistose matrix (Figure 2B). Additionally, a medium- to coarse-grained meta-quartz diorite with preserved igneous(?) mineral zoning (Figure 2C and see below) is a common lithology in core DRB-1. Some rocks contain substantial muscovite (e.g., samples from core DRB-4), but these lithologies are minor compared to rocks dominated by calcic

Table 1. Continued

Core	DRB-7	DRB-7	DRB-7	DRB-8	DRB-8	DRB-8	DRB-8	DRB-8	DRB-8	DRB-9
Sample	DRB7-08	DRB7-09	DRB7-12	DRB8-01	DRB8-02	DRB8-03	DRB8-04	DRB8-05	DRB8-06	DRB9-01
Depth (ft)	1657.0	1777.0	1958.0	1761.0	1638.0	1636.0	1637.0	1292.0	959.6	2648.0
Depth (m)	502.1	538.5	593.3	533.6	496.4	495.8	496.1	391.5	290.8	802.4
Rock Type	2	1	2	5	1	1	1	1	1	5
SiO_2	55.58	49.07	61.31	73.07	65.86	62.01	43.13	57.14	50.48	66.69
TiO_2	1.02	0.92	1.18	0.22	0.64	0.94	1.07	1.16	1.18	0.81
Al_2O_3	17.35	15.41	15.90	13.89	16.34	16.26	14.62	16.53	17.16	13.47
Fe_2O_3[a]	8.65	8.78	7.33	2.04	3.81	5.71	10.84	8.58	11.14	5.46
MnO	0.26	0.22	0.18	0.04	0.07	0.17	0.29	0.19	0.38	0.12
MgO	3.47	6.12	2.84	0.19	1.08	1.74	8.00	2.91	3.93	1.22
CaO	5.72	7.27	4.80	0.67	2.40	3.55	7.66	5.92	7.74	1.83
Na_2O	5.06	3.09	3.51	5.00	6.68	5.91	2.25	4.66	3.81	4.43
K_2O	1.49	3.92	2.01	4.38	1.78	2.12	6.05	1.87	1.90	2.78
P_2O_5	0.46	0.47	0.28	0.03	0.20	0.38	0.31	0.43	0.60	0.18
LOI[c]	0.71	5.46	0.80	0.43	1.08	1.28	5.93	0.63	2.12	1.11
Total	99.77	100.73	100.14	99.96	99.94	100.07	100.15	100.02	100.44	98.10
FeO[b]	7.78	7.90	6.60	1.84	3.43	5.14	9.75	7.72	10.02	4.91
trace elements (ppm)										
Ba	368	748	486	484	669	895	646	656	561	1004
Cr	24	298	49	11	7	21	201	20	28	23
Nb	<3	<3	8	13	6	6	<3	<3	<3	23
Ni	31	94	44	25	25	24	108	38	40	34
Rb	30	78	70	95	46	46	109	39	35	48
Sr	555	346	322	77	409	332	262	579	583	204
V	163	190	148	<3	67	97	259	186	248	69
Y	29	35	45	68	41	45	34	30	25	52
Zr	125	139	188	356	288	240	69	159	80	380

Core	SSW-1	SSW-1	SSW-1	SSW-1	SSW-1	SSW-1	SSW-2	SSW-2	SSW-2	SSW-2	SSW-2
Sample	SSW1-01	SSW1-03	SSW1-06	SW1-07A	SW1-07B	SSW1-10	SSW2-01	SSW2-03	SSW2-04	SSW2-08	SSW2-10
Depth (ft)	1069.0	1158.0	1252.0	1285.0	1285.0	1364.0	892.0	927.0	944.0	1102.0	1192.0
Depth (m)	323.9	350.9	379.4	389.4	389.4	413.3	270.3	280.9	286.1	333.9	361.2
Rock Type	1	1	4	1	1	1	2	1	1*	1	1
SiO_2	61.25	50.46	61.23	65.23	46.60	50.48	68.41	51.11	53.30	48.31	50.75
TiO_2	0.67	1.15	0.18	0.77	1.20	1.07	0.47	0.88	0.77	1.01	0.96
Al_2O_3	18.42	19.18	19.65	15.04	17.43	19.36	15.70	17.52	16.20	17.90	18.61
Fe_2O_3[a]	4.78	11.74	1.17	5.15	11.78	9.10	3.29	9.39	7.97	11.69	10.72
MnO	0.11	0.12	0.05	0.11	0.22	0.21	0.09	0.21	0.17	0.13	0.28
MgO	2.36	2.81	0.32	2.26	6.63	3.37	0.87	5.35	6.27	6.06	4.91
CaO	4.28	9.57	4.17	4.71	7.13	7.74	1.41	8.57	2.48	8.29	8.42
Na_2O	5.42	3.25	8.47	3.89	2.19	4.86	5.02	3.16	1.26	3.94	4.19
K_2O	1.39	0.68	2.32	1.12	2.28	1.43	4.09	1.67	3.86	1.42	0.92
P_2O_5	0.21	0.31	0.03	0.24	0.41	0.33	0.14	0.27	0.22	0.29	0.28
LOI[c]	2.07	1.43	3.62	1.77	5.17	3.13	0.47	1.98	8.55	1.05	0.51
Total	100.96	100.70	101.21	100.29	101.04	101.08	99.96	100.11	101.05	100.09	100.55
FeO[b]	4.30	10.56	1.05	4.63	10.60	8.19	2.96	8.45	7.17	10.52	9.65
trace elements (ppm)											
Ba	415	207	828	486	558	313	815	285	597	376	237
Cr	45	29	<3	59	210	65	15	81	67	105	38
Nb	5	<3	5	<3	<3	<3	11	<3	<3	<3	<3
Ni	30	57	14	54	83	37	39	51	23	47	45
Rb	45	18	46	32	57	35	88	32	110	23	14
Sr	675	596	248	501	447	686	266	524	156	479	542
V	97	270	10	93	291	214	19	230	210	285	263
Y	42	18	17	35	28	33	55	19	31	17	17
Zr	229	89	113	183	107	170	304	82	81	68	82

(a) Total iron given as Fe_2O_3.
(b) Total iron as FeO. Not included in totals.
(c) LOI not corrected for weight gain during oxidation of Fe and others. Complete oxidation cannot be assumed

Rock Types:

1. Mafic schist (Figure 2A)
1* Garnet-bearing mafic schist
2. Blastoporphyritic mafic schist (Figure 2B)
3. Meta-quartz diorite (Figure 2C)
4. Muscovite schist
5. Metagranitoid
6. Biotite gneiss
7. Sediment from above basement
8. Metabase
9. Metavolcanic with well-preserved textures

Table 1. Continued

Core	DRB-3	DRB-3	DRB-3	DRB-3	DRB-4	DRB-4	DRB-4	DRB-4	DRB-4	DRB-4	DRB-4
Sample	DRB3-04	)RB3-06A	)RB3-06B	DRB3-09	DRB4-01	DRB4-04	DRB4-06	DRB4-10	)RB4-11A	)RB4-11B	DRB4-13
Depth (ft)	1184.0	1320.0	1320.0	1444.0	995.0	1123.0	1208.0	1416.0	1454.0	1454.0	1524.0
Depth (m)	358.8	400.0	400.0	437.6	301.5	340.3	366.1	429.1	440.6	440.6	461.8
Rock Type	4	2	2	2	4	4	4	4	5	5	1*
SiO_2	73.70	65.83	52.35	62.02	64.68	59.51	85.98	64.89	63.46	75.25	57.89
TiO_2	0.24	0.78	1.17	0.77	0.84	0.96	0.20	0.93	0.11	0.12	1.05
Al_2O_3	14.26	15.88	17.74	16.00	16.34	19.90	6.06	16.89	19.32	13.77	16.86
$Fe_2O_3^a$	1.48	4.59	10.28	5.13	7.42	7.50	0.92	6.75	1.31	1.18	8.95
MnO	0.05	0.15	0.21	0.08	0.21	0.07	0.04	0.15	0.07	0.02	0.17
MgO	0.37	1.38	3.67	2.74	2.66	1.66	0.35	1.82	0.30	0.24	3.98
CaO	0.81	3.92	7.75	4.60	1.34	2.29	1.15	2.58	3.07	0.76	4.82
Na_2O	5.16	5.66	3.67	4.43	1.93	4.17	1.70	3.39	10.04	7.76	2.45
K_2O	3.05	0.84	1.64	1.97	1.68	2.13	0.79	1.36	0.90	0.23	2.55
P_2O_5	0.04	0.20	0.28	0.48	0.13	0.15	0.01	0.12	0.04	0.02	0.20
LOI^c	0.88	0.62	1.45	2.03	3.83	2.14	1.29	1.80	2.71	0.57	1.55
Total	100.04	99.85	100.21	100.25	101.06	100.48	98.49	100.68	101.33	99.92	100.47
FeO^b	1.33	4.13	9.25	4.62	6.68	6.75	0.83	6.07	1.18	1.06	8.05
trace elements (ppm)											
Ba	629	387	492	987	762	876	130	553	183	36	499
Cr	<3	9	29	41	26	34	30	25	<3	5	123
Nb	5	<3	<3	13	8	8	5	5	22	24	10
Ni	56	28	40	63	32	34	62	38	35	47	69
Rb	64	17	28	40	50	75	38	45	50	13	91
Sr	212	411	523	823	213	348	63	383	92	72	158
V	13	51	238	112	100	105	15	101	18	24	171
Y	35	37	23	15	38	53	20	42	64	83	40
Zr	224	170	97	215	253	262	72	218	373	293	179

Core	DRB-4	DRB-4	DRB-4	DRB-4	DRB-6	DRB-6	DRB-6	DRB-6	DRB-6	DRB-6
Sample	DRB4-15	DRB4-17	DRB4-19	DRB4-24	DRB6-03	DRB6-08	DRB6-11	DRB6-13	RB6-15A	RB6-15B
Depth (ft)	1607.0	1674.0	1748.0	1899.0	1242.0	1417.0	1559.0	1736.0	1844.0	1844.0
Depth (m)	487.0	507.3	529.7	575.5	376.4	429.4	472.4	526.1	558.8	558.8
Rock Type	2	1	1	1	1	2	1	1	2	2
SiO_2	65.92	69.34	52.97	54.60	48.78	48.78	50.52	51.93	48.16	52.28
TiO_2	0.87	0.60	2.03	1.48	1.07	1.00	1.08	1.24	1.08	0.96
Al_2O_3	15.60	13.20	15.85	16.13	17.60	17.44	17.69	16.38	18.45	17.36
$Fe_2O_3^a$	5.06	5.46	13.81	11.11	11.39	11.23	11.89	11.98	10.19	9.47
MnO	0.16	0.12	0.14	0.15	0.21	0.17	0.18	0.23	0.21	0.18
MgO	1.80	1.85	6.20	5.06	5.61	7.91	4.86	4.68	3.70	4.19
CaO	5.09	3.53	2.21	3.86	10.18	7.43	7.84	8.32	10.54	7.33
Na_2O	2.08	2.32	3.04	2.69	3.30	3.85	3.56	3.10	2.41	2.78
K_2O	2.18	1.77	1.32	2.16	0.64	0.95	0.79	0.80	2.92	3.27
P_2O_5	0.19	0.12	0.33	0.23	0.30	0.20	0.16	0.26	0.35	0.30
LOI^c	1.30	1.88	2.49	3.29	1.07	1.70	1.01	1.03	2.57	2.15
Total	100.25	100.19	100.39	100.76	100.15	100.66	99.58	99.95	100.58	100.27
FeO^b	4.55	4.91	12.43	10.00	10.25	10.10	10.70	10.78	9.17	8.52
trace elements (ppm)										
Ba	463	357	454	836	264	324	273	399	589	629
Cr	105	40	391	257	60	132	61	58	33	80
Nb	12	12	13	8	<3	<3	<3	<3	<3	<3
Ni	50	52	223	149	48	82	54	54	49	42
Rb	85	69	36	64	11	17	15	13	52	63
Sr	139	116	107	128	568	342	451	429	636	521
V	142	119	300	273	276	282	320	313	240	211
Y	53	46	23	31	15	16	17	16	24	25
Zr	185	175	119	116	81	58	73	72	103	101

(a) Total iron given as Fe_2O_3.
(b) Total iron as FeO. Not included in totals.
(c) LOI not corrected for weight gain during oxidation of Fe and others. Complete oxidation cannot be assumed

Rock Types:

1. Mafic schist (Figure 2A)
1* Garnet-bearing mafic schist
2. Blastoporphyritic mafic schist (Figure 2B)
3. Meta-quartz diorite (Figure 2C)
4. Muscovite schist
5. Metagranitoid
6. Biotite gneiss
7. Sediment from above basement
8. Metabase
9. Metavolcanic with well-preserved textures

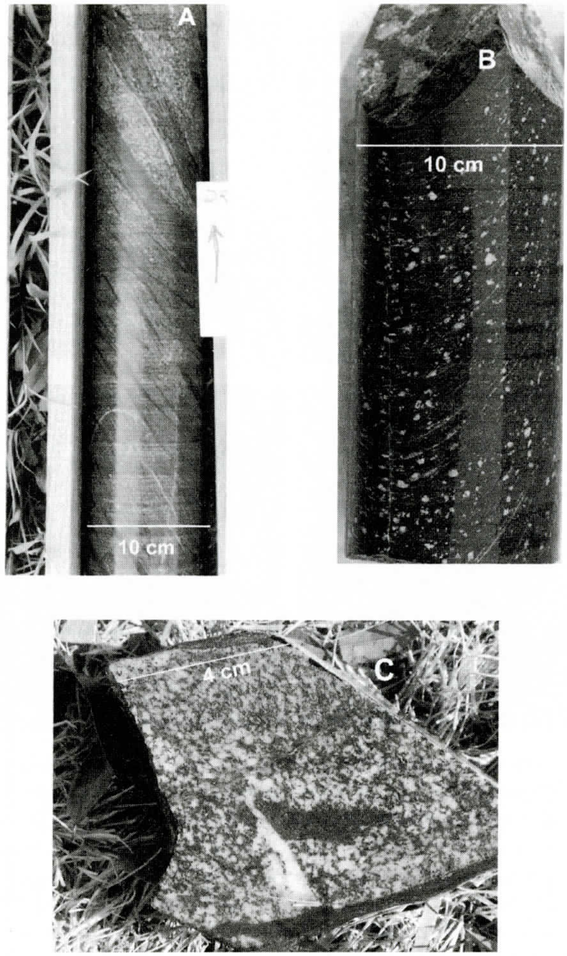

Figure 2. Photographs of drill core specimens. A) typical mafic schist (core DRB-1, 1064 ft depth [324 m]) B) Example of inferred relict igneous texture: porphyroclasts (interpreted as relict phenocrysts) of plagioclase or epidote after plagioclase in a fine-grained matrix (core DRB-1, 1479 feet depth [451 m]; C) Example of meta-quartz diorite from core DRB-1 (1012 ft depth [308 m]).

mineralogy. Occurring locally are zones of "granitic" lithology (K-feldspar and quartz), minor shear zones, and silicified and calcified zones. Quartz-dominated felsic segregations occur locally. Also in some cores, especially those from drill holes near the Pen Branch fault (Figure 1), there are veins of various sizes which contain a variety of minerals, including quartz, calcite, gypsum, and laumontite (Vanko and Capps, 1995; Dowling and others, 1996; Dennis and others, 1997).

The second group of cores (P9R, P11R and P30) from the northwest corner of the SRS consist primarily of Coastal Plain sedimentary rocks, but have a few meters of basement rock in the lowermost portions of the core. These latter lithologies are from the metavolcanic terrane (Figure 1) mapped by Snipes and others (1993), and some rocks have well preserved volcanic textures. Recognized protoliths from hand and thin section textures include lapilli tuffs and porphyritic volcanic rocks. Some rocks contain "water clear" quartz eyes, suggesting essentially no metamorphism. However, metamorphic minerals such as muscovite, chlorite, and epidote occur in the groundmass, and plagioclase phenocrysts have reequilibrated to end member albite compositions (Table 2).

Table 1. Continued

Core	SSW-2	SSW-2	SSW-2	SSW-3	SSW-3	SSW-3	SSW-3	PBF-1	PBF-1	CPC-1	P6R	P6R	P9R	P9R	P9R	P11R	P11R	P11R	P30	P30
Sample	SSW2-11	SW2-12A	SW2-12B	SSW3-01	SSW3-03	SSW3-05	SSW3-07	PBF1-01	PBF1-02	CPC1-01	P6R-01	P6R-02	P9R-01	P9R-04	P9R-06	P11R-01	P11R-02	P11R-03	P30-01	P30-02
Depth (ft)	1224.0	1286.0	1286.0	933.0	966.0	1021.0	1101.0	1065.0	1063.0	1096.0	850.0	855.0	717.0	808.0	1095.0	985.0	995.0	1075.0	786.0	796.0
Depth (m)	370.9	389.7	389.7	282.7	292.7	309.4	333.6	322.7	322.1	332.1	257.6	259.1	217.3	244.8	331.8	298.5	301.5	325.8	238.2	241.2
Rock Type	1	1	1	1	4	2	4	6	6	6	2	1	7	8	2	1	2	8	9	9
SiO_2	57.46	53.39	44.25	50.38	74.72	52.63	69.34	57.29	57.75	70.46	48.97	44.19	82.22	46.77	48.58	48.88	44.99	50.86	68.11	73.11
TiO_2	0.93	1.16	0.94	1.08	0.25	0.98	0.49	0.94	0.84	0.42	0.89	0.84	0.55	1.24	1.01	1.06	0.85	0.81	0.27	0.30
Al_2O_3	16.41	17.12	13.35	17.39	14.06	18.98	15.15	16.75	16.67	15.31	16.47	13.85	11.48	16.75	15.39	13.34	14.95	15.79	14.82	13.10
Fe_2O_3[a]	8.04	9.86	12.64	10.85	1.72	8.82	3.63	7.40	6.74	3.05	8.75	10.29	1.25	11.90	9.80	10.43	9.88	9.44	4.67	3.49
MnO	0.17	0.14	0.27	0.19	0.04	0.15	0.04	0.12	0.13	0.06	0.43	0.29	0.01	0.17	0.17	0.17	0.21	0.18	0.19	0.09
MgO	1.96	4.36	13.29	5.46	0.62	4.54	1.26	4.45	4.01	1.19	5.44	6.76	0.28	6.95	3.73	4.69	5.16	3.49	1.26	0.67
CaO	7.44	6.77	7.07	9.00	1.50	9.38	2.80	4.95	6.04	3.25	8.79	11.57	0.04	8.81	10.85	9.61	11.37	12.13	0.35	1.22
Na_2O	4.33	5.26	1.59	2.99	4.76	3.54	3.02	3.81	4.33	4.00	4.11	2.05	0.03	2.02	3.76	3.23	3.20	2.46	2.08	6.19
K_2O	1.36	1.09	3.95	1.29	1.42	0.79	2.75	3.31	2.59	1.30	0.36	0.82	0.21	0.12	0.61	0.66	0.81	0.01	6.51	0.72
P_2O_5	0.50	0.42	0.33	0.33	0.07	0.31	0.11	0.31	0.28	0.12	0.16	0.17	0.04	0.22	0.18	0.21	0.17	0.15	0.03	0.05
LOI[c]	1.81	0.45	1.39	1.26	0.97	0.62	1.40	0.77	0.95	1.04	6.29	11.27	4.62	6.93	7.65	9.48	10.62	6.24	1.71	0.74
Total	100.41	100.02	99.07	100.22	100.13	100.74	99.99	100.10	100.33	100.20	100.66	102.10	100.73	101.88	101.73	101.76	102.21	101.56	100.00	99.68
FeO[b]	7.23	8.87	11.37	9.76	1.55	7.94	3.27	6.66	6.06	2.74	7.87	9.26	1.12	10.71	8.82	9.38	8.89	8.49	4.20	3.14
trace elements (ppm)																				
Ba	518	372	643	351	742	242	717	716	567	594	92	156	79	33	243	116	119	<10	1731	76
Cr	21	37	1303	119	16	77	18	62	55	40	157	236	30	235	112	118	181	192	4	<3
Nb	<3	<3	3	<3	5	<3	3	9	5	<3	<3	<3	16	<3	<3	<3	<3	<3	12	12
Ni	33	50	415	61	37	43	34	51	39	33	34	96	16	78	73	66	77	62	18	32
Rb	31	16	50	28	35	17	67	150	88	66	6	15	16	4	10	12	12	<3	55	10
Sr	571	544	104	579	216	576	271	443	525	419	156	251	11	252	239	110	147	227	38	127
V	128	290	242	267	19	201	61	174	147	62	238	206	43	286	265	285	257	235	<3	11
Y	32	25	20	20	20	20	38	43	31	22	14	14	144	14	13	15	12	10	54	58
Zr	165	146	55	105	156	122	150	130	135	251	48	50	598	59	40	49	30	33	305	320

(a) Total iron given as Fe_2O_3.
(b) Total iron as FeO. Not included in totals.
(c) LOI not corrected for weight gain during oxidation of Fe and others. Complete oxidation cannot be assumed

Rock Types:
1. Mafic schist (Figure 2A)
1* Garnet-bearing mafic schist
2. Blastoporphyritic mafic schist (Figure 2B)
3. Meta-quartz diorite (Figure 2C)
4. Muscovite schist
5. Metagranitoid
6. Biotite gneiss
7. Sediment from above basement
8. Metabase
9. Metavolcanic with well-preserved textures

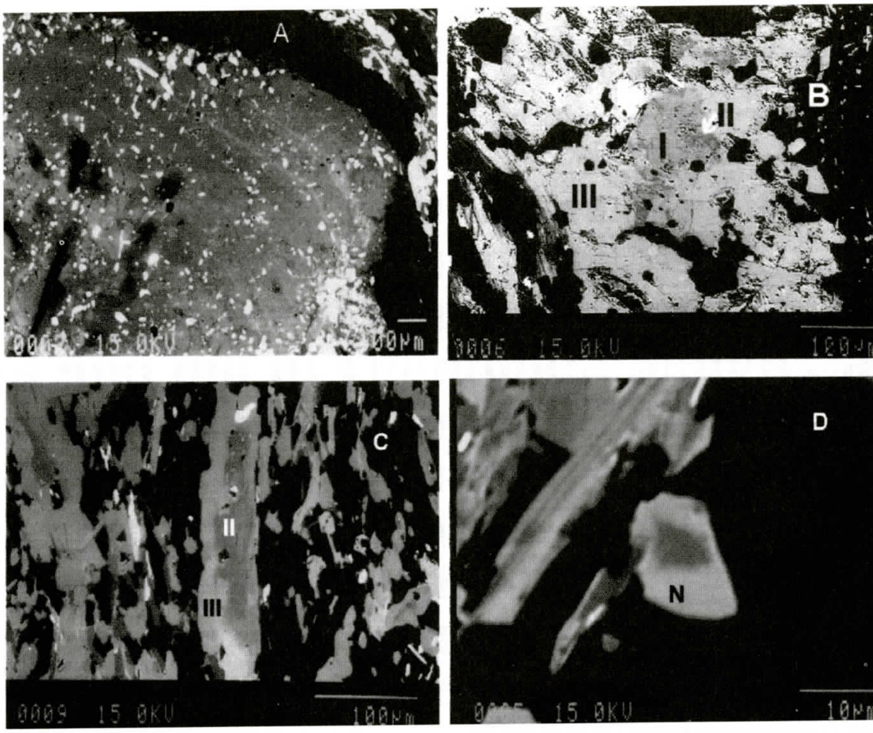

Figure 3. Backscattered electron imagery of zoned plagioclase and amphibole - relatively light grey regions are relatively high atomic number regions. A) Plagioclase porphyroclast with faint but distinct oscillatory zoning (compositional contrast between bright lamella and surrounding darker plagioclase is about 6 mol% an, Table 2). The dark gray streaks and spots in grain center correspond to low average atomic number (Z) areas, contrasting with surrounding light gray high Z areas (sample D1-184-1, 1844 ft depth [562 m]). B). Complexly zoned amphibole in meta-quartz diorite (sample DRB1-02, 1011.5 ft depth [308 m]). The grain center consists of medium gray, high-Ti relict igneous amphibole (I) intergrown with darker gray patches of actinolite (II); the wide rim consists of light gray edenitic hornblende (III). C) Zoned amphibole defining foliation in a fine-grained schist (sample DRB6-08, 1417 ft depth, [429 m]). Core is actinolite (II) and the rim is edenite (III). D) Tiny zoned neoblast (N), in same sample as Fig. 3C, consisting of dark gray actinolite core surrounded by a light gray rim of edenitic/pargasitic hornblende.

phibole + oligoclase + epidote + chlorite + quartz (± biotite, ± muscovite, ± garnet in Ca-poor, Al-rich rocks only). Rocks of greenschist grade are restricted to the northwestern portion of the basement (cores P30, P9R, P11R) and typically contain albite + epidote + chlorite + calcite + quartz.

Plagioclase compositions are variable, ranging from An_0 to An_{56} (Table 2). Some of this variation is probably due to metamorphic grade. For example, a sample from the metavolcanic terrane in the northwestern portion of the SRS has pure albite as porphyroclasts (Table 2; Anderson, 1997). In contrast, samples retrieved from the penetratively deformed rocks of the north-central SRS have more anorthitic plagioclase. In samples from core DRB-1, typical compositions of plagioclase neoblasts and porphyroclasts are An_{20-25}. Some plagioclase porphyroclasts are zoned: both calcic cores (to An_{56}) and calcic lamellae mimicking igneous oscillatory zoning (Figure 3) occur. These zoned porphyroclasts are overgrown with thin oligoclase rims (Table 2). Anderson (1997) reported plagioclase compositions from other DRB cores as well as the SSW2 and PBF1 cores. In these cases, groundmass plagioclase compositions exhibited a significant range and included relatively calcic compositions (to An_{40}; Table 2). Some zoning was observed but

Table 2. Plagioclase compositions (wt.%) in crystalline cores, Savannah River Site

Core	DRB-1	DRB-1	DRB-1	DRB-1	DRB-1	DRB-1	DRB-1	DRB-1	DRB-1	DRB-1	DRB-2	P30	PBF-1
Sample	DRB1-02	DRB1-02	DRB1-02	DRB1-02	DRB1-10	DRB1-10	DRB1-11	D1-184-1	D1-184-1	D1-184-1	DRB2-14	P30-01	PBF1-01
Depth (ft)	1011.5	1011.5	1011.5	1011.5	1879	1879	1885	1844	1844	1844	1632	796	1065
Footnote	(a)	(b)	(c)	(d)	(e)	(d)	(d)	(f)	(g)	(c)	(i)	(h)	(i)
SiO_2	55.42	59.71	63.92	62.48	61.68	62.17	63.78	59.04	57.62	63.77	58.56	67.75	62.3
TiO_2	----	0.07	----	----	----	----	----	0.06	----	----	0.04	----	----
Al_2O_3	29.62	25.67	24.46	24.54	24.69	23.86	23.47	26.28	27.53	23.93	26.42	20.39	23.99
CaO	11.59	8.04	5.22	5.41	5.34	4.87	4.39	7.81	8.74	4.37	7.18	0.31	5.03
MgO	----	----	----	----	----	----	----	----	----	----	----	----	----
FeO	----	0.66	0.04	0.11	0.04	0.12	----	0.06	----	0.08	0.09	0.07	0.09
MnO	----	0.04	----	----	----	----	----	----	0.04	0.07	----	----	----
K_2O	0.06	0.10	0.08	0.07	0.08	0.08	0.09	0.08	0.08	0.1	0.08	0.04	0.09
Na_2O	5.02	7.52	9.12	8.70	8.63	9.35	9.44	7.65	6.92	9.56	7.51	11.73	9.09
BaO	----	----	----	0.10	----	0.07	----	----	0.07	0.08	----	----	----
Total	101.71	101.81	102.84	101.41	100.46	100.52	101.17	100.98	101.00	101.96	99.88	100.29	100.58
Cations normalized to 8 Oxygens													
Si	2.455	2.632	2.755	2.735	2.723	2.748	2.788	2.617	2.559	2.772	2.62	2.96	2.75
Ti	----	0.002	----	----	----	----	----	0.002	----	----	----	----	----
Al	1.546	1.334	1.243	1.266	1.285	1.243	1.209	1.373	1.441	1.226	1.39	1.05	1.24
Ca	0.550	0.380	0.241	0.254	0.253	0.231	0.206	0.371	0.416	0.204	0.34	0.01	0.24
Mg	----	----	----	----	----	----	----	----	----	----	----	----	----
Fe	----	0.024	0.001	0.004	0.001	0.004	----	0.002	----	0.003	0.00	----	0
Mn	----	0.001	----	0.001	----	----	----	----	0.002	0.003	----	----	----
K	0.003	0.006	0.004	0.004	0.004	0.005	0.005	0.005	0.005	0.006	0.00	----	0.01
Na	0.431	0.643	0.762	0.738	0.739	0.801	0.800	0.657	0.596	0.806	0.65	0.99	0.78
Ba	----	----	----	0.002	----	0.001	----	----	0.001	0.001	----	----	----
Total	4.985	5.022	5.006	5.004	5.005	5.033	5.008	5.027	5.02	5.021	5.02	5.02	5.02
Ternary endmembers (molar)													
Ab	0.438	0.625	0.756	0.741	0.742	0.773	0.792	0.637	0.586	0.794	0.652	0.983	0.755
An	0.559	0.396	0.239	0.255	0.254	0.223	0.203	0.359	0.409	0.201	0.344	0.014	0.241
Or	0.003	0.005	0.004	0.004	0.004	0.004	0.005	0.004	0.004	0.005	0.004	0.002	0.005

Footnotes: (a)average (n=2) of calcic core of porphyroclast
(b) point analysis of sodic region in interior of porphyroclast
(c) point analysis of porphyroclast rim
(d) point analysis of neoblast
(e) average (n=2) porphyroclast
(f) point analysis of calcic core of porphyroclast
(g) average calcic lamella (n=2) in porphyroclast
(h) grain core, from Anderson (1997)
(i) grain rim, from Anderson (1997)

A third group of cores (PBF-1, PBF-3, PBF-4, CPC-1) are from the "amphibolite, biotite gneiss" terrane of Snipes et al. (1993); although we logged these cores we examined only 3 thin sections, and did limited microprobe and bulk rock chemistry. The rocks in these cores are comparatively quartz and feldspar-rich, gneissic and contain aluminous amphibole (Table 7) indicative of amphibolite grade metamorphism; Mauldin and others (1997) reported more extensively on these rocks.

MINERAL COMPOSITIONS

Mineralogy typical of greenschist to amphibolite facies characterize rocks of the cores. Rocks of amphibolite grade comprise most of the rocks we examined (cores DRB-1-8, SSW-1-3, PBF-1, CPC-1). In these rocks, typical assemblages include blue-green aluminous am-

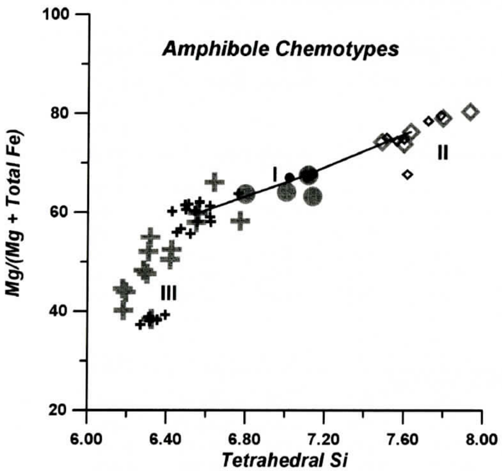

Figure 4. Amphibole chemotypes; data is from Table 3. Tieline connects chemotypes I, II and III from zoned amphibole in sample DRB1-02. The smaller symbols clustered around the large symbols for DRB 1-02 represent individual point analyses used to calculate the average analyses in Table 3 and give an indication of analytical precision. The second cluster of small crosses at the lower left are the individual point analyses of amphiboles in sample DRB 6-08. In this sample the amphibole appeared homogeneous, and the small crosses cluster around the large symbol representing the average of the analyses

most grains were homogeneous and had compositions in the range An_{20}-An_{40}.

Aluminous, blue-green amphibole is a widespread constituent of the rocks from the penetratively deformed rocks of the DRB and SSW cores. A similar amphibole occurs in a sample (PBF1-1) from the amphibolite and biotite gneiss terrane of Snipes and others (1993). Amphibole has not been recognized in the metavolcanic terrane from the northwest corner of the SRS. The most common amphibole composition (Table 3) is a ferroan pargasite but compositions range to actinolite and magnesiohornblende (following Leake and others, 1997; treating all Fe as ferrous). In some rocks the amphibole is complexly zoned and as many as 3 distinct compositions occur within single grains (Figures 3, 4). Even some amphiboles in fine-grained rocks are complexly zoned or at least exhibit sharply defined cores (Figure 3).

Based on petrography, point analyses by electron microprobe and examination of backscattered electron imagery we divided the amphiboles into 3 chemotypes: Amphibole I: brown, Mg- and typically Ti-rich hornblende; amphibole II: pale green actinolite; and amphibole III: blue-green pargasitic hornblende (Figure 4, Table 3). In some amphibole grains all three chemotypes are present and amphiboles I and II are intergrown in the center of the grain and type III forms a rim around I and II (Figure 3). Boundaries between amphibole chemotypes are sharp and not gradational. In other samples, amphiboles I and III or II and III are present; in these samples, amphiboles I or II define a distinct core with sharp boundaries between it and a rim of amphibole III. Where only one amphibole is present, it is consistently amphibole III, a blue-green pargasitic amphibole.

Garnets are sparsely distributed in the cores from the penetratively deformed rocks at the SRS. These garnets are almandine-rich (typically 40-60 mol percent, Table 4) but contain significant amounts of spessartine, grossular and pyrope components (typically 9-20 mol percent of each component). Most garnets are zoned with Mn- and Ca -rich centers and relatively Fe- and Mg-rich rims, but the zoning is not pronounced. One exception is garnet from sample SSW2-4 (Table 4). Anderson (1997) found garnet in one sample from the metavolcanic terrane of the northwest corner of the SRS; this garnet is a spessartine garnet with significant amounts of almandine and grossular components (Table 4) and is relatively unzoned.

Biotite, epidote and chlorite are common constituents of all the cores examined and representative analyses are presented in Tables 5-7. Biotites are homogeneous, moderately Mg-rich (Mg/Fe ~1 to 2), and contain significant amounts of TiO_2 (1.2-2.3 wt.%) and BaO (up to 0.5 wt.%). The chlorites also were homogeneous and relatively Mg-rich (Mg/Fe ~1.4 to 2.8). The epidote is moderately Fe-rich and some grains are zoned: on back scattered electron images, zones with relatively high mean atomic number (Z) were apparent. One zoned epidote was probed in an attempt to determine

Table 3. Amphibole compositions (wt.%) in crystalline cores, Savannah River Site

Core	DRB-1	DRB-1	DRB-1	DRB-1	DRB-1	DRB-1	DRB-1	DRB-1	DRB-1	DRB-1	DRB-1	DRB-1	DRB-1	DRB-2	DRB-2	DRB-4	DRB-6	DRB-6	DRB-6	DRB-6	DRB-8	PBF-1	SSW2
Sample	DRB1-02	DRB1-02	DRB1-02	D1-50-1	D1-50-1	D1-50-1	DRB1-09	DRB1-09	DRB1-10	DRB1-10	DRB1-11	D1-184-1	D1-184-1	DRB2-11	DRB2-14	DRB4-87	DRB6-08	DRB6-08	DRB6-08	DRB6-08	DRB8-05	PBF1-01	SSW2-12
Depth (ft)	1011.5	1011.5	1011.5	1215	1215	1215	1729	1729	1879	1879	1885	1844	1844	1448	1632	1524	1417	1417	1417	1417	1292	210	1286
Chemotype	I	II	III	I	II	III	I	III	II	III	III	I	III	III	III	III	II	III	II	III	III	III	III
footnote	(a)	(b)	(c)	(a)	(d)	(e)	(d)	(e)	(d)	(e)	(f)	(a)	(c)	(f)	(f)	(f)	(d)	(c)	(g)	(h)	(f)	(f)	(f)
n (ave.)	4	6	15	5	----	----	----	----	----	----	8	3	5	2	2	4	----	4	----	----	6	2	4
SiO_2	48.90	53.79	44.46	45.88	52.68	42.76	48.61	41.97	52.23	42.69	42.83	47.99	42.10	41.14	41.21	41.04	56.82	45.89	55.34	44.24	40.95	42.06	45.75
TiO_2	1.72	0.19	0.39	1.64	0.11	0.39	0.41	0.38	0.17	0.43	0.34	1.63	0.38	0.34	0.36	0.26	0.03	0.38	----	0.36	0.73	0.94	0.46
Al_2O_3	6.82	3.35	13.13	8.88	3.47	13.71	7.27	15.04	4.78	14.74	13.88	6.96	14.45	16.39	16.53	17.15	0.49	10.72	2.33	12.68	12.08	12.87	11.74
CaO	11.45	12.12	11.40	11.44	11.71	11.01	11.13	11.17	12.13	11.36	10.75	11.25	11.24	11.46	11.27	10.88	12.62	11.09	12.26	11.54	11.36	11.57	11.36
MgO	14.59	17.60	11.67	13.27	16.88	9.98	13.76	9.15	16.56	10.59	9.47	14.08	9.08	8.00	7.77	6.97	19.62	12.02	18.45	11.35	7.52	10.23	13.61
FeO	12.61	9.73	13.96	13.47	10.68	16.13	14.26	17.42	10.29	15.46	16.96	14.05	17.79	17.72	17.73	18.53	8.55	15.31	8.67	14.63	21.46	16.76	12.41
MnO	0.30	0.30	0.32	0.36	0.49	0.35	0.35	0.32	0.34	0.30	0.50	0.40	0.43	0.48	0.50	0.67	0.16	0.27	0.32	0.34	0.63	0.35	0.27
K_2O	0.28	0.11	0.30	0.21	0.04	0.34	0.32	0.30	0.06	0.34	0.32	0.24	0.43	0.52	0.41	0.29	----	0.26	0.06	0.32	1.39	1.79	0.54
Na_2O	1.05	0.53	1.72	1.35	0.68	1.89	1.10	1.80	0.73	2.07	1.91	1.26	2.04	1.39	1.67	1.66	0.17	1.58	0.32	1.75	1.59	1.67	2.03
BaO	----	----	----	----	----	----	----	----	----	----	----	----	----	----	----	----	----	----	----	----	----	----	----
Cl	0.07	----	----	0.04	----	----	0.05	----	----	----	----	0.07	----	0.12	----	----	----	----	----	----	----	0.09	----
F	0.08	0.07	0.05	0.13	0.06	0.15	----	0.12	na	na	0.16	0.19	0.17	0.14	----	na	----	----	----	0.15	0.18	0.23	0.13
Total	97.82	97.76	97.40	96.61	96.77	96.65	97.25	97.62	97.29	97.98	97.05	98.02	98.04	97.61	97.45	97.45	98.46	97.52	97.75	97.30	97.81	98.44	98.25
Cations normalized to 23 oxygens (anhydrous)																							
Si	7.090	7.631	6.546	6.798	7.597	6.424	7.136	6.282	7.485	6.316	6.416	7.004	6.299	6.179	6.193	6.182	7.931	6.770	7.793	6.548	6.324	6.306	6.638
Ti	0.187	0.020	0.043	0.183	0.012	0.044	0.045	0.043	0.018	0.048	0.040	0.179	0.043	0.038	0.041	0.029	0.003	0.042	----	0.040	0.085	0.106	0.050
Al	1.165	0.560	2.278	1.551	0.590	2.427	1.258	2.653	0.807	2.570	2.451	1.197	2.548	2.900	2.927	3.045	0.081	1.864	0.387	2.212	2.198	2.274	2.007
Ca	1.779	1.843	1.798	1.815	1.809	1.772	1.750	1.791	1.862	1.801	1.730	1.759	1.801	1.843	1.814	1.755	1.887	1.753	1.849	1.830	1.879	1.858	1.765
Mg	3.153	3.722	2.562	2.931	3.629	2.235	3.011	2.042	3.538	2.336	2.153	3.063	2.025	1.790	1.741	1.566	4.083	2.644	3.873	2.505	1.730	2.286	2.944
Fe	1.529	1.154	1.719	1.668	1.288	2.026	1.750	2.180	1.233	1.913	2.114	1.715	2.225	2.225	2.228	2.334	0.998	1.888	1.021	1.811	2.771	2.101	1.506
Mn	0.360	0.035	0.040	0.045	0.060	0.045	0.044	0.041	0.041	0.038	0.054	0.049	0.055	0.060	0.063	0.085	0.019	0.033	0.038	0.043	0.082	0.044	0.033
K	0.051	0.020	0.056	0.039	0.007	0.065	0.060	0.057	0.011	0.064	0.062	0.044	0.082	0.099	0.079	0.055	----	0.049	0.011	0.060	0.273	0.342	0.100
Na	0.294	0.144	0.492	0.389	0.190	0.550	0.313	0.522	0.203	0.594	0.579	0.356	0.593	0.405	0.485	0.483	0.046	0.443	0.087	0.502	0.477	0.484	0.570
Ba	----	----	----	----	----	----	----	----	----	----	----	----	----	----	----	----	----	----	----	----	----	----	----
Sum	15.608	15.129	15.534	15.419	15.182	15.588	15.367	15.611	15.198	15.680	15.599	15.366	15.671	15.539	15.571	15.534	15.048	15.486	15.059	15.551	15.819	15.801	15.613
Assumed Stoichiometry = $AB_2C_5T_8O_{22}(OH)_2$																							
tetrahedral site																							
Si	7.091	7.631	6.546	6.798	7.597	6.424	7.136	6.282	7.485	6.316	6.416	7.004	6.299	6.179	6.193	6.182	7.931	6.770	7.793	6.548	6.324	6.306	6.638
Al	0.910	0.369	1.454	1.202	0.403	1.576	0.864	1.718	0.514	1.684	1.584	0.996	1.701	1.821	1.807	1.818	0.069	1.230	0.207	1.452	1.676	1.694	1.362
Sum	8.001	8.000	8.000	8.000	8.000	8.000	8.000	8.000	7.999	8.000	8.000	8.000	8.000	8.000	8.000	8.000	8.000	8.000	8.000	8.000	8.000	8.000	8.000
C-site																							
Al	0.255	0.191	0.824	0.349	0.186	0.851	0.394	0.935	0.293	0.887	0.867	0.201	0.847	1.079	1.120	1.227	0.011	0.634	0.179	0.760	0.522	0.580	0.645
Ti	0.187	0.020	0.043	0.183	0.012	0.044	0.045	0.043	0.018	0.048	0.040	0.179	0.043	0.038	0.041	0.029	0.003	0.040	0.002	0.040	0.085	0.106	0.050
Fe	1.488	1.134	1.660	1.621	1.258	1.952	1.677	2.077	1.212	1.830	2.027	1.658	2.152	2.152	2.155	2.241	0.979	1.801	1.005	1.762	2.704	2.066	1.457
Mg	3.069	3.655	2.474	2.848	3.544	2.153	2.884	1.945	3.477	2.235	2.065	2.962	1.958	1.732	1.684	1.503	4.006	2.523	3.814	2.438	1.689	2.248	2.849
Sum	4.999	5.000	5.001	5.001	5.000	5.000	5.000	5.000	5.000	5.000	4.999	5.000	5.000	5.001	5.000	5.000	4.999	4.998	5.000	5.000	5.000	5.000	5.001
B-site																							
Fe	0.040	0.021	0.059	0.048	0.030	0.075	0.074	0.103	0.021	0.083	0.086	0.057	0.074	0.073	0.073	0.093	0.019	0.087	0.016	0.048	0.067	0.034	0.049
Mg	0.083	0.067	0.088	0.084	0.085	0.082	0.127	0.096	0.061	0.101	0.088	0.101	0.067	0.058	0.057	0.062	0.076	0.122	0.060	0.067	0.042	0.037	0.096
Mn	0.036	0.035	0.040	0.045	0.060	0.045	0.044	0.041	0.041	0.038	0.054	0.049	0.055	0.060	0.063	0.085	0.019	0.033	0.038	0.043	0.082	0.044	0.033
Ca	1.779	1.843	1.798	1.815	1.809	1.772	1.750	1.791	1.862	1.801	1.730	1.759	1.801	1.843	1.814	1.755	1.888	1.753	1.849	1.830	1.879	1.858	1.765
Na	0.061	0.034	0.016	0.008	0.016	0.026	0.005	0.000	0.014	0.000	0.042	0.033	0.004	0.000	0.000	0.004	0.000	0.005	0.037	0.012	0.000	0.027	0.057
sum	1.999	2.000	2.001	2.000	2.000	2.000	2.000	2.031	1.999	2.023	2.000	1.999	2.001	2.034	2.007	1.999	2.002	2.000	2.000	2.000	2.070	2.000	2.000
A-site																							
Na	0.233	0.110	0.471	0.381	0.174	0.524	0.313	0.522	0.189	0.594	0.537	0.322	0.589	0.405	0.485	0.479	0.046	0.438	0.050	0.490	0.477	0.457	0.514
K	0.051	0.020	0.056	0.039	0.007	0.065	0.060	0.057	0.011	0.064	0.062	0.044	0.082	0.099	0.079	0.055	0.004	0.049	0.011	0.060	0.273	0.342	0.100
sum	0.284	0.130	0.527	0.420	0.181	0.589	0.373	0.579	0.200	0.658	0.599	0.366	0.671	0.504	0.564	0.534	0.050	0.487	0.061	0.550	0.750	0.799	0.614

Footnotes:
(a) Average high-Ti core of zoned porphyroclasts
(b) Average low Al interior region of zoned porphyroclasts
(c) Average high Al rim on zoned porphyroclasts
(d) Point analysis of low Al interior region of zoned porphyroclast
(e) Point analysis of high Al rim of zoned porphyroclast
(f) Average of unzoned porphyroblasts
(g) Point analysis of neoblast center
(h) Point analysis of neoblast rim

Table 6. Chlorite compositions (wt.%) in crystalline cores, Savannah River Site

Core	DRB-1	DRB-1	DRB-1	DRB-1	DRB-1	DRB-1	DRB-2	DRB-2	DRB-4	DRB-6	SSW-2
Sample	DRB1-02	D1-50-1	DRB1-09	DRB1-10	DRB1-11	D1-184-1	DRB2-11	DRB2-14	D4-87-1	DRB6-8	SSW2-4
Depth (ft)	1011.5	1215	1729	1879	1885	1844	1448	1632	1524	1417	944
Footnote	(a)	(a)	(a)	(a)	(a)	(a)	(a)	(a)	(b)	(a)	(c)
n (ave)	3	3	3	2	4	4	2	2	----	2	4
SiO_2	27.30	26.37	26.41	27.28	26.31	26.64	27.10	27.40	25.76	27.97	26.67
TiO_2	0.08	0.10	0.10	0.09	0.07	0.07	0.11	0.13	0.14	0.09	0.07
Al_2O_3	21.54	21.01	21.48	21.27	21.09	21.52	22.02	20.78	21.91	20.22	23.49
CaO	----	0.05	0.06	----	----	----	----	0.04	----	0.05	----
MgO	20.91	19.51	20.31	21.25	19.94	19.50	19.63	17.40	17.63	20.51	21.53
FeO	17.41	19.75	18.55	17.09	18.97	20.09	19.54	22.73	22.46	19.30	16.63
MnO	0.29	0.26	0.15	0.22	0.23	0.26	0.30	0.53	0.34	0.36	0.40
Cl	----	----	----	----	----	----	----	----	----	----	----
F	na	0.11	----	na	----	0.12	0.10	0.09	na	0.05	0.10
Total	87.53	87.11	87.06	87.20	86.61	88.15	88.76	89.06	88.24	88.53	88.85

Footnotes: (a) average neoblast
(b) point analysis of neoblast
(c) average of neoblast and porphyroblast

Table 7. Epidote compositions (wt.%) in crystalline cores, Savannah River Site

Core	DRB-1	DRB-1	DRB-1	DRB-1	DRB-1	DRB-1	DRB-1	DRB-2	DRB-2	DRB-6	DRB-8	SSW-2	P30
Sample	DRB1-02	D1-50-1	DRB1-09	DRB1-10	DRB1-12	D1-184-1	D1-184-1	DRB2-11	DRB2-14	DRB6-8	DRB8-5	SSW2-4	P30-01
Depth (ft)	1011.5	1215	1729	1879	1885	1844	1844	1448	1632	1417	1292	944	786
Footnote	(a)	(b)	(b)	(a)	(c)	(d)	(a)	(b)	(b)	(a)	(a)	(e)	(f)
n (ave)	4	----	----	2	4	----	3	----	----	3	2	2	----
SiO_2	37.94	36.79	37.60	37.51	37.15	37.52	37.28	36.97	36.64	35.79	36.57	36.62	37.09
TiO_2	0.07	0.14	----	----	0.07	----	0.05	0.09	0.09	----	0.09	0.06	----
Al_2O_3	24.73	23.86	23.85	24.32	23.76	25.43	24.13	25.37	23.16	21.46	22.94	25.01	23.06
CaO	23.60	22.97	23.25	23.39	22.73	23.46	23.32	22.91	23.15	23.18	22.99	22.87	22.07
MgO	----	----	----	----	----	----	----	0.09	----	----	----	----	----
Fe_2O_3	11.20	10.76	12.43	11.06	12.07	9.61	11.00	10.13	14.00	14.87	13.37	11.01	11.85
MnO	0.20	0.32	0.29	0.28	0.24	0.26	0.24	0.27	0.24	0.12	0.34	0.79	0.98
Na_2O	----	----	----	----	----	----	----	----	----	----	----	----	----
Total	97.74	94.84	97.42	96.56	96.02	96.28	96.02	95.83	97.28	95.42	96.3	96.36	95.05

Footnotes: (a) average neoblast
(b) point analysis of neoblast
(c) average of inclusions in plagioclase
(d) point analysis of inclusion in plagioclase
(e) average of inclusions in garnet
(f) from Anderson (1997)

ment beneath the Dunbarton basin, and (4) samples from the metavolcanic terrane of Snipes and others (1993). The rocks show a wide variation in composition. For example, SiO_2 varies from 43 to 86 wt.% and MgO from 0.24 to 13.3 wt.% (Figure 5). Other major element oxides and trace element abundances exhibit similar variations, and rock compositions are more or less uniformly distributed through the range. Variable LOI contents reflect the importance of hydrous minerals in the rock assemblages.

There are no striking compositional differences between rocks from the 4 groups, although the metavolcanics tend to be poorer in Al_2O_3 (at similar MgO) than most rocks from the other groups. A number of major element oxides or trace element abundances correlate positively with MgO: these include FeO*, TiO_2, CaO, Cr, V and Ni (Figure 5). Others such as SiO_2, Y, and Zr correlate inversely with MgO. A third group, which encompasses Al_2O_3, the alkalis, Ba and Sr show no correlation with MgO, but Ba and Rb correlate quite well with K_2O. Nb contents are generally very low and below detection limits in many samples. As a group most rocks are relatively sodic and Na_2O/K_2O (weight ratio) is greater than one although exceptions occur (Table 1).

DISCUSSION

Indicators of Low- to Medium Metamorphic Grade

High-grade minerals are generally absent in the core we examined. Even minerals that generally suggest upper low grade or medium grade are not necessarily reliable indicators of that grade. For example, the garnet that occurs locally is considerably manganiferous (Table 4), and

Table 4. Garnet compositions (wt.%) in crystalline cores, Savannah River Site

Core	DRB-2	DRB-2	DRB-2	DRB-2	DRB-4	DRB-4	SSW-2	SSW-2	P30
Sample	DRB2-11	DRB2-11	DRB2-14	DRB2-14	DRB4-13	DRB4-13	SSW2-04	SSW2-04	P30-01
Depth	1448	1448	1632	1632	1524	1524	944	944	786
Footnote	(a)	(b)	(a)	(c)	(d)	(b)	(a)	(b)	(d, e)
n (ave)	2	2	2	----	----	2	5	5	----
SiO_2	36.80	36.88	36.88	36.64	37.23	37.42	36.75	37.13	36.71
TiO_2	0.13	0.10	0.08	----	0.15	----	0.13	0.08	0.13
Al_2O_3	21.19	21.30	21.14	21.13	21.27	21.20	21.27	21.78	20.03
CaO	6.36	5.68	4.85	4.70	5.10	4.21	5.79	4.57	10.48
MgO	2.51	2.94	3.30	2.88	1.89	2.33	2.48	4.45	0.10
FeO	24.56	26.55	26.52	26.73	26.18	27.85	19.55	25.16	13.06
MnO	8.07	6.60	6.57	7.12	9.38	7.63	14.37	7.68	18.94
Cr_2O_3	----	----	----	----	----	----	----	----	----
Na_2O	----	----	----	0.07	----	----	----	----	----
Total	99.62	100.05	99.34	99.27	101.20	100.64	100.34	100.85	99.45
Garnet endmembers (molar proportions)									
alm	0.542	0.580	0.586	0.593	0.574	0.617	0.425	0.538	0.285
gross	0.180	0.159	0.137	0.134	0.143	0.120	0.161	0.125	0.003
pyrope	0.098	0.114	0.130	0.114	0.074	0.092	0.096	0.170	0.292
spess	0.180	0.146	0.147	0.160	0.208	0.171	0.317	0.166	0.420

Footnotes: (a) average grain center; (b) average grain rim; (c) point analysis of grain rim; (d) point analysis of grain center; (e) from Anderson (1997)

Table 5. Biotite compositions (wt.%) in crystalline cores, Savannah River Site

Core	DRB-1	DRB-2	DRB-2	DRB-4	DRB-6	DRB-8	PBF-1	SSW-2	SSW-2	P30
Sample	DRB1-11	DRB2-11	DRB2-14	DRB4-87	DRB6-8	DRB8-5	PBF1-1	SSW2-4	SSW2-12	P30-01
Depth (ft)	1885	1448	1632	1524	1417	1292	1065	944	1286	786
footnote	(a)	(a)	(b)	(a)	(a)	(a)	(c)	(b)	(b)	(d)
n (ave.)	2	2	----	2	3	4	----	----	----	----
SiO_2	37.97	37.65	37.40	36.71	38.75	37.51	39.06	39.07	38.54	36.57
TiO_2	2.03	1.77	1.86	2.27	1.64	2.19	1.59	1.17	1.56	2.02
Al_2O_3	16.62	17.50	17.23	17.76	16.78	15.73	16.32	17.83	17.30	14.71
CaO	0.04	0.05	----	----	0.05	----	----	0.05	----	0.04
MgO	13.34	12.10	10.73	10.91	13.30	10.95	13.38	14.77	16.33	7.98
FeO	16.69	17.70	18.46	19.35	17.77	20.23	16.74	14.56	13.85	24.13
MnO	0.12	0.23	0.24	0.23	0.15	0.45	0.24	0.41	0.13	1.15
K_2O	9.39	9.45	8.58	9.58	9.75	9.42	9.02	8.85	8.84	8.92
Na_2O	0.06	----	0.06	0.05	----	0.04	0.06	----	0.06	----
BaO	0.41	0.49	0.54	0.15	0.31	0.37	0.08	0.23	0.16	0.15
Cl	----	0.10	----	----	----	----	----	----	----	----
F	0.30	0.36	0.23	na	0.16	0.27	0.49	0.66	0.18	1.46
Total	96.84	97.23	95.23	97.01	98.59	97.05	96.77	97.32	96.87	97.14
Mg# [(e)]	0.59	0.55	0.51	0.50	0.57	0.49	0.59	0.64	0.68	0.37

Footnotes: (a) average neoblast; (b) point analysis of neoblast; (c) biotite rim on amphibole; (d) from Anderson (1997); (e) molar Mg/(Mg+Fe) ratio

the cause of the zoning. Although Fe_2O_3 varied slightly between high Z (13.3 wt.% Fe_2O_3) area and low Z (12.7 wt.% Fe_2O_3) areas, the small amount of variation is unlikely to be the cause of the apparent difference in mean Z. The zoned element probably is an element such as Ce which was not analyzed.

WHOLE ROCK COMPOSITIONS

Bulk rock chemical compositions are illustrated in a series of MgO variation diagrams (Figure 5). We divided the rocks into 4 groups based on the distribution of drill holes and the inferred basement geology of Snipes et al. (1993): (1) samples from the tightly clustered DRB 1-8 holes which sampled the central portion of the "penetratively deformed mafic to ultramafic" terrane, (2) samples from the more widely spaced SSW and P6R holes which sampled the same terrane, (3) samples from the CPC, PBF and DRB-9 holes which sampled the amphibolite and biotite gneiss of Snipes and others (1993) or in the case of DRB-9, base-samples from core. The felsic enclaves could be, at least in some cases, "sweat" segregations formed under middle to upper amphibolite conditions. Fibrolite forms at or near the first sillimanite isograd (Kerrick, 1990) and its presence does not require upper amphibolite grade conditions. In fact, fibrolite could be stable at lower temperatures than coarse grained sillimanite (Holdaway, 1971), although understanding of the relative stabilities of these two textural types of sillimanite is currently incomplete (Essene, 1982). Middle amphibolite conditions are indicated by the sillimanite and are presumably related to the regional metamorphic events. Rocks from the biotite gneiss terrane contain a metamorphic assemblage similar to that of the rocks from the penetratively deformed terrane including pargasitic amphibole and oligoclase (Tables 2, 3). Hence these rocks also experienced amphibolite grade metamorphism but Anderson (1997) noted overprinted, retrograde greenschist assemblages in both samples she studied from this terrane.

Rocks from the northwestern portion of the SRS equilibrated at lower-grade metamorphic conditions than the rest of the basement. Some of these rocks have perfectly preserved metavolcanic textures, but the mineralogy is metamorphic and characterized by albite + epidote + chlorite + muscovite + calcite + quartz. Hence, the rocks appear to have experienced greenschist facies metamorphism and Anderson (1997) estimated metamorphic conditions of 400-530°C and approximately 8 kb for those rocks.

Thus, the core reveals abundant evidence that the rocks were regionally metamorphosed under conditions of greenschist to middle amphibolite facies. Whether metamorphic grade increases continuously from the metavolcanic terrane in the northwest to the penetratively deformed terrane in the southeast, or whether the variation in grade reflects a structural discontinuity (Anderson, 1997) is uncertain.

Metamorphic Structures

Some of the drill core has metamorphic structures that indicate tectonic grain size reduction at low metamorphic grade, i.e. mylonitic or cataclastic deformation (e.g. Babaie and La Tour, 1994). Rocks of DRB-4 show this feature very well: biotite-bearing rocks are folded into microfolds, with extensive alteration of biotite to chlorite, some of which has grown in the axial surfaces of the microfolds. Moreover, some muscovite has recrystallized to chlorite. Sigmoidal porphyroclasts of micas and of larger zones of rocks are enclosed by fine grained layer silicates, primarily muscovite and chlorite. These fine grained fabrics are phyllonitic (micaceous mylonitic), and are consistent with strong deformation at low grade (La Tour, 1979). Moreover, in DRB-4 felsic segregations are lenticular or bulbous with narrowed tails. At least some of these are discontinuous (attenuated) fold noses, forming "hooks". These features are also indicative of high strain rates and represent dismembered and "sheared out" parts of the felsic segregations.

Generally, the deformation features observed appear to have formed at low metamorphic grade. These features include mineral foliation and lineation, microfolding, and small shear zones. In some core samples, mineralogy that is of distinctly higher metamorphic grade has overprinted these low-grade deformational features. Syn- or even post-metamorphic, larger-scale structures, e.g. macrofolds, are not commonly evident in the core. However, in hole DRB-4 there are larger fold structures that clearly post-date the fine grained fabric that was sheared out by earlier folds. It is not clear, however, how the latter folds relate to the regional metamorphism or deformation.

The most recent deformational feature in the rocks are veins associated with brittle, throughgoing(?) fractures that cut all other structures (La Tour and others, 1996; Dowling and others, 1996). These appear to have formed as a result of the brittle behavior of the basement rocks, presumably during rifting in Triassic to Jurassic time. The rifting also caused numerous large normal faults, one of which is the Pen Branch fault that runs through the SRS and is marginal to the Dunbarton basin (Stieve and Stephenson, 1995).

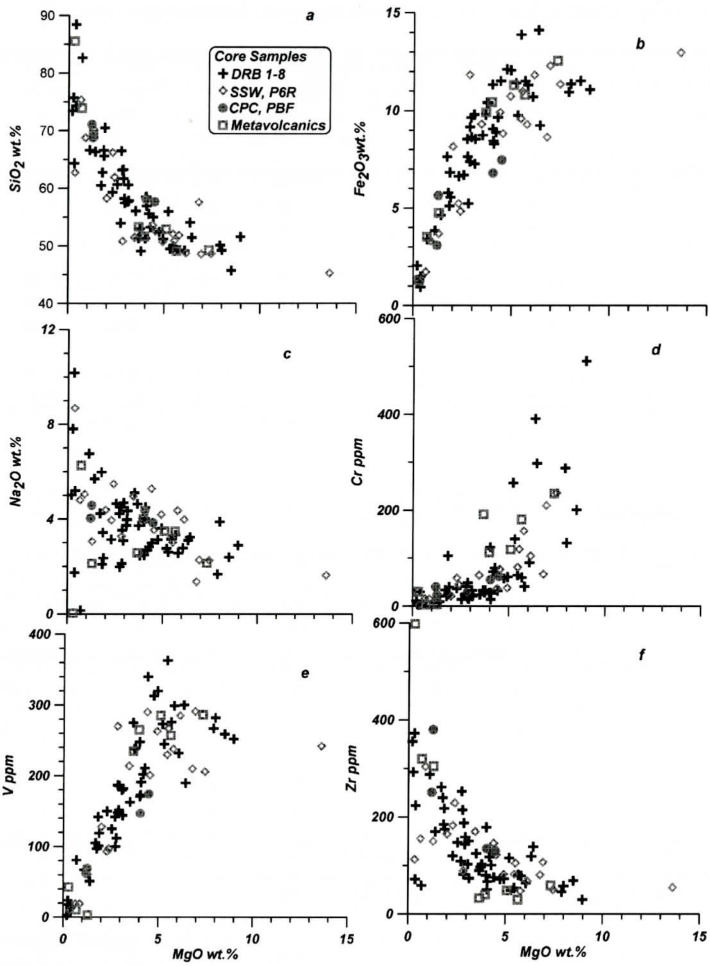

Figure. 5. MgO variation diagrams showing bulk rock compositions of SRS core samples (Table 1). Metavolcanic samples are from drill cores P11R, P30 and P9R. Major elements are plotted on an anhydrous basis

therefore capable of having been stabilized at a relatively low grade (Miyashiro, 1973; Symmes and Ferry, 1992; Yardley, 1989). However, the dominant amphibole composition is not actinolitic, but edenitic or pargasitic, and the metamorphic plagioclase is oligoclase (Table 2), suggesting at least moderate metamorphic temperatures (e.g., Wenk and others, 1974; Winkler, 1979; Yardley, 1989).

Most of the mafic rocks from the penetratively deformed terrane contain abundant epidote. Thin section examination reveals that much of the epidote did not form during retrograde metamorphism from higher grade metamorphic mineralogy but rather from metamorphism of the original igneous mineralogy, primarily plagioclase. Thus, the key mineral indicators of metamorphic grade are pargasitic or edenitic amphibole + oligoclase + epidote which are indicative of lower amphibolite facies (Winkler, 1979).

Anderson (1997) quantified these qualitative ideas for four samples from cores DRB-2 and DRB-4 through thermodynamic modelling of mineral compositions. She estimated peak metamorphic conditions ranging from epidote amphibolite to amphibolite facies (i.e., 540-700°C at about 6 kbar). Consistent with her calculation is the occurrence of minor sillimanite (fibrolite) as well as felsic enclaves in some

Amphibole II - Alteration Amphiboles (Actinolite)

These amphibole domains are green, low in Ti and Al (high Si^{IV}), and have relatively high Mg/Fe ratios (Figure 4). They are actinolite (Leake and others, 1997), not hornblende, and probably formed at low metamorphic grade and in some cases by alteration of original Ti-rich igneous amphiboles (amphibole I). This latter interpretation is supported by the occurrence of composite cores consisting of patchy intergrowths of amphiboles I (magnesiohornblende) and II (actinolite). This texture probably reflects incomplete reaction of amphibole I at relatively low metamorphic grade (Grapes and Graham, 1978).

In situ replacement of amphibole I by amphibole II suggests that the geologic conditions proceeded from high temperature igneous conditions to relatively low temperature, metamorphic conditions without an accompanying deformational event. The amphibole II is probably a pretectonic feature that could have formed, for example, in a hot volcanic pile through which seawater circulated. Alteration of igneous mineralogy in seafloor rocks (so-called seafloor metamorphism) is common (e.g. Alt and others, 1994, 1996; Gillis and others, 1993), and extends to depths of several kilometres in oceanic crust. The alteration can be completely pervasive or occur along microveins and along grain boundaries (e.g. Vanko and Stakes, 1991). In the former case, the rocks may appear simply as greenstones or classic spilites (e.g. Cann, 1969), and may have preserved igneous textures such as the case for some SRS samples.

Amphibole III - Regional Metamorphic Amphibole (Edenitic or Pargasitic Hornblende)

Occurring as the sole amphibole, or constituting rims on cores of either or both of the above amphiboles (Figure 3), is blue-green hornblende. This hornblende is compositionally homogeneous and is relatively low in Ti but relatively high in Al^{IV} (Table 3). This indicates that the amphibole is edenitic or pargasitic hornblende, characteristic of so-called epidote-amphibolite facies of regional metamorphism (Leake, 1968). Hornblende at this grade typically coexists with low-Ca plagioclase and epidote (Winkler, 1979). In the present case, the plagioclase coexisting with the blue-green hornblende is oligoclase to sodic andesine (Table 2), in contrast to Ca-rich plagioclase (calcic andesine, bytownite, etc.) found in amphibolite-grade mafic rocks (Wenk and others, 1974). Moreover, epidote is common in these rocks and is absent in true amphibolites (Wenk and others, 1974).

Amphibole III is the most extensively developed amphibole in the basement samples that we examined, and is commonly the only amphibole in a given sample. In grains where amphibole III forms rims around amphibole I and/or amphibole II, amphibole III rims have a sharp contact with the other amphibole domains. These sharp contacts could result from a solvus in the Ca-amphiboles, particularly at low to medium grades of metamorphism (e.g. Cooper, 1972; Misch and Rice, 1975). More likely, however, the sharp boundaries reflect a change in nature or composition of coexisting phases (e.g., plagioclase) during prograde metamorphism (Grapes and Graham, 1978). Sharp contacts between distinct amphiboles are a common feature in epidote amphibolites, corresponding approximately to the subsolidus jump from albite to oligoclase in the plagioclases (e.g. Hyndman, 1985, p. 586-588).

Recognition of a Dioritic Intrusion

An intriguing lithology found in drill core DRB-1 is a medium to coarse grained felsic rock (Figure 2C) interpreted to be a meta-quartz diorite on the basis of relict igneous textures, mineral zoning and compositions, and bulk composition. Similar rocks are rare in other DRB cores. In DRB-1 the meta-quartz diorite is intimately intermingled with dark fine-grained schists. In some samples the meta-quartz diorite is strongly foliated with no preserved igneous mineralogy. In these rocks, the mineral assemblage, edenitic-pargasitic amphibole, oligoclase, epidote, chlorite, quartz $\pm$ biotite, reflects only peak metamorphic conditions. Other samples, however, have blastoporphyritic textures

Interpretation of Mineral Zoning

Zoned plagioclase and amphibole are only common in the DRB-1 core and even in this core the occurrence of zoned minerals is sporadic. Moreover, zoning is only found in the interior of grains; zoned plagioclase and amphibole always have a rim of oligoclase or pargasitic amphibole, respectively, which are indicative of peak amphibolite grade metamorphism. These characteristics of the zoned minerals indicate that their centers record earlier metamorphic or igneous events which are preserved only where complete chemical equilibrium was not achieved during metamorphism.

Plagioclase porphyroclasts preserve two types of zoning: relatively calcic cores and delicate lamellae of relatively calcic compositions that mimic the oscillatory zoning common in the igneous plagioclases of intermediate volcanic and hypabyssal rocks. Generally, oscillatory zoning of plagioclase is rare in metamorphic rocks (Smith, 1974); in one example, Cannon (1966) interpreted thick (60-100 micrometers) oscillatory zones in matrix plagioclase of amphibolites and granulites from British Columbia as metamorphic in origin. However, the lamellae preserved in the DRB-1 samples are thin (<10 microns thick, Figure 3) and similar to oscillatory zones in igneous plagioclases in thickness and compositional contrasts (Smith, 1974). This similarity combined with extremely sluggish CaAl-NaSi coupled diffusion under metamorphic conditions (e.g., Grove and others, 1984) indicates that igneous oscillatory zoning could easily be preserved during amphibolite grade metamorphism. Hence, we interpret these thin compositional zones in some plagioclases of core DRB-1 to be igneous in origin, and by association, the relatively calcic cores are also thought to be igneous.

As noted, three chemotypes of amphibole occur, and we infer that Amphibole III records the P-T conditions for peak metamorphism based on its volumetric dominance over the other chemotypes, its occurrence as homogeneous grains in equilibrated assemblages, and its occurrence as grain rims on zoned amphiboles. In these latter samples the amphibole III rims are in contact with the other phases (including oligoclase) believed to have formed during peak metamorphism. Most significantly, in all the zoned amphiboles, no matter how small, the rims are consistently composed of amphibole III. In some cases amphibole III forms a rim on a relict porphyroblast of amphibole or on an amphibole that defines the dominant schistosity (Figure 3). It also occurs as rims on tiny grains formed by tectonic grain size reduction or on small neoblasts nucleated during metamorphism (Figure 3). Furthermore, in no sample is amphibole III deformed. All these relations indicate that the deformational event(s) responsible for producing or modifying the metamorphic fabric occurred before the growth of amphibole III.

Amphibole I - Igneous Amphibole Cores (Magnesiohornblende)

This amphibole, occurring only in hole DRB-1, is brown in color and occupies the cores of composite grains (Figure 3). In many cases it contains wisps of apparently exsolved material similar to that seen in pyroxenes of metagabbros. The brown cores are high in Mg, Ti and Al, but their Ti contents are highly variable, even in a single sample. The variation in Ti and tetrahedral Al contents is consistently sympathetic, and is interpreted to represent various degrees of modification of amphibole I. Retrograde breakdown of igneous or metamorphic amphiboles proceeds first with loss of Ti, followed by other adjustments such as loss of Al and rise in Mg/Fe (La Tour, 1979). The color of amphiboles is strongly dependent on Ti (Fyfe, 1964), and the mottled appearance of the brownish cores reflects this variable and incomplete Ti loss. The grain shapes, exsolution features, and composition of the brown amphibole cores (magnesiohornblende) are interpreted as original igneous features, some of which have been modified or obliterated during metamorphism. These partially preserved igneous features are consistent with the partially preserved oscillatory zoning in the co-existing relict igneous plagioclases in the same rocks of DRB-1.

crease (e.g., Pettijohn, 1975). One way to illustrate this point is to calculate ratios of relatively soluble oxides torelatively immobile oxides such as Fe_2O_3 or Al_2O_3 (Garrels and Mackenzie, 1971). Mature sediments such as shales or their metamorphic equivalents, mica schists, are characterized by relatively high K_2O/Al_2O_3 but low Na_2O/Al_2O_3 ratios (Figure 6) compared to igneous rocks. In contrast most of the core samples have relatively high Na_2O/Al_2O_3. In fact, the bulk chemical trends of the core samples mimic the variability in FeO/CaO, FeO/K_2O and Na_2O/Al_2O_3 of average igneous rocks and are distinct from mature sediments such as shales and their metamorphic equivalents (Figure 6). Moreover, the compositional variation as well as absolute abundances of oxides (e.g., increasing SiO_2, Zr and decreasing FeO*, Cr, V with decreasing MgO, Figure 5) are similar to trends and absolute abundances in igneous rock series (LeMaitre, 1976; Cox and others, 1979). Some rocks have silica contents higher than typical igneous rocks (Figure 5) or are aluminous based on the abundance of metamorphic muscovite in them and these rocks probably represent silicified igneous rocks, clastic sediments or metamorphosed pelites. However, based on the bulk compositional similarity in a relative and absolute sense to igneous rock series, we conclude that the SRS core samples are dominated by a heterogeneous group of meta-igneous rocks and relatively immature sediments derived from them. The relative proportions of the igneous and sedimentary components is uncertain and probably impossible to determine but the data are permissive of a dominantly igneous pile of rocks and minimal amounts of sediments.

Most rocks have relatively high Na_2O and $Na_2O/ K_2O >1$ (Table 1). The possibility of alkali mobility during metamorphism complicates the interpretation of the alkali abundances and the low Na_2O contents of a few MgO-poor rocks (Figure 5) points to some alkali mobility. However most MgO-poor rocks are relatively Na_2O-rich and as noted in the previous paragraph the Na_2O/Al_2O_3 ratios of most rocks are consistent with an igneous source, and in fact point to nearly closed system (excluding H_2O)

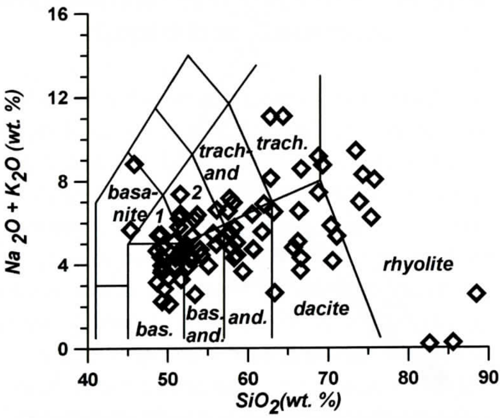

Figure 7. SRS core samples (anhydrous) plotted on the IUGS total alkali-silica classification grid (Le Bas and Streckeisen, 1991).Fields 1 and 2 are for trachybasalt and basaltic trachy andesite, respectively.

metamorphism. Most core samples are relatively potassium-poor and potassic phases (except biotite) are uncommon to rare, and vein mineralogy is dominated by Ca- and Si- rich phases rather than alkali phases (Vanko and Capps, 1995). These observations point towards a potassium-poor igneous series although minor amounts of potassic, foliated granite (K-feldspar dominated) occur in the core.

Based on the discussion above we plotted bulk compositions of the SRS core samples on on the IUGS total alkali-silica classification grid for volcanic rocks (Figure 7). Compositions are variable and range from basalt to rhyolite; most compositions are subalkaline but mildly alkaline compositions such as trachybasalts also occur. Although Snipes and others (1993) describe the terrane sampled by the DRB 1-8 holes as "penetratively deformed mafic to *ultramafic* rocks" (our italics) there are common felsic compositions and only one sample that we analyzed could be considered to be ultramafic. Evolved alkaline compositions are uncommon and most evolved compositions plot in the rhyolite or dacite fields, and hence, if the variation is viewed as one of an igneous series, the series appears to be dominantly subalkaline, and the wide variation in composition is suggestive of a volcanic arc origin. Bulk compositions plotted on an AFM diagram (Figure 8), are conwith large plagioclase porphyroclasts that are commonly zoned. The most striking zoned minerals are plagioclase porphyroclasts with calcic cores (to An_{56}) and oscillatory zoning (Figure 3) surrounded by a metamorphic rim of oligoclase (An_{20}). This zoning is interpreted to record igneous crystallization as noted above. Some amphibole porphyroclasts also contain a brown Ti-rich magnesiohornblende core also interpreted to be igneous in origin.

Bulk chemical analyses of samples of the meta-quartz diorite (samples DRB1-02, 05, 07, 08, 10, 11, 12, Table 1) are relatively low in K_2O (<1%) and intermediate in SiO_2 (~56%) contents and thus the rocks are approximately equivalent to a diorite or quartz diorite. Calculated CIPW norms confirm these ideas: most samples plot within the IUGS fields for quartz diorite or quartz monzodiorite.

The medium- to coarse-grain size and the blastoporphyritic texture of some samples suggests that the meta-quartz diorite was a relatively shallow intrusion. The intimate intermingling of the meta-quartz diorite and fine grained schists in core DRB-1 indicate that the original quartz diorite intruded wallrocks which we interpret to be fine-grained volcanic ejecta or sediments as discussed below. The entire package of rocks were deformed together. The rarity of the meta-quartz diorite in adjacent cores of the DRB cluster suggest that the original intrusion was small.

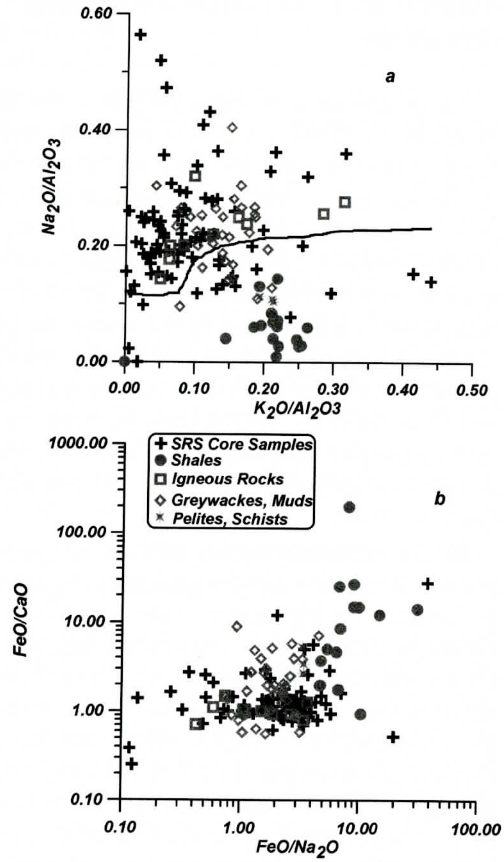

Figure 6. Bulk rock compositions of SRS core samples compared to average shales (Pettijohn, 1975; Taylor and McLennan, 1985), average igneous rocks (basalts/gabbros to rhyolites/granites; Taylor and McLennan, 1985; Clark, 1966), graywackes and deep sea muds and sands (Pettijohn, 1975; Taylor and McLennan, 1985, and average pelites and schists (Miyashiro, 1994). The black line in 6A is the discriminant line separating igneous rocks from shales, slates, pelites and schists (generalized from Garrels and Mackenzie, 1971). All iron is treated as ferrous

Basement Protoliths

The remnant igneous textures of some core samples points to an igneous protolith for these samples (Figures 2B, 2C). Mineral zoning, i.e., oscillatory zoning and relatively calcic cores of some plagioclases and the preservation of Ti-rich, brown hornblende cores in some amphiboles (Figure 3) are also indicative of an igneous protolith in that the mineral zoning and/or compositions are typical of igneous rocks. However, many of the rocks are fine-grained schists (Figure 2A) and their protoliths are not readily deduced from textures or mineral compositions. Nonetheless, the bulk compositions of most core samples are consistent with an igneous (or immature sediment derived from an igneous) source (see also Mauldin and others, 1997; La Tour and others, 1997).

As sediments mature due to mechanical sorting and chemical reactions, their bulk compositions become distinct from their protoliths. Relative to igneous sources, mature sediments are relatively depleted in Na_2O and commonly in CaO while K_2O contents remain high or in-plutonism, and attendant erosion and sedimentation related to a volcanic arc which formed over a subduction zone during the early Paleozoic era or earlier. The geochemical characteristics and the inferred convergent tectonic setting suggest a similarity between these rocks and those of other nearby terranes of Georgia and South Carolina. Whitney and others (1977) interpreted the Carolina slate belt rocks as parts of a primitive island arc sequence, dominated by low-K arc tholeiites. However, the extensive compositional variation for the SRS rocks suggests a mature arc setting rather than the primitive arc setting envisioned for the slate belt rocks to the northwest. During and following development of the arc, interaction of the hot rocks with seawater caused localized conversion of the igneous mineralogy to relatively low temperature metamorphic mineralogy (amphibole II: actinolite), without apparent deformation. Subsequent thrusting associated with accretion of this terrane caused thickening of the stack and development of pervasive schistosity and strong mineral lineations in the volcanic and volcaniclastic rocks. Locally, massive, coarse grained, and perhaps drier rocks such as the meta-quartz diorite escaped complete penetrative deformation, as less competent rocks deformed around them. Shear zones of high internal deformation formed in places, cutting across the earlier penetrative schistosity, and reducing the grain size of earlier metamorphic mineralogy.

During and following thrusting, the thickened pile sank isostatically, and heat migrated upward in the pile. Heating continued well after the pile had been thickened, forming the metamorphic mineralogy (e.g., pargasitic amphibole rims, oligoclase to sodic andesine overgrowths, and neoblasts) as an overprint on the tectonic fabric. Any later deformation apparently occurred as macrofolds and mesofolds (and faults?), but these structures do not appear to have been associated with a distinct metamorphic event. These post-metamorphic structures were not evident enough in the core for thorough study, and their significance cannot be properly assessed at this time.

Appalachian Tectonics and the SRS Crystalline Basement

The SRS basement appears to represent an example of another volcanic/intrusive terrane which was deformed and metamorphosed during accretion onto the proto-North American continent. In general terms, these rocks are comparable to those of the Carolina (Avalon) terrane to the northwest which consists of accreted arc rocks (Hatcher, 1972, 1987). The igneous age of the SRS basement may be similar to that of the Lincolnton metavolcanics of the Carolina terrane, i.e. Cambrian (Whitney and others, 1977), but its accretion age is most likely similar to that of other nearby terranes, i.e., Carboniferous (Hatcher, 1972).

In the Carolina terrane high and low grade rocks alternate in "belts" approximately parallel to the boundaries of the terrane (e.g., Rankin and others, 1989). For example, in Georgia and South Carolina, Carolina slate belt and higher grade Charlotte belt lithologies occur adjacent to each other to the southeast of the Inner Piedmont (e.g. Secor and others, 1986a; Whitney and Allard, 1990). The Carolina slate belt consists of weakly metamorphosed and deformed volcanic rocks and associated volcanic sediments, whereas Charlotte belt lithologies consist of higher grade metamorphic rocks and associated granitic rocks. Rocks of both belts are believed to be related to the same volcanic arc now exposed at different erosional levels due to thrusting and folding (Dallmeyer and others, 1986; Secor and others, 1986a). To the southeast the repetition of belts of distinct metamorphic grades is repeated in the Kiokee and Belair belts (Secor and others, 1986b). The juxtaposition of relatively low grade rocks at the northwest corner of the SRS with higher grade rocks to the southeast suggest that the alternation of high and low grade belts extends to the southeast of surface outcrops of the Carolina terrane.

As indicated by amphibolite assemblages and granitic intrusions, high temperatures affected the Charlotte belt rocks. Mineral compositions in rocks from the SRS drill core indicates metamorphism at relatively deep lev-

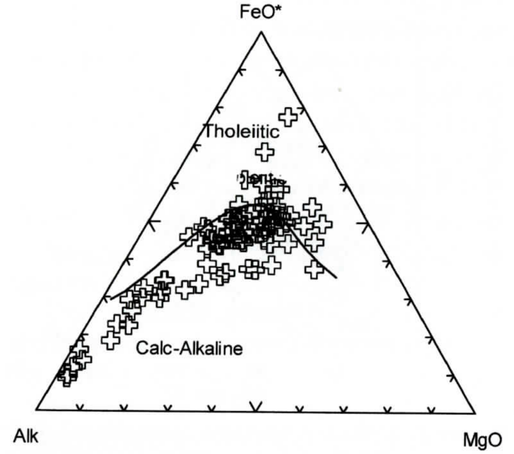

Figure 8. SRS core samples (anhydrous) plotted on the AFM discriminant diagram; line dividing tholeiitic from calc-alkaline trends is taken from Irvine and Baragar (1971).

sistent with this idea: the rocks define a trend without significant Fe-enrichment, consistent with a fundamentally calc-alkaline lineage. This idea is also supported by a more detailed look at 5 fine-grained schists and 7 medium- to coarse-grained meta-quartz diorites from core DRB-1. These samples can plausibly be related to each other by magmatic processes based on their close spatial association and the common occurrence of remnant igneous zoning and textures in the samples from this core. Moreover, variations of oxides and trace elements relative to MgO are consistent with closed system crystallization of a mafic magma. On a plot of MgO vs FeO* (Figure 9) the DRB-1 samples lack the distinct iron enrichment typical of the tholeiitic magmatic systems (e.g., Wright and Fiske, 1971) and instead define a trend of declining FeO* with decreasing MgO as is typical in arc volcanic rocks (Maaloe and Peterson, 1981). Also consistent with this magmatic setting are low TiO_2 abundances (near 1 wt.% for a rock with 8 wt.% MgO), and Nb abundances (many below detection limits) in rocks of basaltic composition (Table 1). All of these chemical characteristics suggest that most of the rocks represent a combination of calc-alkaline mafic to intermediate extrusive and intrusive rocks (and related immature sediments) such as are found in convergent margin volcanic settings (Gill, 1981).

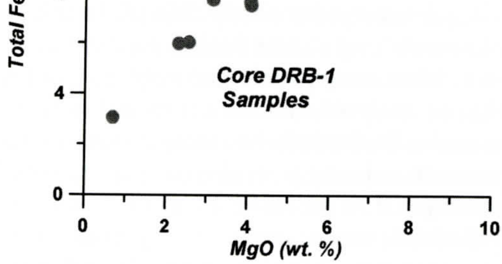

Figure 9. MgO variation diagram for DRB-1 core samples; Makaopuhi lava lake (Kilauea) liquid line of descent from Wright and Okamura (1977).

Identification of protoliths for many metamorphic rocks can be difficult; however, many factors including textures and stratigraphic relations as well as bulk rock compositions can yield important constraints on the nature of the protoliths. In the present rocks, variable bulk compositions and especially compositions similar in key respects (Na_2O/Al_2O_3, CaO/FeO) to igneous rock compositions as well as compositional variations (e.g., decreasing Cr, increasing Zr with decreasing MgO) consistent with magmatic differentiation and blastoporphyritic textures and igneous-style mineral zoning of some rocks, all point to dominantly (but not exclusively) igneous protoliths. Although some rocks may be metasediments, and a few are clearly altered, the majority of the rocks have mafic to intermediate (locally felsic) compositions that can be interpreted in terms of original igneous geochemistry.

For the purposes of this discussion we include the relatively low grade metavolcanic rocks from the northwestern corner of the site with the rest of the SRS core that we investigated. Limited "exposure" in the form of incomplete drill core allows only tentative interpretation of the tectonic history of the rocks. Rocks of the SRS core reflect volcanism,

tile shear zone: Tectonophysics, v. 229, p. 19-30.

Cann, J.R., 1969, Spilites from the Carlsbad Ridge, Indian Ocean: Journal of Petrology, v. 10, p. 1-19.

Cannon, R.T., 1966, Plagioclase zoning and twinning in relation to the metamorphic history of some amphibolites and granulites: American Journal of Science, v. 264, p. 526-542.

Capps, R.C., Whitney, J.A., Roden, M.F., La Tour, T.E., and Vanko, D.A., 1995, Crystalline basement lithologies from beneath the Savannah River Site (SRS): Geological Society of America Abstracts with Programs, v. 27, no. 2, p. A41.

Cooper, A.F., 1972, Progressive metamorphism of metabasic rocks from the Haast schist group of southern New Zealand: Journal of Petrology, v. 13, p. 457-492.

Cooper, A.F. and Lovering, J.F., 1970, Greenschist amphiboles from Haast River, New Zealand: Contributions to Mineralogy and Petrology, v. 27, p. 11-24.

Cox, K.G., Bell, J.D., and Pankhurst, R.J., 1979, The Interpretation of Igneous Rocks: Allen and Unwin: London, 450 p.

Clark, S.P., 1966, Composition of rocks: Geological Society of America Memoir 97, p. 1-6.

Dallmeyer, R.D., Wright, J.E., Secor, D.T., Jr., and Snoke, A.W., 1986, Character of the Alleghanina orogeny in the southern Appalachians: Part II. Geochronological constraints on the tectonothermal evolution of the eastern Piedmont in South Carolina: Geological Society of America Bulletin, v. 97, p. 1329-1344.

Dennis, A.J., Maher, H.D. Jr., Shervais, J.W., and Wright, J.E., 1997, Tectonic inheritance at the Savannah River `Site, SC: Geological Society of America Abstracts with Programs, v. 29, N. 3, p. 12.

Dowling, S.M., Hunter, M.A., Rhodes, G.B., Yatabe, A.P., Rose, S.E., and Vanko, D.A., 1996, Mineralogic controls on deep ground water within crystalline basement rocks, Savannah River Site, SC: Geological Society of America Abstracts with Programs, v. 28, no. 2, p. A10.

Essene, E.J., 1982, Geologic thermometry and barometry, *in*: Characterization of metamorphism through mineral equilibria: Reviews in Mineralogy, v. 10, Mineralogical Society of America, p. 153-206.

Fyfe, W.S., 1964, Geochemistry of Solids: McGraw-Hill, New York, 199 p.

Garrels, R.M., and Mackenzie, F.T., 1971, Evolution of Sedimentary Rocks: Norton, New York, 397 p.

Gill, J., 1981, Orogenic Andesites and Plate Tectonics: Springer-Verlag, New York, 390 p.

Gillis, K.M., Thompson, G., and Kelley, D.S., 1993, A view of the lower crustal component of hydrothermal systems at the mid-atlantic ridge: Journal of Geophysical Research-Solid Earth, v. 98, p. 19597-19619.

Grapes, R.H. and Graham, C.M., 1978, The actinolite-hornblende series in metabasites and the so-called miscibility gap: a review: Lithos, v. 11, p. 85-97.

Grove, T.L., Baker, M.B. and Kinzler, R.J., 1984) Coupled CaAl-NaSi diffusion in plagioclase feldspars: Experiments and applications to cooling rate speedometry: Geochimica et Cosmochimica Acta, v. 48, p. 2113-2122.

Hatcher, R.D. Jr., 1972, Developmental model for the southern Appalachians: Geological Society of America Bulletin, v. 83, p. 2735-2760.

Hatcher, R.D. Jr., 1987, Tectonics of the southern and central Appalachian internides: Annual Review of Earth and Planetary Science, v. 15, p. 337-362.

Hatcher, R.D., Jr., Thomas, W.A. and Viele, G.W. (eds.), 1989, The Appalachian-Ouachita Orogen in the United States: Geological Society of America, Boulder CO, 767 p.

Holdaway, M.J., 1971, Stability of andalusite and the aluminum silicate phase diagram: American Journal of Science, v. 271, p. 97-131.

Hyndman, D.A., 1985, Petrology of Igneous and Metamorphic Rocks: McGraw-Hill Book Co., New York, 786 p.

Irvine, T.N. and Baragar, W.R.A., 1971, A guide to the chemical classification of the common volcanic rocks: Canadian Journal of Earth Sciences, v. 8, p. 523-548.

Kerrick, D.M., 1990, The Al_2SiO_5 Polymorphs: Reviews in Mineralogy, v. 22: The Mineralogical Society of America, Washington, 406 p.

La Tour, T.E., 1979, The nature and origin of the Grenville front: A reinterpretation: unpublished Ph.D. thesis, University of Western Ontario, 344 p.

La Tour, T.E., 1989, Analysis of rocks using X-ray fluorescence spectrometry: The Rigaku Journal, v. 6, p. 3-9.

La Tour, T.E., Roden, M.F., Vanko, D.A., and Whitney, J.A., 1996, Crystalline basement core --Savannah River Site. ERDA Task 53 Final Report to Westinghouse Savannah River Company, 305 p.

La Tour, T.E., Roden, M.F., Whitney, J.A. and Capps, R.C., 1997, Geochemistry of metavolcanic rocks below the Savannah River Site: speculation s on affinity and origin: Geological Society of America Abstracts with Programs, v. 29, number 3, p. 29.

Leake, B.E., 1968, A catalog of analyzed calciferous and subcalciferous amphiboles together with their nomenclature and associated minerals: Geological Society of America Special Paper 98, 210 p.

Leake, B.E., Woolley, A.R., Arps, C.E.S., Birch, W.D., Gilbert, M.C., Grice, J.D., Hawthorne, F.C., Kato, A., Kisch, H.J., Krivovichev, V.G., Linthout, K., Laird, J., Mandarino, J.A., Haresch, W.V., Nickel, E.H., Rock, N.M.S., Schumacher, J.C., Smith, D.C., Stephenson, N.C.N., Ungaretti, L., Whittaker, E.J.W., Youzhi, G., 1997, Nomenclature of amphiboles: report of the Subcommittee on Amphiboles of the International Mineralogical Association, Commission on New Minerals and Mineral Names: Canadian Mineralogist, v. 35, p. 219-246.

Le Bas, M.J. and Streckeisen, A.L., 1991, The IUGS systematics of igneous rocks: Journal of the Geological Society of London, v. 148, p. 824-833.

Le Maitre, R.W., 1976, The chemical variability of some common igneous rocks: Journal of Petrology, v. 17, p.587-637.

Maaloe, S. and Petersen, T.S., 1981, Petrogenesis of oceanic andesites: Journal of Geophysical Research, v. 86, p.

els without widespread granitic plutonism (Anderson, 1997). Except for these differences, rocks of the SRS drill cores and Charlotte belt and Carolina Slate belt may have formed in similar environments. The high pressure metamorphism of the SRS drill core is consistent with common regional metamorphism, ranging from greenschist to middle amphibolite grade. This would mean that the SRS rocks acquired their metamorphic characteristics at depths similar to those of the Charlotte belt, probably as part of the regional metamorphism associated with accretion and crustal thickening. General absence of granitic or other post-volcanic intrusive lithologies in the drill core suggests that widespread melting such as occurred in the Charlotte belt did not occur in the SRS basement. This difference may be a simple function of the more southeasterly position of the SRS rocks, off the thermal axis of the orogen.

CONCLUSIONS

The petrology and bulk compositions of core samples from crystalline basement at the SRS are consistent with derivation from a terrane composed mainly of greenschist to amphibolite grade metavolcanic rocks, related hypabyssal metaplutonic rocks as well as immature metasediments. A small area in the northwestern part of the SRS is underlain by metavolcanic rocks that have been little metamorphosed and little deformed. However, higher grade, amphibolite facies rocks underlie most of the northwestern half of the SRS. These rocks have been severely deformed more than once and are metamorphosed to at least first sillimanite isograd. Bulk compositions of these rocks are consistent with protoliths that were dominated by volcanic rocks, shallow plutonic rocks and immature sediments derived from the magmatic rocks. Sporadically preserved igneous mineral zoning and textures confirm an igneous protolith for at least some rocks and complexly zoned amphibole porphyroclasts record progressive metamorphism through greenschist and amphibolite facies. All these rocks appear to be part of a fundamentally calc-alkaline lineage that formed in a convergent margin setting. These observations suggest that the rocks exposed in the core may be similar to other rocks exposed at the surface elsewhere in the Georgia and South Carolina Piedmont and form another portion of the accreted arc terranes of the southeastern United States.

ACKNOWLEDGEMENTS

Research supported by Education, Research, and Development Association of Georgia Universities (ERDA), Task 53, Prime Contract No. DE-AC09-89SR18035. We thank Dr. Ratib Karam, Executive Director of ERDA, for his cooperation and support, and the Westinghouse Savannah River Company (WSRC) for access to the core samples. In particular, Dr. Richard Strom (WSRC) was instrumental in the conception of the work, and Drs. Sharon Lewis and R.J. Cumbest of WSRC acted as the technical liaisons for the task period. The electron microprobe facility is maintained by support from the University of Georgia and the National Science Foundation. We thank Chris Fleisher for help with operation of the microprobe, Scott Vetter and Allen Dennis for their reviews and Gilles Allard for his comments on the manuscript.

REFERENCES CITED

Alt, J.C., Laverne, C., Vanko, D.A., Tartarotti, P., Teagle, D.A.H., Bach, W., Zuleger, E., Erzinger, J., Honnorez, H., Pezard, P., Becker, K., Salisbury, M.H., and Wilkens, R.H., 1996, Hydrothermal alteration of a section of upper oceanic crust in the eastern equatorial Pacific: A synthesis of results from Site 504 (DSDP Legs 69, 70, and 83, and ODP Legs 111, 137, 140, and 148), *in*: J.C. Alt, H. Kinoshita, L.B. Stokking, P.J. Michael, eds. Proceedings of the Ocean Drilling Program, Scientific Results, vol. 148. College Station, TX, Ocean Drilling Program, 1996, p. 417-434.

Alt, J.C., Honnorez, J., Laverne, C., and Emmermann, R., 1994, Hydrothermal alteration of a 1 km section through the upper oceanic crust, Deep Sea Drilling Project Hole 504B: Mineralogy, chemistry, and evolution of seawater-basalt interactions: Journal of Geophysics, v. 91, p. 10309-10335.

Anderson, V.M., 1997, The metamorphic conditions of the crystalline basement rocks beneath the Savannah River Site, South Carolina, unpublished M.S. thesis, University of Georgia, 135 p.

Babaie, H.A. and La Tour, T.E., 1994, Semibrittle and cataclastic deformation of hornblende-quartz rocks in a duc-

SOUTHEASTERN GEOLOGY
V. 41, No. 1, March 2002, p. 63-73

THE OCCURRENCE OF SEPTARIAN AND NON-SEPTARIAN CONCRETIONS IN THE UPPER CRETACEOUS BLUFFTOWN FORMATION, SOUTHWESTERN GEORGIA, U.S.A., AND THEIR RELATIONSHIP TO SYNSEDIMENTARY SEISMICITY

CARL R. FROEDE JR.

RALPH O. HOWARD JR.

United States Environmental Protection Agency
Region 4
61 Forsyth Street
Atlanta, GA 30303-8960

ABSTRACT

Septarian and non-septarian concretions have been found in the upper portion of the Blufftown Formation at several locations along a section of Hannahatchee Creek, in Stewart County, Georgia. These diagenetic features likely originated under shallow burial conditions before the surrounding sediment was compacted. Their general north-south outcrop orientation within the east to west flowing creek suggests they formed due to channelized diagenetic fluid flow. The origin of the forces necessary to create the cracks and brecciation inside the septarian concretions remains unresolved. However, the septaria in this study exhibit features consistent with seismically-induced crack development in keeping with a recently proposed mechanism. The Chattahoochee River Valley has experienced seismic events throughout its history. This area has likely experienced one or more seismic events during the late Cretaceous which has resulted in the formation and development of septarian concretions.

INTRODUCTION

Concretions occur in the upper portion of the Blufftown Formation, which is exposed along Hannahatchee Creek, in Stewart County, Georgia. Although non-septarian concretions have previously been reported from the Blufftown Formation, little has been written about them or their relationship to septarian concretions also found in the same formation. This paper presents a brief outline of the size and significance of both septarian and non-septarian concretions, their possible origin, and their areal extent in the upper portion of the Blufftown Formation. A recent proposal that septarian cracks may result from seismic forces operating on concretions during their initial diagenesis (Pratt, 2001) was also considered, and the initial results of this investigation appear to support this synsedimentary seismic origin. The terms concretion, septaria, septarian, and septarium are defined in the appendix.

GEOLOGIC SETTING

Location

The septarian and non-septarian concretions described in this report were noted at several locations along Hannahatchee Creek in southwestern Georgia (Figure 1). The creek drains a small watershed and flows west, generally along regional strike, to Lake Eufaula. It has incised into Upper Cretaceous strata including, from oldest to youngest, the Eutaw Formation, Blufftown Formation, and the Cusseta Sand. This investigation only examined strata from the upper Blufftown Formation to the lower Cusseta Sand. Septarian and non-septarian concretions were only observed in the upper few meters of the Blufftown Formation.

10273-10286.

Maher, H.D. Jr., Dallmeryer, R.D., Secor, D.T. and Sacks, P.E., 1994, 40Ar/39Ar constraints on chronology of Augusta fault zone movement and late Alleghanian extension, southern Appalachian Piedmont, South Carolina and Georgia: American Journal of Science, v. 294, p. 428-448.

Marine, I.W., and Siple, G.E., 1974, Buried Triassic basin in the central Savannah River area, South Carolina and Georgia: Geological Society of America Bulletin, v. 85, p. 311-320.

Mauldin, J., Shervais, J., and Dennis, A.,J., 1997, Basement core from the Savannah River Site, South Carolina: Petrology and geochemistry of an accreted island arc: Geological Society of America Abstracts with Programs, v. 29, p. 57.

Miyashiro, A., 1973, Metamorphism and Metamorphic Belts: John Wiley and Sons, New York, 492 p.

Miyashiro, A., 1994, Metamorphic Petrology: Oxford, New York, 404 p.

Misch, P. and Rice, J.M., 1975, Miscibility of tremolite and hornblende in progressive Skagit metamorphic suite, north Cascades, Washington: Journal of Petrology, v. 16, p. 1-21.

Norrish, K. and Hutton, J.T., 1969, An accurate X-ray spectrographic method for the analysis of a wide range of geological samples: Geochimica et Cosmochimica Acta, v. 33, p. 431-453.

Pettijohn, F.J., 1975, Sedimentary Rocks: Harper and Row, New York, 628 p.

Rankin, D.W., Drake, A.A. Jr., Glover, L. III, Goldsmith, R., Hall, L.M., Murray, D.P. Ratcliffe, N.M., Read, J.F., Secor, D.T. Jr. and Stanley, R.S., 1989, Pre-orogenic terranes, *in* Hatcher, R.D. Jr., Thomas, W.A., and Viele, G.W., eds., The Appalachian-Ouachita Orogen in the United States: Geological Society of America, Boulder CO, p. 7-100.

Roden, M.F. and Shimizu, N., 1993, Ion microprobe analyses bearing on the composition of the upper mantle beneath the Basin and Range and Colorado Plateau Provinces: Journal of Geophysical Research, v. 98, p. 14091-14108.

Secor, D.T. Jr., Snoke A.W. and Dallmeyer, R.D., 1986a, Character of the Alleghanian orogeny in the southern Appalachians: Part III: Regional tectonic relations: Geological Society of America Bulletin v. 97, p. 1345-1353.

Secor, D.T. Jr., Snoke, A.W., Bramlett, K. W., Costello, O.P., and Kimbrtell, O.P., 1986b, Character of the Alleghanian orogeny in the southern Appalachians: Part I. Alleghaninan deformation in the eastern Piedmont of South Carolina, Geological Society of America Bulletin v. 97, p. 1319-1328.

Smith, J.V., 1974, Feldspar Minerals, v. 2, Chemistry and Textures: Springer-Verlag, New York, 690 p.

Snipes, D.S., Fallaw, W.C., Price, V. Jr., and Cumbest, R.J., 1993, The Pen Branch Fault: Documentation of late Cretaceous-Tertiary faulting in the coastal plain of South Carolina: Southeastern Geology v. 33, 195-218.

Stieve, A., and Stephenson, D., 1995, Geophysical evidence for post late Cretaceous reactivation of basement structures in the central Savannah River area: Southeastern Geology, v. 35, p. 1-20.

Symmes, G.H. and Ferry, J.M., 1992, The effect of whole-rock MnO content on the stability of garnet in pelitic schists during metamorphism: Journal of Metamorphic Geology, v. 10, p. 221-237.

Taylor, S.R. and McLennan, S.M., 1985, The Continental Crust: Its Composition and Evolution: Blackwell: Oxford, 312 p.

Thomas, W.A., Chowns, T.M., Daniels, D.L., Neathery, T.L., Glover, L. III, and Gleason, R.J., 1989a, The subsurface Appalachians beneath the Atlantic and Gulf Coastal Plains, *in* Hatcher, R.D. Jr., Thomas, W.A., and Viele, G.W., eds., The Appalachian-Ouachita Orogen in the United States: Geological Society of America, Boulder CO, p. 445-458.

Thomas, W.A., Chowns, T.M., Daniels, D.L., Neathery, T.L., Glover, L. III, and Gleason, R. J., 1989b, Pre-Mesozoic paleogeologic map of Appalachian-Ouchita orogen beneath Atlantic and Gulf Coastal Plains, *in* Hatcher, R.D. Jr., Thomas, W.A., and Viele, G.W., eds., The Appalachian-Ouachita Orogen in the United States: Geological Society of America, Boulder CO, plate 6.

Vanko, D.A. and Stakes, D.S., 1991, Fluids in oceanic layer 3: evidence from veined rocks, hole 735B, southwest Indian ridge, *in:* R.P. Von Herzen, P.T. Robinson, et al., eds., Proceedings of the Ocean Drilling Program, Scientific Results, v. 118:Ocean Drilling Program, College Station, TX, p. 181-215.

Vanko, D.A. and Capps, R.C., 1995, History of fluids in the basement, Savannah River Site, South Carolina: Vein mineralogy and fluid inclusions: Geological Society of America Abstracts with Programs, v. 27, no. 2, p. A94.

Wenk, E., Schwander, H. and Stern, W., 1974, On calcic amphiboles and amphibolites from the Lepontine Alps: Schweiz. Mineral. Petrol. Mitt., v. 54, p. 97-149.

Winkler, H.G.F., 1979, Petrogenesis of Metamorphic Rocks: Springer Verlag, New York, 348p.

Whitney, J.A., Paris, T.A., Carpenter, R.H., and Hartley, M.E., 1977, Volcanic evolution of the southern slate belt of Georgia and South Carolina: a primitive oceanic island arc: Journal of Geology, v. 86, pp. 173-192.

Whitney, J.A. and Allard, G.O., 1990, Structure, tectonics, and ore potential along a transect across the Inner Piedmont, Charlotte belt, and Slate belt of eastern Georgia. Georgia Geological Society Guidebooks, v. 10, 45 p.

Wright, T.L., and Fiske, R.S., 1971, Origin of differentiated and hybrid lavas of Kilauea volcano, Hawaii: Journal of Petrology, v. 12, p. 1-66.

Wright, T.L. and Okamura, R.T., 1977, Cooling and crystallization of Tholeiitic basalt, 1965 Makaopuhi Lava Lake, Hawaii, U.S. Geological Survey Professional Paper 1004, 78 p.

Yardley, B.W.D., 1989, An Introduction to Metamorphic Petrology: Longman Scientific and Technical and John Wiley and Sons, New York, 248 p.

Figure 2. Small concretions, 15 to 45 cm in diameter (location C-2) exposed in the Blufftown Formation, in Hannahatchee Creek.

Skotnicki, 1986a, 1986b; 1994). The formation reflects at least two sea-level highstand to lowstand cycles (Reinhardt, 1982), with the latter regression ending in a shoaling event as indicated by the transition of the Blufftown Formation micaceous clays to cross-bedded and bioturbated sands of the Cusseta Sand.

According to Schwimmer (1981, 1986), Schwimmer and Case (1987), and Frazier (1997), the Blufftown strata represent a back-barrier to estuarine paleoenvironment at near-normal salinity. However, we noted an abundance of carbonized plant fragments compressed within the thinly-layered micaceous clays, suggesting a lower energy estuarine paleoenvironment. This type of facies is typically clay-rich with high primary porosities ranging from 70 to 90 percent. Such porosities are notable as they are thought necessary for concretion development (e.g., Raiswell, 1971; Hudson, 1978; Criss and others, 1988; Andrews and others, 1991; Middleton and Nelson, 1996). Wide, shallow channels within this estuarine setting appear to have concentrated organic materials as lag deposits, which later served in some cases as the nucleus for concretion formation.

Paleontology

The Blufftown Formation contains a plethora of terrestrial vertebrate fossils, plant fragments, and petrified wood fragments. Additionally, the petrified teeth of marine fish and macro-invertebrate fossils have also been recovered. Much of the paleontology of the Blufftown Formation has been documented and reviewed by Schwimmer (1981, 1986a, 1986b), Schwimmer and Case (1987), Case and Schwimmer (1988), Schwimmer and Best (1989), and Schwimmer and others (1993). Although microfossils have not yet been reported in the Blufftown, such fauna may be present in septarian and non-septarian concretions due to their ability to protect and preserve fossilized material long lost from the compacted host sediments (Weeks, 1953; Blome and Albert, 1985; Maples, 1986; Allison, 1988).

FIELD OBSERVATIONS AND ANALYSIS

Approximately 5.5 kilometers of Hannahatchee Creek was traversed during this investigation. The septarian and non-septarian concretions were observed in the creek bed, where they are exposed due to differential erosion of the harder concretions from the sur-

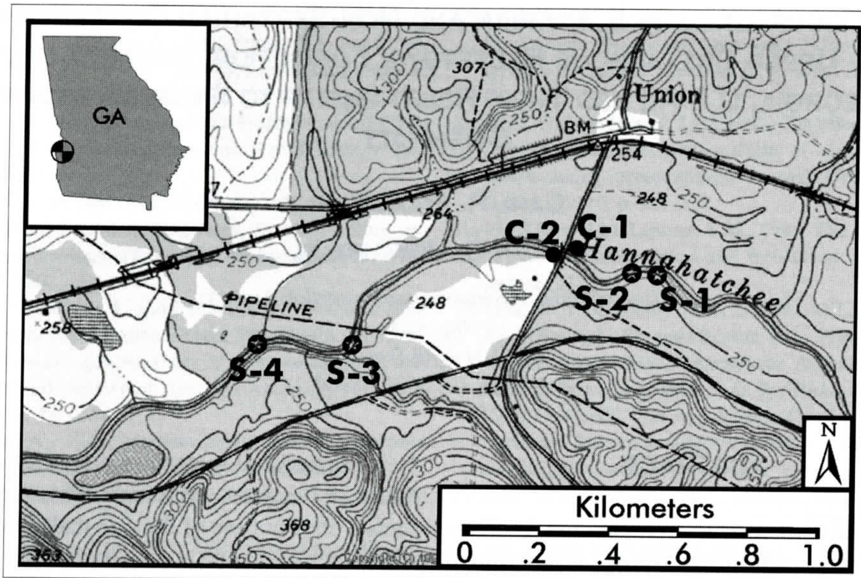

Figure 1. Isolated outcrops of septaria (S) and concretions (C) along Hannahatchee Creek. The septaria exposed within the creek bed trend in a general north-south direction (see Table I for descriptions). Modified from the United States Geological Survey 7.5 minute quadrangle for Union, GA-ALA, 1955, revised 1993.

Table 1. Septarian and Non-septarian Concretions Found in the upper portion of the Blufftown Formation exposed along Hannahatchee Creek

Latitude	Longitude	Long-Axis Orientation	Description and Location (Figure 1)
N 32E 09.126	W 84E 54.143	N 15E°	Septaria (S-1)
N 32E 09.127	W 84E 54.197	N 15E°	Septaria (S-2)
N 32E 09.172	W 84E 54.312	No Clear Orientation	Concretions (C-1)
N 32E 09.164	W 84E 54.362	No Clear Orientation	Concretions (C-2)
N 32E 08.995	W 84E 54.779	N 20E°	Septaria (S-3)
N 32E 08.995	W 84E 54.978	N 20E°	Septaria (S-4)

Stratigraphy

The Blufftown's typical micaceous clay composition was originally identified by Veatch (1909) from an exposure near Blufftown, a small town (now abandoned) along the Chattahoochee River in Stewart County, Georgia. Veatch and Stephenson (1911) were the first to record "indurated, nodular, concretionary layers" in their description of the strata. Cooke (1943) recognized the Blufftown Formation as a formal stratigraphic unit and identified it in exposures in western Georgia. Veatch and Stephenson (1911) and Cooke (1943) collected a variety of invertebrate fossils from concretion-bearing zones within the Blufftown. Marsalis and Friddell (1975) determined its stratigraphic variation, outcrop expression, regional dip, and thickness of the formation, and Reinhardt and Gibson (1980) defined its up- and down-dip lithofacies.

The Blufftown Formation is an early to middle Campanian unit (Sohl and Smith, 1980), that extends from western Georgia to east-central Alabama (Skotnicki, 1985; King and Skotnicki, 1986a, 1986b). Its general stratigraphic sequence reflects an overall regression through the Late Cretaceous (Reinhardt, 1980; King and

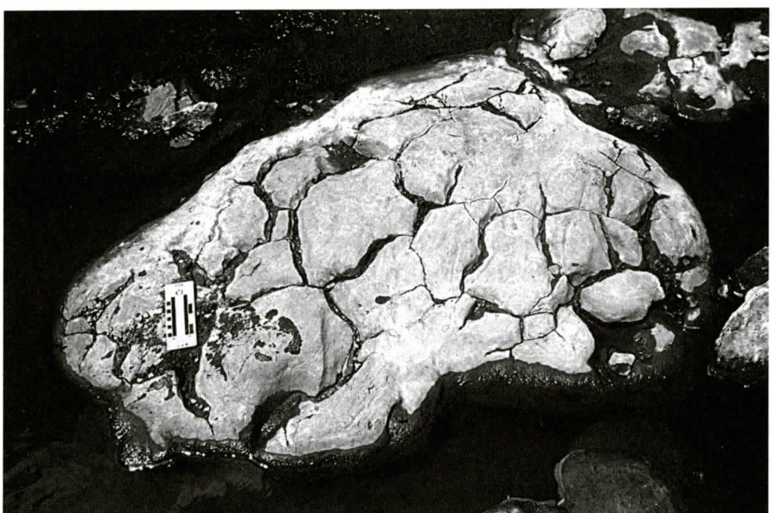

Figure 5. a (top). Large septarium (location S-3) with its broken and blocky interior exposed due to the erosion of its outer surface. Scale in inches and centimeters. b (bottom). Large septarium (location S-4) and its jig-saw-puzzle-like interior. Scale in inches and centimeters.

meters to greater than 1 meter in their longest dimension (Figure 4) which is parallel to the bedding plane. They vary from long flat ellipsoids to discoidal spheres (Figures 5a and 5b). Calcite cement, where not eroded, fills the cracks in the septaria, resulting in the typical irregular polygonal grid appearance. Cement thickness ranges up to 15 mm. Initial microscopic examination of the calcite cements indicates that clear, subhedral crystals fill the cracks, with smaller, blocky crystals lining the fracture surfaces. Several features described by Pratt (2001) were observed within the septaria, including lenticular shrinkage cracks, branching cracks, and cross-cutting cracks.

The septarian concretions occur in discrete rows, whose axis align in a general north-south direction (Table 1). Two areas with large septaria located on the east side of Union Bridge (S1 and S2) have an alignment bearing north 15 degrees east, while the two areas of large septaria to the west of the bridge (S3 and S4) align north 20 degrees east. This orientation, which is roughly parallel to regional dip and perpendicu-

Figure 3. Host micaceous clayey-shale eroded away from around a septarium (location S-3) exposing its outer surface. Scale in inches and centimeters.

Figure 4. Septarian concretions exposed in Hannahatchee Creek (location S-4). Erosion of their upper surface has exposed their cracked interiors. The alignment of their north-south axes is perpendicular to creek flow.

rounding clay matrix (Figure1). Non-septarian concretions (Figure 2) are approximately 15 to 45 cm in diameter, and in many cases contain small particles of plant debris and macro- and micro-invertebrate fossils in their interiors. No evidence of internal layering or zonation was observed in either the septarian or non-septarian concretions.

The contact between the septaria and the host sediment is distinct, with micaceous clay laminae having compacted around each concretion (Figure 3). Septaria range in size from 30 centi-

Scotchman (1991) set the initiation of the development of septarian cracks soon after burial below the sediment-water interface, with growth continuing over a long period of time to substantial burial depths. Within the deep-burial setting, multiple cracks (which are later filled with calcite and other cements) are believed to reflect multiple episodes of burial (Astin, 1986; Scotchman, 1991).

A third theory for the origin and development of septaria involves seismic events that supply the shear stresses necessary to create cracks in the interiors of developing concretions. Pratt (1996, 2001) proposed that cracks form in concretions at shallow burial depths due to earthquake-induced ground motion, and more specifically, that seismic events create instantaneous, chaotic, and high stresses which cause shrinkage, fracturing, and/or brecciation inside the developing concretionary bodies. He suggested that septaria exhibit features best explained by formation in response to the passage of seismic waves through water-saturated sediments. These include: 1) lenticular shrinkage cracks; 2) broken macrofossils; 3) broken, dislodged, and shingled macrofossil fragments from loss of shear strength in the matrix; 4) flaky surface of shrinkage cracks; 5) parallel-sided cracks cutting matrix and first stage of cement; 6) breccia fragments of matrix and first stage cements; 7) reticulate arrays of parallel-sided cracks; 8) branching cracks; 9) en échelon sigmoidal cracks; 10) plumose cracks; and 11) geopetal sediment injected from outside the concretion after the first stage of fibrous calcite cementation has occurred in the shrinkage cracks (Pratt, 2001).

Certain sedimentary structures and deformed beds, identified as "seismites," are known to record the effects of syndepositional tectonic activity (Seilacher, 1984; Plaziat and others, 1990; Pratt, 1994, 1998a; 1998b; 2001). While seismites can be documented quite easily, problems arise in that they are not necessarily accurate monitors of seismic activity, because the sediments do not always faithfully record the events, or the record can be subsequently erased through erosion. The possibility that diagenetic features such as septaria might lend themselves to recording these rather unique events makes their documentation important, if as Pratt (2001) suggested, they can be linked to such occurrences.

DISCUSSION

Lithological and paleontological features of the upper portion of the Blufftown Formation exposed along Hannahatchee Creek support an estuarine paleoenvironment. Concentrations of lag deposits suggestive of paleochannels contain varying amounts of carbonized plant material, petrified wood fragments, and invertebrate and vertebrate fossil debris. With in-filling and burial, these former channels likely continued to influence or serve as conduits in the dewatering and fluid migration of the compacting organic-rich clay sediments within the shallow burial setting (cf. Wood and Hewett, 1986). The septarian and non-septarian concretions do occur within clearly defined areas, suggesting they may represent compartmentalized fluid flow or discrete flow pathways in several individual channels. The preferential orientation of concretions along what were interpreted as paleochannels has been described by Colton (1967) in his investigation of carbonate concretions in the Upper Devonian in New York. Additionally, Raiswell and White (1978) attributed a consistent concretion orientation to a preferred direction of pore water transport during sediment compaction and fluid expulsion. However, the details of this process are unclear.

Of the three general theories used to account for the formation of septarian concretions, the seismic event model best supports the physical setting of these features in the upper Blufftown Formation. The shallow burial setting of the study area eliminates the deep-burial model. Invoking over-pressurization or dehydration of non-septarian concretion interiors in a shallow burial setting fails to explain the variety of internal crack features suggestive of one or more violent forcing agents which are better explained as seismically derived (see Pratt, 2001). The septarian concretions contain cross-cutting cracks which lend a brecciated appearance to their interiors. The best way to create these fraclar to strike, suggests that they may have formed due to channelized diagenetic fluid flow. The two areas of concretions exposed immediately adjacent to the east and west sides of Union Bridge were too eroded to permit any clear axial determination.

DIAGENETIC ORIGIN

Concretions

Concretions are believed to be accurate recorders of changing sedimentology and geochemistry (Curtis and Coleman, 1986; Ludvigson and others, 1994; Coniglio and others, 2000). Pantin (1958) proposed three different periods for concretion development: 1) synsedimentary, i.e., formed at the time of deposition, 2) diagenetic, i.e., formed in the enclosing sediments while they were still soft and unconsolidated, and 3) epigenetic, i.e., formed after the consolidation of the enclosing sediments. Presently, it is generally held that concretion development begins shortly following burial with the onset of diagenetic activity (e.g., Woodland and Richardson, 1975; Dix and Mullins, 1987; Coniglio and Cameron, 1990; Pirrie and Marshall, 1991; Huggett, 1994).

Ritger and others (1987), Raiswell (1988), Morad and Eshete (1990), and Andrews and others (1991), have argued that concretion growth begins within one meter of the submerged sediment surface in uncompacted and highly porous sediment. Raiswell (1976) speculated that each concretion nucleated and developed at the site of an active accumulation of microorganisms. He later postulated that methane (diffused from below) was consumed by microbes to stimulate a late phase of locally intense sulfate reduction, which caused the precipitation of $CaCO_3$ and isotopically heavy FeS_2 (Raiswell, 1987). Sulfate reduction is thought to occur primarily within the top three meters of sediment (Berner, 1968; Coleman and Raiswell, 1981). Below the sulfate reduction zone, methanogenesis is believed to occur as a result of microbial metabolization of the organic content of the uncompacted clay sediment (Siegel and others, 1987). Raiswell and Fisher (2000) concluded that concretion growth may continue beyond the period of sulfate reduction and thus generate cements during methanogenesis, contributing to an extended cementation history.

Concretion formation and development is not believed to require long intervals of geological time (Berner, 1968). Coleman and Raiswell (1993) proposed that even with low rates of microbial sulfate reduction, concretions can form on the order of thousands of years. The rate at which concretions form in the subsurface remains unresolved, but their formation within a short geological interval appears probable.

Septaria

At present there are various processes which can be broadly grouped into three theories that have been proposed to explain the origin and development of septarian cracks: 1) shallow burial with external case hardening and internal geochemical dehydration (and potentially some internal overpressurization); 2) deep-burial with external case hardening and internal overpressurization; and 3) shallow burial with seismic events opening cracks in the interiors of externally case hardened concretions.

The first theory proposes that septaria only form close to the sediment water interface (Raiswell, 1971; Hesselbo and Palmer, 1992; Wetzel, 1992; Duck, 1995; Raiswell and Fisher, 2000). Septarian cracks open by either geochemical dehydration or possibly the overpressurization of the interior. Pore waters supersaturated with calcium carbonate derived from the surrounding sediments pass through the case-hardened exterior and precipitate calcite cement in the open cracks within the interiors of the septarian concretions.

The deep-burial theory envisions septaria developing at depth due to rapid burial and overpressurization (Astin, 1986; Hounslow, 1997). Cracks formed within the deeply buried concretions are viewed as tensile-derived features. However, Hounslow (1997) suggested that crack development could occur at depths less than 10 m if tensional failure resulted as a consequence of localized excess pore pressure.

the epigenetic mineral deposits that may occur as fillings of these cracks.

Septarium - A large roughly spheroidal concretion, 8 to 90 cm in diameter, usually of an impure argillaceous carbonate such as clay ironstone. It is characterized internally by irregular polyhedral blocks formed by a series of radiating cracks that widen toward the center and that intersect a series of cracks concentric with the margins, the cracks invariably filled or partly filled by crystalline minerals (most commonly calcite) that cement the blocks together.

REFERENCES

Allison, P. A., 1988, The role of anoxia in the decay and mineralization of proteinaceous macro-fossils: Paleobiology 14:139-154.

Andrews, J. E., Turner, M. S., Nabi, G., and Spiro, B., 1991, The anatomy of an early Dinantian terraced floodplain: Palaeo-environment and early diagenesis: Sedimentology 38:271-287.

Astin, T. R., 1986, Septarian crack formation in carbonate concretions from shales and mudstones: Clay Minerals 21:617-631.

Bates, R. L., and Jackson, J. A., eds., 1987, Glossary of geology: Third edition, American Geological Institute, 603 p.

Berner, R. A., 1968, Rate of concretion growth: Geochimica et Cosmochimica Acta 32:477-483.

Blome, C. D., and Albert, N. R., 1985, Carbonate concretions: An ideal sedimentary host for microfossils: Geology 13:212-215.

Case, G. R., and Schwimmer, D. R.,1988, Late Cretaceous fish from the Blufftown Formation (Campanian) in western Georgia: Journal of Paleontology 62:290-301.

Coleman, M. L., and Raiswell, R., 1981, Carbon, oxygen and sulphur isotope variations in concretions–from the Upper Lias of N. E. England: Geochimica et Cosmochimica Acta 45:329-340.

Coleman, M. L., and Raiswell, R., 1993, Microbial mineralization of organic matter: Mechanisms of self-organization and inferred rates of precipitation of diagenetic materials: Philosophical Transactions of the Royal Society of London A344:69-87.

Colton, G. W., 1967, Orientation of carbonate concretions in the Upper Devonian of New York: U.S. Geological Survey Professional Paper 575-B, Washington, D.C., pp. B57-B59.

Coniglio, M., and J. S. Cameron, 1990, Early diagenesis in a potential oil shale: Evidence from calcite concretions in the Upper Devonian Kettle Point Formation, southwestern Ontario: Bulletin of Canadian Petroleum Geology 38:64-77.

Coniglio, M., Myrow, P., and White, T., 2000, Stable carbon and oxygen isotope evidence of Cretaceous sea-level fluctuations recorded in septarian concretions from Pueblo, Colorado, U.S.A.: Journal of Sedimentary Research 70:700-714.

Cooke, C. W., 1943, Geology of the coastal plain of Georgia: United States Geological Survey Bulletin 941, Washington, D. C., 121 p.

Criss, R. E., Cooke, G. A., and Day, S. D., 1988, An organic origin for the carbonate concretions of the Ohio Shale: U. S. Geological Survey Bulletin 1836, Washington, D. C., 21 p.

Curtis, C. D., and Coleman, M. L., 1986, Controls on the precipitation of early diagenetic calcite, dolomite and siderite concretions in complex depositional sequences, *in* Gautier, D. L., ed., Roles of organic matter in sedimentary diagenesis, Special Publication No. 38, Society of Economic Paleontologists and Mineralogists, p. 23-33.

Dix, G. R., and Mullins, H. T., 1987, Shallow, subsurface growth and burial alteration of middle Devonian calcite concretions: Journal of Sedimentary Petrology 57:140-152.

Duck, R. W., 1995, Subaqueous shrinkage cracks and early sediment fabrics preserved in Pleistocene calcareous concretions: Journal of the Geological Society of London 152:151-156.

Frazier, W. J., 1997, Upper Cretaceous strata in southwestern Georgia and adjacent Alabama: Atlanta Geological Society Field Trip Guidebook., Atlanta, 22 p.

Hesselbo, S. P., and Palmer, T. J., 1992, Reworked early diagenetic concretions and the bioerosional origin of a regional discontinuity within British Jurassic marine mudstones: Sedimentology 39:1045-1065.

Hounslow, M. W., 1997, Significance of localized pore pressure to the genesis of septarian concretions: Sedimentology 44:1133-1147.

Hudson, J. D., 1978, Concretions, isotopes, and the diagenetic history of the Oxford Clay (Jurassic) of central England: Sedimentology 25:339-370.

Huggett, J. M., 1994, Diagenesis of mudrocks and concretions from the London Clay Formation in the London Basin: Clay Minerals 29:693-707.

King, D. T., Jr., 1994a, Upper Cretaceous depositional sequences in the Alabama Gulf Coastal Plain: Characteristics, origin, and constituent clastic aquifers: Journal of Sedimentary Research B64:258-265.

King, D. T., Jr., 1994b, Upper Cretaceous marine depositional sequences in Alabama and their probable correlation with the Western Interior Seaway: Transactions of the Gulf Coast Association of Geological Societies v. 44: 315-320.

King, D. T., Jr., and Skotnicki, M. C., 1986a, Depositional facies and sea-level dynamics of the Blufftown Formation, Lower Campanian of east Alabama: Southeastern Geology 27(2):53-67.

King, D. T., Jr., and Skotnicki, M. C., 1986b, Facies relationships and depositional history of the Upper Cretaceous Blufftown Formation in eastern Alabama and coeval shelf sediments in central Alabama, Field Trip

ture relationships is by one or more synsedimentary seismic events which occurred periodically during the deposition of the upper portions of the Blufftown Formation.

Seismic events linking clastic dikes and concretions have been documented in the geologic literature (e.g., Martill and Hudson, 1989). Certain exposures of the Blufftown Formation within the Chattahoochee River Valley, approximately 15 and 22 kilometers to the south and northeast of the study area, respectively, contain seismic-derived features such as ball-and-pillow structures and injection dikes (Reinhardt and Donovan, 1986; Reinhardt and Gibson, 1980), along with non-septarian concretions (Marsalis and Friddell, 1975; Reinhardt and Gibson, 1980). The seismic energy necessary to disrupt the interiors of the developing concretions found along sections of Hannahatchee Creek could have been derived from one or more earthquakes within the Chattahoochee River Valley, an area which has had a long history of seismic activity (King, 1994a, 1994b). Therefore it seems reasonable to link seismic events and septaria formation in the manner proposed by Pratt (2001).

SUMMARY AND CONCLUSIONS

The upper Blufftown Formation exposed along Hannahatchee Creek contains concentrations of lag deposits with carbonized particles of plant material and petrified wood fragments along with vertebrate and invertebrate fossils. These plant and animal fossils contained within the micaceous clay matrix suggest a quiet-water setting analogous to an estuarine paleoenvironment. The septarian and non-septarian concretions were only observed at specific locations in the creek. The septarian concretions occur in a linear, near north-south alignment. Their alignment, where it could be determined, suggests that they may be associated with diagenetic fluid flow related to former channels of the estuary.

A seismic origin is proposed for the septarian concretions found in Hannahatchee Creek. This interpretation is based on their irregular polygonal appearance and the presence of internal features similar to those described by Pratt (2001), along with seismic evidence located nearby from other outcrops of the upper Blufftown Formation. One or more seismic events likely disrupted the synsedimentary concretion interiors, forming internal cracks, which were later filled with calcite cement derived from the surrounding sediments.

ACKNOWLEDGMENTS

We are appreciative to Mr. Tony Best for providing field assistance during our investigation. Dr. E. F. McBride contributed very helpful information about his work on septaria. Canadian geologist Dr. B. R. Pratt generously provided us with a prepublication copy of his work on septaria. We also thank Ms. Joellen O'Neill for her capable assistance in locating some obscure references for us. We acknowledge the constructive review provided by Dr. Brian R. Pratt. Any mistakes which remain are our own. This investigation was conducted outside of the official duties associated with our work for the U.S. Environmental Protection Agency.

APPENDIX

The word septaria is often confused with septarian, and septarium. Septarian concretions are a subset of concretions. The words septarium and septaria are not commonly used when describing septarian concretions. The definitions of these terms are noted below (Bates and Jackson, 1987):

Concretion - A hard, compact mass or aggregate of mineral matter, normally subspherical but commonly oblate, disk-shaped, or irregular with odd or fantastic outlines; formed by precipitation from aqueous solution about a nucleus or center. Most concretions were formed during diagenesis, and many (especially in limestone or shale) shortly after sediment deposition.

Septaria - Plural of septarium.

Septarian - Descriptive term for the irregular polygonal pattern of internal cracks developed in septaria, closely resembling the desiccation structure of mud cracks; also said of

Reinhardt, J., and Gibson, T. G., 1980, Field trip 20 road log, Upper Cretaceous-Lower Tertiary, Chattahoochee River Valley, *in* Frey, R. W., ed., Excursions in southeastern geology v. II.: Geological Society of America, Annual Meeting, Atlanta, GA, Field trip guidebooks, American Geological Institute, Virginia, p. 431-463.

Ritger, S., Carson, B., and Suess, E., 1987, Methane-derived authigenic carbonates formed by subduction-induced pore-water expulsion along the Oregon/Washington margin: Geological Society of America Bulletin 98:147-156.

Schwimmer, D. R., 1981, A distinctive Upper Cretaceous fauna, 3-4 meters below the Blufftown-Cusseta contact in the Chattahoochee River Valley, *in* Reinhardt, J., and Gibson, T. G., eds., Upper Cretaceous and lower Tertiary geology of the Chattahoochee River Valley, western Georgia and eastern Alabama: Georgia Geological Society, 16th Annual Field Trip Guidebook, Atlanta, p. 81-88.

Schwimmer, D. R. 1986a, Late Cretaceous fossils from the Blufftown Formation (Campanian) in western Georgia: The Mosasaur 3:109-123.

Schwimmer, D. R., 1986b, A distinctive biofacies near the Blufftown-Cusseta contact in a downdip exposure, Stewart County, Georgia, Field Trip #3 for the Annual Meeting of the Society of Economic Paleontologists and Mineralogists and American Association of Petroleum Geologists: Georgia Geological Society, Atlanta, p. 19-28.

Schwimmer, D. R., and Best, R. H., 1989, First dinosaur fossils from Georgia, with notes on additional Cretaceous vertebrates from the state: Georgia Journal of Science 47:147-157.

Schwimmer, D. R., and Case, G. R., 1987, Cretaceous fish fossils in western Georgia, *in* Frazier, W. J., and Hanley, T. B., eds., Geology of the Fall Line: A field guide to structure and petrology of the Uchee Belt and facies stratigraphy of the Eutaw Formation in southwestern Georgia and adjacent Alabama: Georgia Geological Society, 22nd Annual Field Trip Guidebook, Atlanta, p. C-1 -- C-18.

Schwimmer, D. R., Williams, G. D., Dobie, J. L., and Siesser, W. G., 1993, Late Cretaceous dinosaurs from the Blufftown Formation in western Georgia and eastern Alabama: Journal of Paleontology 67:288-296.

Scotchman, I. C., 1991, The geochemistry of concretions from the Kimmeridge Clay Formation of southern and eastern England: Sedimentology 38:79-106.

Seilacher, A., 1984, Sedimentary structures tentatively attributed to seismic events: Marine Geology 55:1-12.

Siegel, D. I., Chamberlain, S. C., and Dossert, W. P., 1987, The isotopic and chemical evolution of mineralization in septarian concretions: Evidence for episodic paleohydrogeologic methanogenesis: Geological Society of America Bulletin 99:385-394.

Skotnicki, M. C., 1985, Stratigraphy and depositional environments of the Upper Cretaceous Blufftown Formation, eastern Gulf Coastal Plain of Alabama: unpublished M.S. thesis, Auburn Univ., 162 p.

Sohl, N. F., and Smith, C. C., 1980, Notes on Cretaceous biostratigraphy, *in* Reinhardt, J., and Gibson, T. G., Upper Cretaceous and lower Tertiary geology of the Chattahoochee River Valley, western Georgia and eastern Alabama, *in* Frey, R. W., ed., Excursions in southeastern geology v. II.: Geological Society of America, Annual Meeting, Atlanta, GA, Field trip guidebooks, p. 392-402.

Veatch, O., 1909, Second report on the clay deposits of Georgia: Geological Survey of Georgia Bulletin 18, Atlanta, GA. 453 p.

Veatch, O., and Stephenson, L. W., 1911. Preliminary report on the geology of the coastal plain of Georgia, Geological Survey of Georgia Bulletin 26, Atlanta, GA, 466 p.

Weeks, L. G., 1953, Environment and mode of origin and facies relationships of carbonate concretions in shales: Journal of Sedimentary Petrology 23:162-173.

Wetzel, A., 1992, An apparent concretionary paradox: Zentralblatt für Geologie und Paläontologie [1992], Teil I, H12, p. 2823-2830.

Wood, J. R., and Hewett, T. A., 1986, Forced fluid flow and diagenesis in porous reservoirs--controls on the spatial distribution, *in* Gautier, D. L., ed., Roles of organic matter in sedimentary diagenesis, Special Publication No. 38, Society of Economic Paleontologists and Mineralogists, p. 181-187.

Woodland, B. G., and Richardson, C. K., 1975, Time factors of differentially preserved wood in two calcitic concretions in Pennsylvanian black shale from Indiana: Fieldiana Geology 33:179-192.

#3 for the Annual Meeting of the Society of Economic Paleontologists and Mineralogists and American Association of Petroleum Geologists: Georgia Geological Society, Atlanta, p. 10-18.

King, D. T., Jr., and Skotnicki, M. C., 1994, Upper Cretaceous stratigraphy and sea-level history, Gulf Coastal Plain of central and eastern Alabama, *in* Shurr, G. W., Ludvigson, G. A., and Hammond, R. H., eds., Perspectives on the Eastern Margin of the Cretaceous Western Interior Basin: Geological Society of America, Special Paper 287, p. 27-42.

Ludvigson, G. A., Witzke, B. J., González, L. A., Hammond, R. H., and Plocher, O. W., 1994, Sedimentology and carbonate geochemistry of concretions from the Greenhorn marine cycle (Cenomanian-Turonian), eastern margin of the Western Interior Seaway, *in* Shurr, G. W., Ludvigson, G. A., and Hammond, R. H., eds., Perspectives on the Eastern Margin of the Cretaceous Western Interior Basin: Geological Society of America, Special Paper 287, p. 145-173.

Maples, C. G. 1986. Enhanced paleological and paleoenvironmental interpretations result from analysis of early diagenetic concretions in Pennsylvanian shales: Palaios 1:512-516.

Marsalis, W. E., and Friddell, M. S., 1975, A guide to selected Upper Cretaceous and lower Tertiary outcrops in the lower Chattahoochee River Valley of Georgia: Georgia Geological Survey, Guidebook 15, Atlanta, GA, 87 p.

Martill, D. M., and Hudson, J. D., 1989, Injection clastic dykes in the Lower Oxford Clay (Jurassic) of central England: Relationship to compaction and concretion formation: Sedimentology 36:1127-1133.

Middleton, H. A., and Nelson, C. S., 1996, Origin and timing of siderite and calcite concretions in late Palaeogene non- to marginal-marine facies of the Te Kuiti Group, New Zealand: Sedimentary Geology 103:93-115.

Morad, S, and Eshete, M., 1990. Petrology, chemistry and diagenesis of calcite concretions in Silurian shales from central Sweden: Sedimentary Geology 66:113-134.

Pantin, H. M., 1958, Rate of formation of a diagenetic calcareous concretion: Journal of Sedimentary Petrology 28:366-371.

Pirrie, D., and Marshall, J. D., 1991, Field relationships and stable isotope geochemistry of concretions from James Ross Island, Antarctica: Sedimentary Geology 71:137-150.

Plaziat, J.-C., Purser, B. H., and Philobbos, E., 1990, Seismic deformation structures (seismites) in the syn-rift sediments of the NW Red Sea (Egypt): Bulletin de la Société Géologique de France, Series 8(6):419-434.

Pratt, B. R., 1994, Seismites in the Mesoproterozoic Altyn Formation (Belt Supergroup), Montana: A test for tectonic control of peritidal cyclicity: Geology 22:1091-1094.

Pratt, B. R., 1996, Septarian fissures in marine carbonate concretions: Origin through cracking and shrinkage during syndepositional earthquakes: Geological Society of America Annual Meeting, Abstracts with Programs v. 28, p. A-407.

Pratt, B. R., 1998a, Syneresis cracks: Subaqueous shrinkage in argillaceous sediments caused by earthquake-induced dewatering: Sedimentary Geology 117:1-10.

Pratt, B. R., 1998b, The origin of molar-tooth structure in Proterozoic carbonate rocks by synsedimentary earthquake-induced shrinkage and fluidization, and implications for the nature and evolution of basins and marine sediment: Geological Society of America Bulletin 110:1028-1045.

Pratt, B. R., 2001, Septarian concretions: Internal cracking caused by synsedimentary earthquakes: Sedimentology 48:189-213.

Raiswell, R., 1971, The growth of Cambrian and Liassic concretions: Sedimentology 17:147-171.

Raiswell, R., 1976, The microbiological formation of carbonate concretions in the Upper Lias of NE England: Chemical Geology 18:227-244.

Raiswell, R., 1987, Non-steady state microbiological diagenesis and the origin of concretions and nodular limestones, *in* Marshall, J. D., ed., Diagenesis of sedimentary sequences: Geological Society Special Publication No. 36, p. 41-54.

Raiswell, R., 1988, Chemical model for the origin of minor limestone-shale cycles by anaerobic methane oxidation: Geology 16:641-644.

Raiswell, R., and Fisher, Q. J., 2000, Mudrock-hosted carbonate concretions: A review of growth mechanisms and their influence on chemical and isotopic composition: Journal of the Geological Society of London 157:239-251.

Raiswell, R., and White, N. J. M., 1978, Spatial aspects of concretionary growth in the Upper Lias of northern England: Sedimentary Geology 20:291-300.

Reinhardt, J., 1980, Upper Cretaceous stratigraphy and depositional environments, *in* Reinhardt, J., and Gibson, T. G., Upper Cretaceous and lower Tertiary geology of the Chattahoochee River Valley, western Georgia and eastern Alabama, *in* Frey, R. W., ed., Excursions in southeastern geology v. II.: Geological Society of America, Annual Meeting, Atlanta, GA, Field trip guidebooks, Atlanta, p. 386-392.

Reinhardt, J., 1982, Lithofacies and depositional cycles in Upper Cretaceous rocks, central Georgia to eastern Alabama, *in* Arden, D. D., Beck, B. F., and Morrow, E., eds., Proceedings of the second symposium on the geology of the southeastern coastal plain: Information Circular 53, Georgia Department of Natural Resources, Atlanta, GA, p. 89-96.

Reinhardt, J., and Donovan, A. A., 1986, Roadlog, *in* Reinhardt, J., ed., Stratigraphy and sedimentology of continental, nearshore, and marine Cretaceous sediments of the eastern Gulf coastal plain, Field Trip #3 for the Annual Meeting of the Society of Economic Paleontologists and Mineralogists and American Association of Petroleum Geologists: Georgia Geological Society, Atlanta, p. 71-91.